UNIVERSIDADE
BEIRA INTERIOR

Development of a CNC Milling machine

DIY kit for a vertical desktop milling machine

(Versão final após defesa)

Miguel Filipe Estevão da Cruz

Dissertação para obtenção do Grau de Mestre em

Engenharia Eletromecânica

(2º ciclo de estudos)

Orientador: Prof. André Ferreira Costa Vieira

Janeiro de 2025

Declaração de Integridade

Eu, Miguel filipe Estevão da Cruz, que abaixo assino, estudante com o número de inscrição M11619 no 2º ciclo de estudos do curso de enegenharia eletromecânica da Faculdade de enegenharias, declaro ter desenvolvido o presente trabalho e elaborado o presente texto em total consonância com o **Código de Integridades da Universidade da Beira Interior**.

Mais concretamente afirmo não ter incorrido em qualquer das variedades de Fraude Académica, e que aqui declaro conhecer, que em particular atendi à exigida referenciação de frases, extratos, imagens e outras formas de trabalho intelectual, e assumindo assim na íntegra as responsabilidades da autoria.

Universidade da Beira Interior, Covilhã 05 / 01 / 25

(assinatura conforme Cartão de Cidadão ou preferencialmente
assinatura digital no documento original se naquele mesmo formato)

Acknowledgements

Firstly, I would like to express my gratitude to Professor André Ferreira Costa Vieira for sharing his knowledge and for his availability. His lectures at Universidade da Beira Interior have deepened my interest in manufacturing processes and project development. Next, I'd like to thank Lara Sales for all the love, support and patience during the writing of this work, to my parents for allowing me to pursue my academic course and for all the support during my life. A huge thanks to Rodrigo Antunes for his partnership and availability, without him this work would have taken longer. Thanks to Rat Rig for all the resources, shared knowledge and availability to teach. Lastly, thank you to everyone who was a part of my academic journey and shaped it somehow, friends, teachers and roommates.

Abstract

This thesis presents the design and development of a DIY CNC vertical milling machine aimed at small-scale, precise machining for materials such as wood, plastics, and light metals like aluminium. The motivation behind this project is to make precision machining more accessible to hobbyists, educators, and small workshops by providing a compact and affordable solution. The design focuses on optimizing structural components, electronics, and software to balance cost with performance. Key challenges in mechanical design, such as force distribution, material selection, and operational stability, are addressed to ensure the mill's precision and reliability. The opensource approach of this project allows users to further customize the platform to their specific needs. This research also discusses the importance of desktop CNC machines in fostering innovation and accessibility in engineering, education, and product development. The Rat Rig mill is developed with a modular design that enables users to adapt and modify the machine according to specific project requirements.

Keywords

CNC milling, DIY, Rat Rig, desktop manufacturing, open source

Table of Contents

Table of Figures

List of tables

Nomenclature

Acronyms:

DIY	Do it yourself
CNC	Computer numerical control
3D	3-dimensional
AM	Additive manufacturing
IoT	Internet of things
AI	Artificial intelligence
Vc	Cutting velocity
N	Spindle speed
F	Feed rate
DOC	Depth of cut
Fz	Chip load
MMR	Material removal rate
Af	Feed per tooth
Ae	Width of cut
Ap	Depth of cut
Fa	Axial force
Fc	Cutting force
Fr	Radial force
Ft	Tangential force
D	Diameter
P	Power
T	Torque
CAD	Computer aided design
Xf	X offset
Yf	Y offset
Zf	Z offset
ACME	American trapezoidal thread
P_{cr}	Critical buckling load
E	Modulos of elasticity
I	Second momentum of inertia
K	End condition factor
L	Length
C	Supporting configuration factor
$N_{critical}$	Critical speed
SPI	Serial communication interface
TMC	Trinamic
PWM	Pulse width modulation
VFD	Variable frequency drive
V	Voltage
I	Current
PSU	Power supply

1. Introduction

1.1 Motivation and Objectives

Due to the technological evolution of the machining processes with CNC (Computer Numerical Control) machines and the worldwide spread of information, thanks to the internet, anyone can have the resources and knowledge to assemble and operate a small CNC device at home. The 'Industry 4.0' which refers to a fourth industrial revolution based on using the Internet of Things (IoT) concept, allows for cyber-physical systems and other modern technologies, which are to bring full digital interconnection of all manufacturing processes (from development to distribution of the product) (SEVIC & KELLER, 2019).

Desktop vertical mills have revolutionised small-scale manufacturing, offering precision machining capabilities that were once only available in industrial-sized equipment. These compact machines, capable of cutting and drilling a variety of materials, have become indispensable tools in various fields, including engineering, product design, and education. This document explores the origins, technological advancements, and significant benefits of such machines, including their mechanical build and electronics and controls. This passion led me to pursue a job at Rat Rig, a small company based in the south of Portugal with a huge community around the world, they design and produce do-it-yourself (DIY) desktop 3D printers as well as CNC routers. A huge ambition to learn the design and production processes involved in making such a machine was the motivation to embrace the Mill project. This project consists of a small DIY desktop milling machine, providing the end user with a milling machine suited to their needs at an affordable price. In the beginning, the goals were very clear, to accomplish a mill that can cut wood, acrylics, plastics, and soft metals, like aluminum.

1.2 Purpose of the Essay

The primary aim of this essay is to delve into the dynamic and static forces acting on milling machines and to elucidate the principles of dimensioning and designing these sophisticated tools. Understanding these aspects is crucial for designing, optimising, and operating milling machines that meet the rigorous demands of modern manufacturing. By integrating advanced materials, control systems, and innovative design features, milling machines can meet the evolving demands of modern manufacturing. This comprehensive approach enhances machine performance and ensures the longevity and reliability of these critical tools in the manufacturing ecosystem.

This essay aims to provide a detailed exploration of these aspects, offering insights that will aid in the development and optimization of milling machines for diverse desktop and semi-industrial applications.

2. State of the art

2.1 Vertical mill machine

A vertical milling machine is a versatile piece of machinery used in the manufacturing industry. It features a vertically oriented spindle that holds and rotates the cutting tool against the workpiece, which is typically clamped to a worktable. The machine allows for precise milling, drilling, boring, and cutting operations on a variety of materials. Vertical milling machines come in both manual and CNC versions, with the latter offering advanced automation and precision. Key components include the spindle (located in the head), worktable, column, knee, and base, as shown in Fig. 1 below, all designed to provide stability and accuracy during machining tasks (Carlsson, 1984).

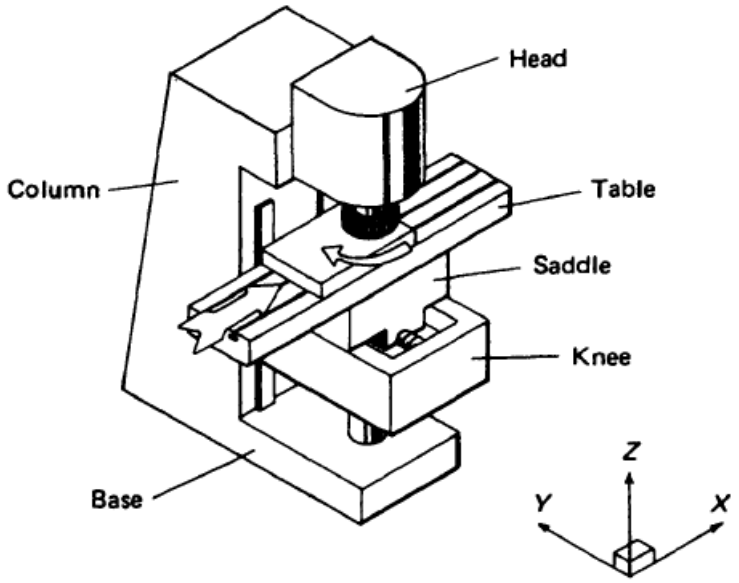

Fig. 1 Vertical Mill machine illustration (Boothroyd, 1988)

2.2 Brief overview of desktop vertical milling machines

Desktop vertical milling machines are compact versions of traditional milling machines, designed for precision machining of metal, plastic, and other materials within a smaller footprint. These machines have been pivotal in democratising access to precision machining, enabling small-scale workshops, educational institutions, and hobbyists to produce intricate parts and prototypes without the need for large industrial machinery. The advantage of desktop vertical mills lies in their versatility and precision. Despite their compact size, these machines offer capabilities similar to their larger counterparts, including drilling, slotting, keyway cutting, and contouring, with accurate precision. This has been crucial in fostering innovation and creativity in various fields, including engineering, design, and art. The emergence of desktop vertical milling machines is part of a trend toward miniaturization and affordability in manufacturing technology. The development of CNC technology has been a significant driver behind this trend. CNC technology

allows for the automated control of the milling machine, enabling complex parts to be manufactured with high precision and repeatability (Abd Rahman et al., 2023). The integration of CNC technology with desktop milling machines has expanded their functionality and appeal, making them accessible to a wider audience. Recent advancements have further enhanced the capabilities of desktop vertical mills. For instance, the incorporation of 3D (3-dimensional) printing technology into the fabrication of machine components reduced costs and allowed for greater customization and innovation in machine design. Research has shown that combining 3D printing and CNC milling technologies in desktop machines can significantly impact the prototyping and manufacturing processes, offering a versatile tool for modern maker spaces and educational settings (Krimpenis & Iordanidis, 2023).

2.3 Importance of manufacturing and prototyping

Manufacturing is the process of producing goods by transforming raw materials using labour, and machines. Manufacturing sectors are pivotal for economic stability and growth, providing a substantial employment base and fostering ancillary industries. The sector's health is often a reflection of economic prosperity. Studies like those conducted by (Hoffmann et al., 2020) analyse the correlation between manufacturing output and employment rates, illustrating how manufacturing serves as an important economic stabilizer.

The manufacturing industry is a key point in global supply chains, affecting everything from local labour markets to international trade policies. The intricate network of suppliers, manufacturers, and distributors ensures the movement of goods across borders, allowing for global trade. Manufacturing is also synonymous of innovation. The development of new manufacturing processes and technologies often leads to significant advancements in product efficiency, sustainability, and affordability. The research highlighted in (SEVIC & KELLER, 2019) discusses the role of manufacturing in driving technological innovation, particularly through the adoption of Industry 4.0 technologies, which is just a small example of how important manufacturing is to technology improvement. All the benefits manufacturing brings, don’t come for free as the environmental impact of manufacturing processes has spurred research into sustainable practices. Studies, such as those published in (Gupta et al., 2018), explore methods to reduce waste, improve energy efficiency, and utilize renewable resources in manufacturing processes, aiming to mitigate the industry's environmental footprint.

Along with manufacturing, there is always the prototyping stage, which is an iterative process crucial in the design and development of new products. It allows for the exploration of ideas, testing of functionality, and refinement of designs before full-scale production begins. Prototyping empowers innovation, allowing designers and engineers to test and refine their ideas. Studies, like those found in (Chaoji & Martinsuo, 2019), investigate the role of prototyping in the creative process, highlighting how it enables rapid iteration and innovation. Effective prototyping can greatly reduce development time and costs by identifying design flaws and manufacturability issues early in the process. If a fatal flaw in a product is not caught during prototyping and it reaches the production stage, it can result in significant waste and financial loss for the company.

Research presented by (Pitt et al., 2021) examines how prototyping practices influence product development timelines and budget adherence.

Last but not least, prototypes serve as a tangible representation of products for stakeholders, including investors, customers, and marketing teams (Pitt et al., 2021). The intertwined roles of manufacturing and prototyping in product development, economic growth, and innovation cannot be overstated. They have a huge impact on the improvement of product quality, the fostering of economic stability, and the advancement of sustainable practices.

2.4 History of milling machines

The evolution of milling machines dates back to the 19th century, with the inception of the first milling machine credited to Eli Whitney in 1818, as shown in Fig. 2 below. Designed to produce musket balls in standardised sizes, this machine laid the groundwork for future developments in milling technology (Usher, 1961). The journey from these early machines to today's sophisticated desktop vertical mills spans over two centuries of engineering innovation.

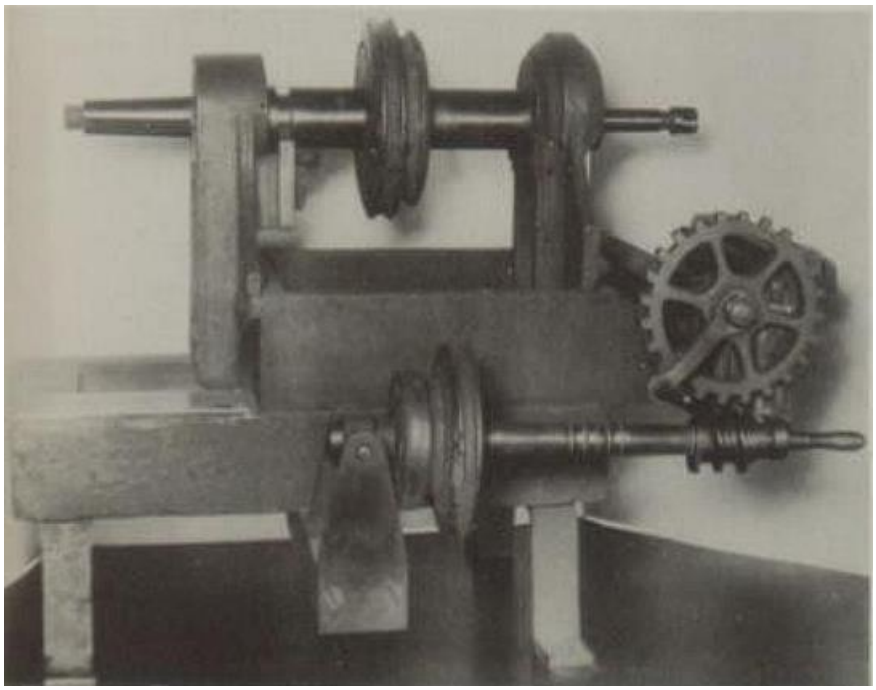

Fig. 2 Eli Whitney's 1818 milling machine, a pioneering innovation made primarily from iron and wood, was used to create uniform, interchangeable parts for firearms. (Martins, 2015)

In the late 19th and early 20th centuries, advancements in materials and precision engineering led to the development of the first vertical mills. These machines introduced a vertical milling spindle, enabling more complex shapes and surfaces to be machined with higher precision. The introduction of computer numerical control technology in the latter half of the 20th century was a pivotal moment. It allowed for precise control over the milling process, transforming the capabilities of milling machines. The first-ever CNC controller was developed in the late 1940s

and early 1950s by John T. Parsons and Frank L. Stulen at the Massachusetts Institute of Technology. This early CNC system used punched tape as a data storage method to control the movements of a milling machine, marking a significant advancement in automated machine control and precision manufacturing. This pioneering development laid the foundation for modern CNC technology (Usher, 1961).

The miniaturization of CNC technology and the rise of digital manufacturing in the 21st century have culminated in the development of desktop vertical mills. These compact machines bring the power of CNC machining to small-scale operations, workshops, and educational institutions, making advanced manufacturing techniques more accessible than ever before (Ro et al., 2008).

2.5 Key technological innovations in desktop vertical mills

Exploring the key technological innovations in desktop vertical mills, we dive into the realms of advanced materials, precision engineering, and digital control systems that have significantly enhanced their capabilities, accuracy, and usability over the years. Although new improvements in desktop vertical mills and their technological innovations are limited for the time being, we can extrapolate from broader research in related fields, such as additive manufacturing and smart manufacturing systems, to understand the trends and advancements likely impacting desktop vertical milling technologies.

The advancements in additive manufacturing (AM) allow the use of 3D printing technologies with traditional milling processes which has led to innovative hybrid manufacturing systems. These systems leverage the flexibility of additive manufacturing for complex geometries with the precision of subtractive milling for finishing surfaces (Krimpenis & Iordanidis, 2023). The integration of digital control systems, such as CNC technology, into desktop vertical mills has transformed their capabilities. These systems allow for precise control over the milling process, enabling the execution of complex designs with high accuracy and repeatability as machining is one of the most versatile and accurate of all manufacturing processes (Akinnuli et al., 2015). Nowadays research focuses on improving these digital systems to enhance user interfaces, increase automation, and integrate with software tools for better design and manufacturing workflows (Anania et al., 2021). The application of Internet of Things (IoT) technologies in manufacturing equipment, including desktop vertical mills, introduces smart capabilities. These include remote monitoring and control, predictive maintenance, and process optimization based on real-time data analytics. Such technological innovations aim to increase efficiency, reduce downtime, and dynamically adapt manufacturing processes to changing requirements (Siddhartha et al., 2021).

2.6 Accessibility for small-scale operations and education

The integration of technology in small businesses and educational initiatives significantly impacts accessibility for small-scale operations, fostering an environment where innovation and efficiency thrive. According to a report by the U.S. Chamber of Commerce, a staggering 95% of small

businesses in the U.S. utilize at least one type of technology platform, highlighting the deep penetration of technology in the small business sector. This widespread adoption correlates with growth in sales, employment, and profits, particularly for those who have embraced Artificial Intelligence (AI), showcasing technology's pivotal role in navigating post-pandemic economic challenges and fuelling optimism among small business owners. However, the report also notes a concern among these owners regarding potential tech regulations that could introduce increased costs and complexities (U.S. Chamber of Commerce, 2022).

On a similar note, agricultural mechanization in China presents an illustrative example of how technology can enhance accessibility and efficiency in small-scale operations, especially in agriculture. Despite the prevalent misconception that machinery is unsuitable for small-scale businesses, China's experience underscores the transformative potential of agricultural productivity. The development of agricultural automation in China has been an evolutionary process focused on self-reliance, demonstrating that appropriate mechanization theories and strong, pro-farmer policies are essential. This approach has successfully increased agricultural productivity, contributing to sustainable food security and poverty alleviation. It's a testament to the idea that, with the right strategies and policies, technology can be adapted to benefit small-scale operations significantly (U.S. Chamber of Commerce, 2022).

These insights collectively underscore the transformative potential of technology and mechanization across diverse sectors. They highlight the importance of policy frameworks, the adoption of appropriate technologies, and the need for strategic leadership to navigate the challenges and opportunities presented by technological innovation. For small businesses and agricultural operations alike, leveraging technology not only enhances operational efficiency but also opens new pathways for growth and development (U.S. Chamber of Commerce, 2022).

2.7 Comparison with traditional manufacturing methods

Comparing desktop CNC milling machines with traditional manufacturing methods offers a clear view of the evolution in precision machining. Desktop CNC mills, such as the SYIL X5 Pro CNC machine, provide significant advantages, including a compact design that saves space, cost-effectiveness, and ease of use, without sacrificing quality or performance. These machines are particularly suitable for small-scale operations and education, where precision, affordability, and space savings are crucial (SYIL, 2023).

On the other hand, traditional manufacturing methods, which often rely on manual operations, have their own set of benefits, especially in terms of robustness and handling heavy-duty tasks. However, they tend to lack the precision and flexibility offered by CNC machining. Traditional methods are more suitable for large-scale production where the high volume justifies the setup and operational costs (SYIL, 2023).

CNC machining outperforms traditional methods in efficiency, precision, and flexibility. It's fully automated, requires minimal human intervention, and can operate continuously, making it more efficient and cost-effective for production. Its computer-controlled nature results in extremely precise parts, essential in industries where accuracy is paramount. Moreover, CNC machining's

software-driven process allows for quick adaptations to produce various parts with minimal setup time, making it ideal for customized or small-batch production (Liang et al., 2018).

2.8 Overview of leading models in the market

There are already some desktop DIY milling machines on the market, birthing from the early RepRap days, many projects emerged so it's hard to say which was first but the first to become popular in 2019 was the Mini Mill from Openbuilds. Openbuilds is an American company dedicated to open-source hardware and design. They introduced the V-Slot extrusions to the market and laid the foundations for thousands of projects, companies, and products worldwide. This small milling machine is still available to purchase at Openbuildspartstore.com for 943.96$. Being a DIY kit, some components are optional, like the router, interface, and probe, allowing the users to customize the machine to their needs. It has a work area of 120mm on the X-axis, 180mm on the Y-axis, and 80mm on the Z-axis, the motion system uses lead screws and V-wheels, along with NEMA 23 stepper motors. The manufacturer provides the BlackBox X32 motion controller, which is a 32-bit processor board with Toshiba tb67s109A stepper drivers capable of outputting a 4A current. The BlackBox X32 runs a customized version of GrblHAL firmware, which is the successor of the 8-bit Grbl firmware, allowing Openbuilds to implement more functionalities on the machine as the 32-bit processor has an increased computing power. They provide the user a software called Openbuilds Control to visually control the mini mill, along with their Openbuilds CAM webpage. This combo is aimed at being intuitive and easy to use, the user doesn't need to have previous CNC or CAM experience to get the machine up and running. This small mill is advertised as capable of milling and cutting cast acrylics, wood, and non-ferrous metals, like copper and aluminium (Mark Carew, 2019). This small machine can be observed below in Fig. 3.

Fig. 3 OpenBuilds Mini Mill: A versatile and compact CNC milling machine, designed for precision and efficiency in small-scale projects and DIY manufacturing (Mark Carew, 2019).

Nowadays the most popular desktop DIY milling machine is the Milo1.5, Fig. 4. This is an open-source project aimed at being low-cost and powerful, starting at 1261$. The main difference from the Openbuilds MiniMill is that the Milo1.5 is a project, not a product from a company, so the developers of the project made a public bill of materials which is used by *LDO motors*, a Chinese company focused on reselling open-source machine kits, to produce a full kit for everyone. This kit is sold by a wide variety of resellers worldwide, it has a work area of 340mm on the X-axis, 160mm on the Y-axis, and 60mm on the Z-axis, the motion system uses lead screws and linear rails, along with nema 23 stepper motors. The frame is made of 2020 aluminium extrusion profiles along with aluminium plates and 3D-printed parts. The kit comes with a 1.5KW air-cooled spindle capable of speeds from 10000 to 24000 rpm and claims a maximum cutting speed of 1000mm/min, along with the FLY CDY V3 controller board, this board has a 32-bit processor and TMC2209 stepper motor drivers, this board is designed to run RepRap firmware, which is a comprehensive motion control firmware intended primarily for controlling 3D printers, but with applications in laser engraving/cutting and CNC too. At this point, this is one of the most popular firmware for budget/open-source CNC machines. The Milo1.5 is advertised as capable of milling and cutting cast acrylics, wood, aluminium, and even mild steel (MilleniumMills, n.d.).

Fig. 4 MILO 1.5: Advanced robotic system and DIY kit with 3D printed components, designed for precision manufacturing and automation, offering high efficiency and flexibility (MilleniumMills, n.d.).

3. Mechanical analysis of a milling machine

3.1 Chapter 1: Types of milling operations

The two most commonly used types of milling on a vertical mill are: end milling and face milling, as illustrated below, a) and b) respectively:

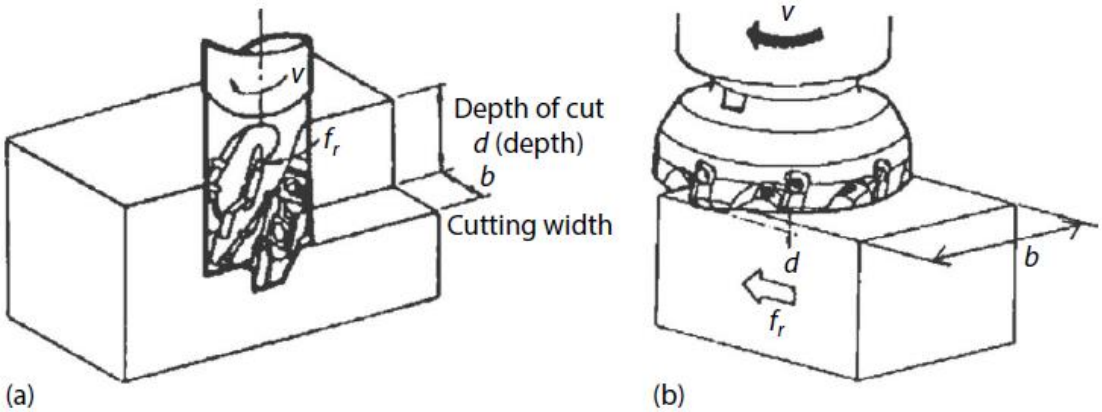

Fig. 5 Types of milling operations: (a) end milling, (b) face milling (Lee et al., 2020)

3.1.1 End Milling

End milling involves the use of a rotating cutting tool called an end mill, which has cutting edges on both the end and the sides. The tool moves along the surface of the workpiece to remove material. This operation can be used to create grooves or slots within the workpiece, which is named Slotting, cutting intricate profiles/contours, named profiling, drilling into the material which is called Plunging and lastly, remove material from the interior area of a workpiece, which is called pocketing (Boothroyd, 1988).

End mills can handle a wide range of tasks due to their multiple cutting edges, making them a super versatile tool. They are also capable of achieving accurate and consistent cuts, due to their high precision. Lastly, these come in various shapes, e.g. flat mill, ball-nose, radius, etc… and numerous sizes and materials to suit different applications and workpiece materials (Boothroyd, 1988), as illustrated in Fig. 6.

Fig. 6 Different types of end mills (Mekanika, n.d.).

3.1.2 End mill parameters

A comprehensive understanding of the endmill characteristics allows the user to select the appropriate tool for the specific milling operation, optimizing performance, tool life, and the quality of the machined part. An end mill has the following characteristics: Number of teeth or number of flutes (n), diameter (d), helix angle (α) and length (L) (Stephenson & Agapiou, 2018)

The number of flutes on an end mill directly impacts chip removal capacity, surface finish and tool strength. Fig. 7illustrates the number of fluted on an end mill, 2 Flute end mills are the most commonly used for slotting operations in aluminium and non-ferrous materials. Provides excellent chip evacuation due to the large flute volume but sacrifices surface finish. 3 Flutes provide a compromise between the chip evacuation capacity of 2 flutes and the surface finish of 4 flutes. Often used in softer materials. End mills with 4 Flutes and more are used for harder materials like steel and also for finishing operations. More flutes result in a smoother surface finish but reduce chip space, potentially leading to clogging in deeper cuts (Stephenson & Agapiou, 2018).

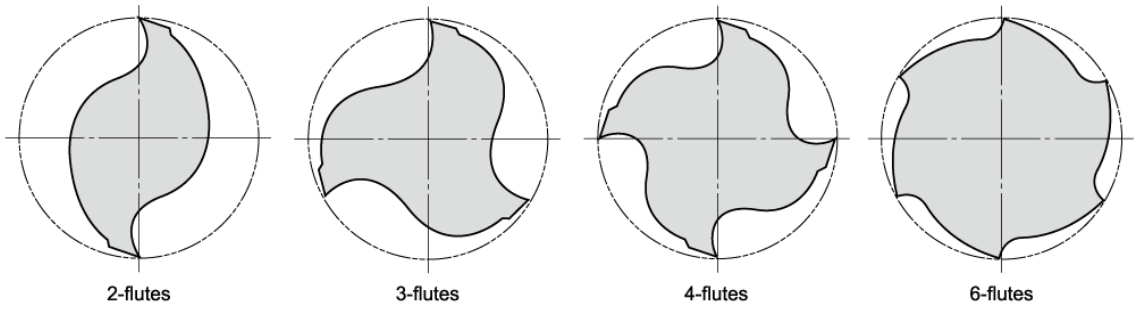

Fig. 7 Visual representation of the number of flutes on an end mill (Wayken, 2022)

The diameter of the end mill determines the width of the cut and the rigidity of the tool. Larger diameters offer greater stiffness and can handle more aggressive cutting parameters, while smaller diameters allow for more precise details at the cost of way more conservative cutting parameters. It's very important to consider the machine's spindle power, the rigidity of the setup, and the required cutting depth. Larger diameters require more power and may introduce deflection in less rigid setups (Stephenson & Agapiou, 2018).

The helix angle affects chip evacuation, cutting forces, and tool vibration. This feature can be described as the "pitch" of the flutes when compared to a screw thread for example. The choice of helix angle depends on the material being machined and the type of operation. For example, high helix angles are beneficial in aluminium machining, while lower angles are better for tough steels (Stephenson & Agapiou, 2018).

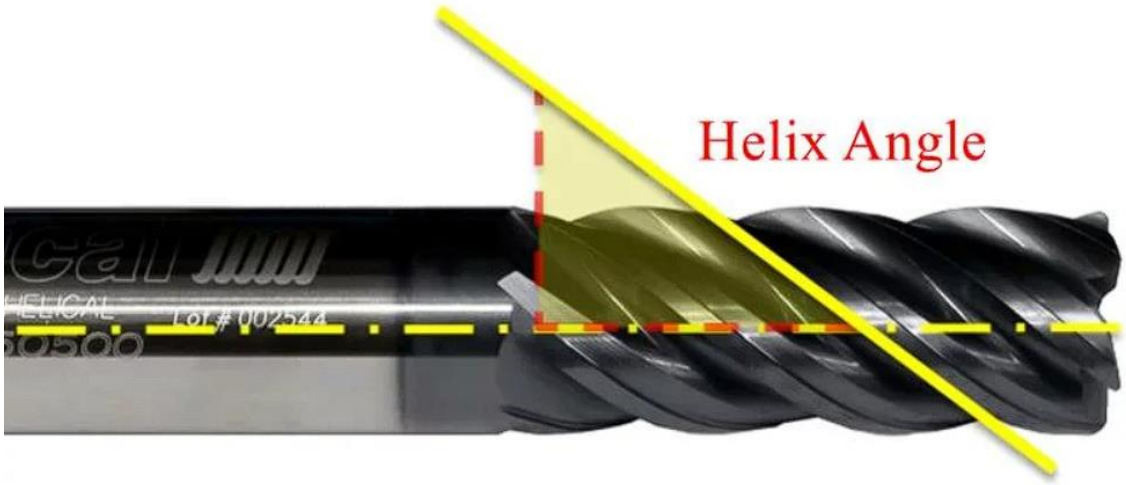

Fig. 8 Visual representation of the helix angle (Wayken, 2022).

Lastly, the overall length and the flute length of the end mill affect tool rigidity and maximum depth of cut. Short end mills provide maximum rigidity and are preferred for high-precision operations and hard materials. Minimize deflection and vibrations, while long end mills are necessary for deep pocketing and extended reach applications but can introduce deflection and vibration, especially in less rigid setups. Choosing the shortest possible end mill that can reach

the cutting depth required is the best approach. For deep cuts, consider using reduced shank tools or specialized long-reach end mills designed to minimize deflection (Stephenson & Agapiou, 2018).

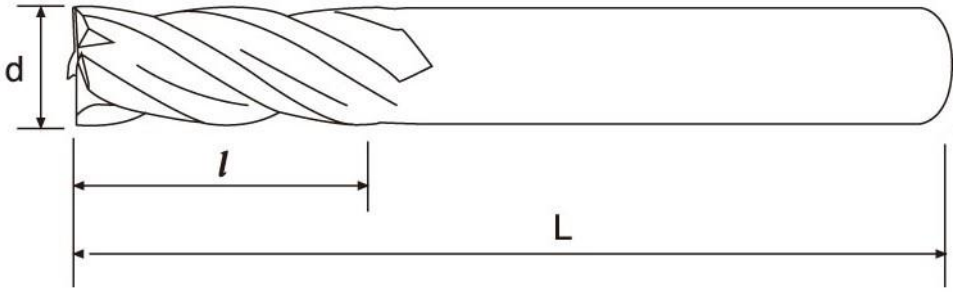

Fig. 9 End mill diameter (d), flute length (l) and overall length (L) (Speedtiger, n.d.)

3.1.3 Face Milling

Face milling is a machining process where the cutting tool has a broad face that moves perpendicular to the surface of the workpiece. The cutting edges are located on the periphery and the face of the cutter. This process is aimed at the surface finish and material removal, the right face mill can achieve a smooth and flat surface to the workpiece, this is not only great for manufacturing quality but also precision and face milling ensures all operations done afterwards are perfectly perpendicular to the workpiece surface (Boothroyd, 1988).

The picture below illustrates what a face mill generally looks like, it has three major parts, the Body, the cutting inserts and the Arbor hole. The main body of a face mill is typically made of a sturdy material, such as high-speed steel or carbide. The body can vary in diameter, commonly ranging from a few centimetres to several decimetres, depending on the size of the workpiece and the required material removal rate. The cutting inserts (or teeth) are mounted on the face of the tool. These inserts are usually replaceable and can be made from various materials, including carbide, ceramics, and high-speed steel. The inserts are secured in the body using screws or clamps. There are numerous types of inserts, ranging from square inserts, round inserts and triangular/diamond inserts, etc… Choosing the right type of insert involves considering the material to be machined, the type of milling operation, and the desired surface finish. Understanding the various insert shapes, materials, and coatings can significantly enhance milling efficiency and tool performance. Lastly, the centre of the face mill has an arbor hole for mounting onto the spindle of the milling machine. The arbor hole size must match the spindle specifications of the machine (Boothroyd, 1988).

Fig. 10 Face mill example (Avantec, n.d.)

3.1.4 Conventional milling VS climb milling

Conventional milling and climb milling are two distinct machining techniques used in milling operations, each with its advantages and disadvantages. Understanding these differences is crucial for selecting the appropriate milling method based on the specific requirements of the machining operation, such as the desired surface finish, the rigidity of the setup, and the type of material being machined.

In conventional milling, the cutter rotates against the direction of feed of the workpiece. The cutter teeth engage the material at the bottom of the cut and remove the material upward. The cutting force tends to pull the workpiece upward and away from the cutting tool, which can cause vibrations and chatter, especially if the setup is not rigid. It also begins with a small chip thickness and increases to a maximum at the end of the cut. This can lead to higher friction and increased heat generation, resulting in more wear on the cutting tool. Generally, the surface finish is rougher compared to climb milling because of the gradual increase in chip thickness and the tendency for tool deflection. This cutting method requires stronger clamping as the workpiece tends to be lifted from the table due to the upward cutting forces (Shaw & Cookson, 2005)

On the other hand, in climb milling, the cutter rotates in the same direction as the feed of the workpiece. The cutter teeth engage the material at the top of the cut and remove the material downward. The cutting force pushes the workpiece downward and into the fixture, providing better support and reducing vibrations and chatter. It starts cutting at a maximum chip thickness and decreases to zero. This generally results in lower friction and heat generation, reducing tool wear. It also provides a better surface finish due to the cleaner shearing action of the tool and reduced tool deflection and requires less clamping force because the downward cutting force helps to stabilise the workpiece (Shaw & Cookson, 2005).

Conventional milling is often used for machining cast surfaces, roughing operations, and when a machine or workpiece setup is not rigid enough for climb milling. While climb milling is preferred for finishing operations, precision machining, and when the machine and setup are rigid enough to handle the cutting forces.

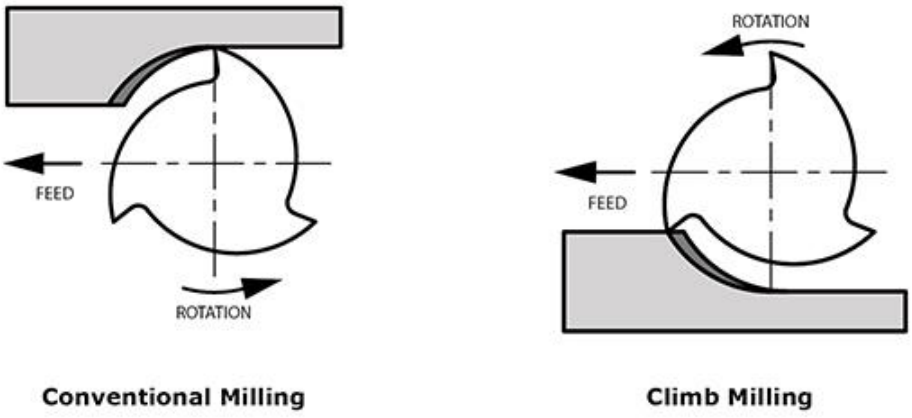

Fig. 11 Conventional milling versus climb milling, where feed and rotation are illustrated to better understand the cutting strategy.

3.2 Milling Concepts

Mastering these basic milling concepts is crucial for optimising machining operations, ensuring high-quality results, and maximising tool life. Proper selection and adjustment of cutting parameters, along with a thorough understanding of the material properties and machine capabilities, are essential for successful milling.

3.2.1 Cutting speed (Vc)

Cutting speed is the speed at which the cutting edge of the tool moves relative to the workpiece. It is typically measured in meters per minute (m/min). The important aspects of speed are the diameter of the end mill (D) in millimetres and the spindle speed (N) in rpm, and it can be determined via equation (1). (Vieira, A. C. (2021). Aula 05 – Manufatura subtrativa Notas de Aulas 2021 [PowerPoint slides]. Unpublished classroom notes)

$$Vc = \frac{\pi \times D \times N}{1000} \qquad (1)$$

Proper cutting speed is essential to ensure tool longevity and optimal surface finish. A too high cutting speed can cause excessive tool wear and thermal damage to the workpiece, while a too low a speed can lead to inefficient material removal and poor surface quality (Burek et al., 2019).

3.2.2 Spindle speed (N)

Spindle speed refers to the rotational speed of the spindle and the attached cutting tool, measured in revolutions per minute (rpm), whenever speed is mentioned in the milling context, it is always associated with the spindle speed, it's easy to mistake with cutting speed. Equation 2 defines speed:

$$N = \frac{Vc \times 1000}{\pi \times D} \qquad (2)$$

Setting the correct spindle speed is critical for balancing the cutting forces and heat generation during milling (Maiyar et al., 2013).

3.2.3 Feed rate (F)

The feed rate is the distance the tool advances along the workpiece per revolution of the spindle. It is measured in millimetres per minute (mm/min). The feed rate affects the cutting force, surface finish, and tool wear. An optimal feed rate ensures efficient material removal and prolongs tool life. Equation 3 describes feed rate, where f_z represents feed per tooth in mm/tooth and Z the number of teeth on the end mill (Vieira, A. C. (2021). Aula 05 – Manufatura subtrativa Notas de Aulas 2021 [PowerPoint slides]. Unpublished classroom notes).

$$F = fz \times Z \times N \qquad (3)$$

3.2.4 Depth of cut (DOC)

Depth of cut refers to the thickness of the material removed in one pass of the cutting tool, measured in millimetres (mm) or inches (in). It can be categorised into axial depth of cut (A_p) and radial depth of cut (A_e). A_p is the depth of cut along the axis of the end mill, and A_e is the depth perpendicular to the axis of the end mill, as the Fig. 12 below shows:

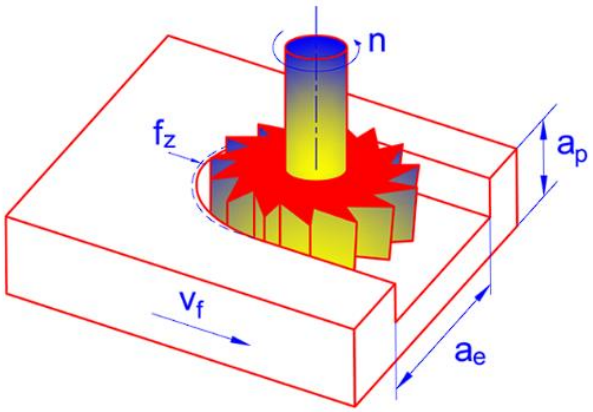

Fig. 12 Visual representation of the DOC parameters (Vieira, A. C. (2021). Aula 05 – Manufatura subtrativa Notas de Aulas 2021 [PowerPoint slides]. Unpublished classroom notes)

3.2.5 Chip Load (fz)

Chip load is the amount of material removed by each tooth of the cutter per revolution, measured in millimetres per tooth (mm/tooth). Proper chip load ensures efficient material removal and prevents tool overload. It also influences the surface finish and heat generation during milling (Vieira, A. C. (2021). Aula 05 – Manufatura subtrativa Notas de Aulas 2021 [PowerPoint slides]. Unpublished classroom notes).

3.2.6 Material removal rate (MRR)

MRR is the volume of material removed per unit of time, measured in cubic millimetres per minute (mm^3/min). MRR is a critical metric for evaluating the efficiency of the milling process. Higher MRR indicates more efficient material removal. Equation 4 describes MMR. (Vieira, A. C. (2021). Aula 05 – Manufatura subtrativa Notas de Aulas 2021 [PowerPoint slides]. Unpublished classroom notes).

$$MRR = Ae \times Ap \times F \quad (4)$$

3.2.7 Feed per tooth (af)

This is the linear distance that a single tooth of the milling cutter travels into the material being cut for each revolution of the cutter. It is typically measured in millimetres (mm). The feed per tooth influences the cutting force, surface finish, and overall machining efficiency. It can be described via equation 5, where n represents the number of teeth in the end mill (Shaw & Cookson, 2005).

$$af = \frac{F}{N \times n} \quad (5)$$

3.2.7 Spindle power and torque (P, T)

Spindle power refers to the amount of power that a spindle motor can deliver to perform machining operations. It is typically measured in watts (W) or kilowatts (kW). The spindle power determines the capability of the machine to perform work, such as cutting, drilling, or milling materials. Torque is the rotational force that the spindle motor generates to turn the cutting tool. It is typically measured in Newton meters (Nm). Torque is a critical factor in determining the machine's ability to maintain a consistent cutting force, especially at lower spindle speeds.

Both parameters are crucial as they determine the maximum amount of force that can be applied by the tool to remove material without stalling or overloading the machine.

$$P = \frac{Ae \times Ap \times Kc \times F}{6 \times 10^7 \times n} \quad (6) \; ; \; T = \frac{F_c \times D}{2} \quad (7)$$

3.3 Forces Acting on Milling Machines

Understanding the forces that act on milling machines is fundamental to the design, operation, and optimization of these critical manufacturing tools. In milling operations, the interaction between the cutting tool and the workpiece generates complex forces that must be carefully managed to ensure precision, efficiency, and tool longevity. These forces can be broadly categorised into cutting forces and static forces, each playing a unique role in the machining process.

3.3.1 Cutting Forces

Cutting forces arise directly from the material removal process and are influenced by various factors such as tool geometry, material properties of both the tool and the workpiece, cutting parameters, and the type of milling operation being performed. These forces are crucial in determining the power requirements of the machine, the potential for tool deflection, and the quality of the finished product (Koenigsberger & Tlusty, 2016).

The total cutting force (Fc) in milling operations can be approximated using empirical formulas and depends on specific cutting forces and cutting power. A general form of the cutting force equation (8) is:

$$Fc = \frac{P}{V_c} \quad (8)$$

Where P is the spindle power (depends on its speed). The total cutting force can be divided into three main components: axial, radial, and tangential forces. Each element plays a distinct role in the machining process:

3.3.2 Axial Force (Fa):

This force acts parallel to the axis of the tool and is responsible for the penetration of the tool into the workpiece. It mostly affects the DOC and the load on the spindle bearings. Proper management of axial force is crucial to avoid excessive tool deflection and maintain dimensional accuracy (Koenigsberger & Tlusty, 2016). This force is extremely complex to determine, many scientific articles develop complex algorithms according to their specific endmill geometry and workpiece to get an estimate of this value. This paper will take into consideration the following hypothesis: The cutting force is the maximum force the spindle is able to sustain before stalling or overloading, so the axial force will never be bigger than the cutting force. For this reason, the largest value axial force can be assumed is the cutting force: Fc=Fa.

3.3.3 Radial Force (Fr):

This force acts perpendicular to the axis of the tool and contributes to the sideways movement of the tool. It influences the stability of the tool and the machine's structural integrity. High radial forces can lead to vibrations and chatter, which negatively impact surface finish and tool life (Koenigsberger & Tlusty, 2016). This force can be calculated via equation (9):

$$F_r = F_c \times \cos(\lambda) \quad (9)$$

Where λ represents the angle of the endmill on the XY plane. The radial force can be broken down into the force on the X-axis (Fx) and the force on the Y-axis (Fy), but similar to the axial force, this is a very complex and demanding work. Nonetheless, both Fx and Fy can have the same value as the cutting force, when the right angle is observed, for this reason, both Fx and Fy will be considered to have the same value as the cutting force.

3.3.4 Tangential Force (Ft):

This force acts tangentially to the cutting edge of the tool and is primarily responsible for the material removal process. It determines the cutting power required and the heat generated during machining. The tangential force is the same as the cutting force (Koenigsberger & Tlusty, 2016). This force can be calculated via equation (10):

$$F_t = F_c \quad (10)$$

It's important to note that these equations describe the basic theoretical force values, they do not account for vibrations, tool deflection, heat generation, etc... To accurately account for these parameters advanced models and simulations need to be used.

3.3.5 Factors Influencing Cutting Forces

Several factors influence the magnitude and direction of cutting forces in a milling operation, like tool geometry, workpiece material, cutting parameters and tool wear. Tool geometry refers to the shape and design of the cutting tool, including rake angle, clearance angle, and cutting edge radius. The material properties of the workpiece, such as hardness, toughness, and thermal conductivity, affect the resistance to cutting. For instance, harder materials generally produce higher cutting forces, requiring more robust tooling and machine rigidity. On the other hand, the parameters defined by the user, like cutting speed, feed rate, and depth of cut are critical in determining cutting forces. For example, higher cutting speeds can reduce cutting forces but may increase the thermal load, while higher feed rates and depths of cut typically increase cutting forces. Lastly the cutting tool condition, wear is crucial for cutting forces, these tend to increase due to the deterioration of the cutting edge. Monitoring tool wear and implementing timely tool changes are essential to maintain optimal cutting conditions.

Understanding and managing cutting forces are fundamental to the success of CNC milling operations. By considering the components of cutting forces, the factors influencing them, and the methods for measuring and analysing these forces, is possible to achieve higher precision, improved efficiency, and extended tool life (Wang et al., 2014).

3.3.6 Static Forces

Static forces, on the other hand, are primarily concerned with the structural integrity and stability of the milling machine. These include the weight of the machine components, the forces exerted by clamping mechanisms, and other loads that impact the machine's ability to maintain precise alignment and positioning during operation. While operating, the cutting forces cause deflection in the machine structure, this deflection can alter the cutting conditions, leading to changes in the cutting forces themselves. This feedback loop can amplify inaccuracies if not properly managed. Many components of the motion system need to be carefully thought out and dimensioned for such a machine, as they handle most forces and directly impact the production results (Cheng et al., 2014).

4. Product development

4.1 Machine specifications

The Rat Rig Mill will be designed to have a work area of 340mm in the X-axis, 160mm in the Y-axis, and a minimum of 100mm in the Z-axis. The machine will feature a modular setup, enabling users to modify it according to their specific requirements. Additionally, it will be engineered for ease of assembly and setup. It will be capable of cutting a wide range of materials, including softwoods, hardwoods, acrylic, polycarbonate, and aluminium. It will be equipped with the 2.2KW spindle sold by Rat Rig, a powerful and cheap alternative for any CNC machine at 5.3 kg. This

spindle features a constant speed regulator, capable of maintaining the router speed regardless of the resistance from the workpiece, as well as an active water cooling system. It has an electronic speed input dial, ranging from 6000 to 24000 RPM. This spindle can handle tools from 1mm to 13mm in diameter, although it only comes with every standard-size collet. The Rat Rig Mill must achieve a precision of at least 0.1mm, setting a cutting error of 0.05mm, as these values are the standard of the lower-cost milling industries. To machine aluminium, manufacturers advise a 1 flute flat endmill, since the equipped router comes with the largest collet of 13mm, all calculations and tests will be done with a 13mm 1 flute flat endmill. Even though some parameters were defined above, many more variables need to be set for the next steps, such as Ap, N and F. The forces to which the mill is subject, are defined by Fc. Table 2 reflects all the requirements set above for this project.

Parameter	Endmill	Speed	Max Spindle Power	Spindle weight	D
Unit	-	RPM	W	Kg	mm
value	13mm 1 flute	6000-24000	2200	5.3	13

Table 1. Machine requirements for the mill project.

With the values present in the above table and the spindle Power/Torque curve, we can easily determine the maximum forces to which the machine will be subject, in equation 11.

$$F_c = \frac{P}{V_c} \times 60 = \frac{P \times 1000 \times 60}{\pi \times D \times N} = \frac{P \times 60000}{\pi \times D \times N} \quad (11)$$

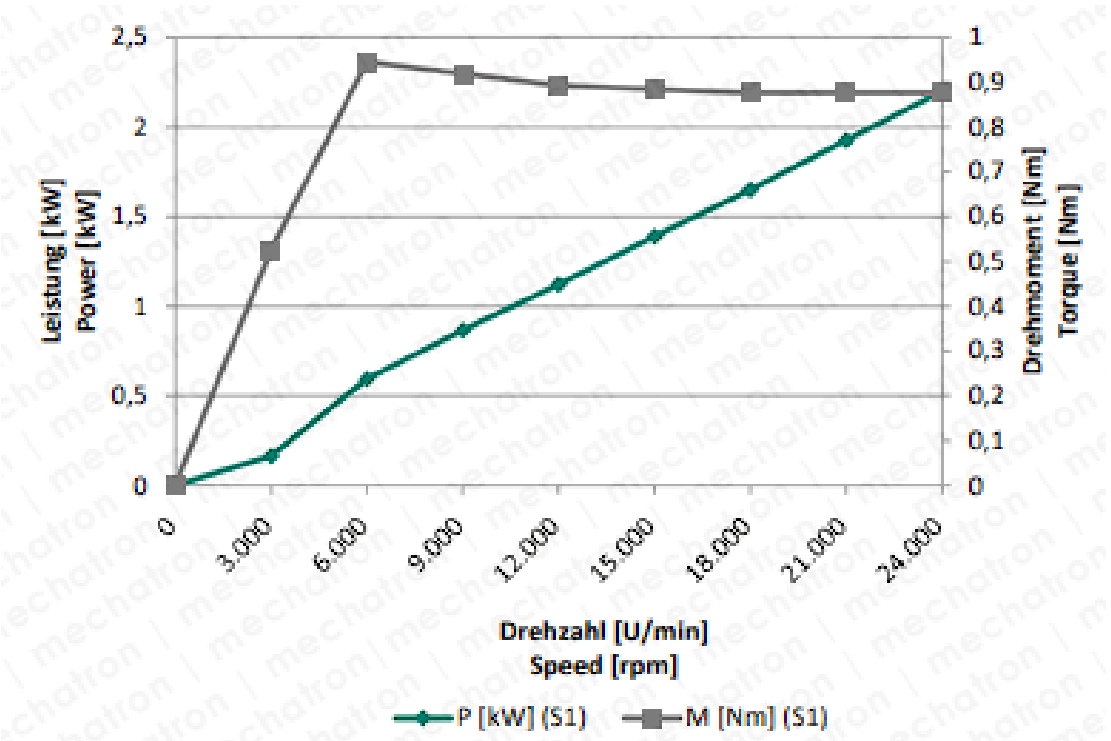

Fig. 13 Spindle power[KW] and torque[Nm] curve versus speed [RPM], provided by the spindle manufacturer.

By analysing the Spindle power and Torque versus Speed we are able to determine the remaining parameters for both ends of the spindle speed range:

If N=6000RPM, then it has approximately 0,6KW of power and the maximum torque available is approximately 0,97 Nm, which is equivalent to the spindle's maximum torque. Calculating the maximum total cutting force and required torque, in equation 12 and 13 respectively:

$$F_c = \frac{P \times 60000}{\pi \times D \times N} = \frac{600 \times 60000}{\pi \times 13 \times 6000} = 146\ N \quad (12)$$

$$T = \frac{F_c \times D}{2} = \frac{146 \times 0{,}013}{2} = 0{,}95\ Nm \quad (13)$$

If N=24000RPM, then it has approximately 2,2 KW of power and the maximum torque available is approximately 0,95 Nm. Calculating the maximum total cutting force and required torque, in equation 14 and 15 respectively:

$$F_c = \frac{P \times 60000}{\pi \times D \times N} = \frac{2200 \times 60000}{\pi \times 13 \times 24000} = 134\ N \quad (14)$$

$$T = \frac{F_c \times D}{2} = \frac{134 \times 0{,}013}{2} = 0{,}85\ Nm \quad (15)$$

After verifying at which settings the spindle is able to achieve it's highest cutting power and still meet the required torque, the machine will be projected to take maximum advantage of its cutting power at 24000RPM and 134,669N of cutting force.

4.2 Material selection

The material selection for this project is based on Rat Rig's modular build style and stock inventory.

4.2.1 Structural frame

The Mill aims to be a premium DIY kit at a friendly price point. Most Rat Rig DIY kits have an aluminium extrusion frame, these extrusions are made out of 6060-T5 aluminium. This aluminium offers an excellent balance of strength and ductility. It has a moderate tensile strength (about 170-220 MPa) and yield strength (about 110-160 MPa), making it suitable for many structural applications. Adding a T5 tempering process increases the hardness and mechanical strength of the alloy, enhancing its durability. It also has a thin, protective oxide layer when exposed to air, which helps prevent corrosion. Rat Rig offers the extrusion anodized in black for a better look as Fig. 14 shows. The 6060-T5 is easy to machine, making it ideal for parts that require precision machining, this is a big advantage since all extrusions are cut at the Rat Rig headquarters, offering a cut precision of up to +/- 0.25mm. While it's not the cheapest material, 6060-T5 offers a good balance of cost and performance, making it a cost-effective option for many applications requiring moderate strength and good corrosion resistance, allowing the company to still offer good price points at premium quality. Lastly, this alloy is fully recyclable without losing its properties, making it a sustainable choice in an era of increasing environmental awareness.

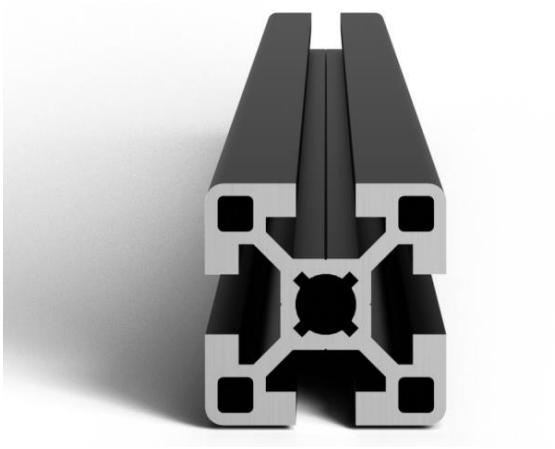

Fig. 14 4040 T-Slot profile, anodized black, by Rat Rig (Rat Rig, n.d.)

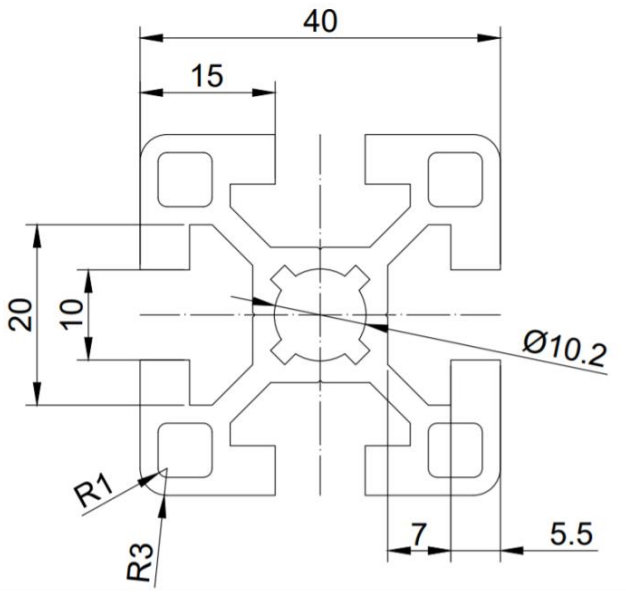

Fig. 15 4040 T-Slot extrusion profile, by Rat Rig (Rat Rig, n.d.)

The aluminium is extruded as a T-slot extrusion, as shown in Fig. 15. These are a type of structural aluminium profile designed with longitudinal T-shaped slots that run along the length of the extrusion. These slots allow for the easy attachment of connectors, brackets, and other hardware, facilitating the creation of modular and adjustable frameworks. They provide an excellent balance between modularity and structural integrity. They are highly suitable for a wide range of applications, from light-duty frames and workstations to more demanding applications like machine frames and 3D printers. Proper design and assembly techniques are key to maximising their potential and ensuring that they meet the application's specific requirements. The Mill will use these types of profiles for the structure. There are numerous variations of the 4040 T-Slot extrusion profiles. By placing the same pattern side by side, one can effortlessly create a 4080 T-Slot extrusion profile. This pattern can be further extended to achieve a 40120 T-Slot or even a 40160 T-Slot extrusion profile, as illustrated in Fig. 16.

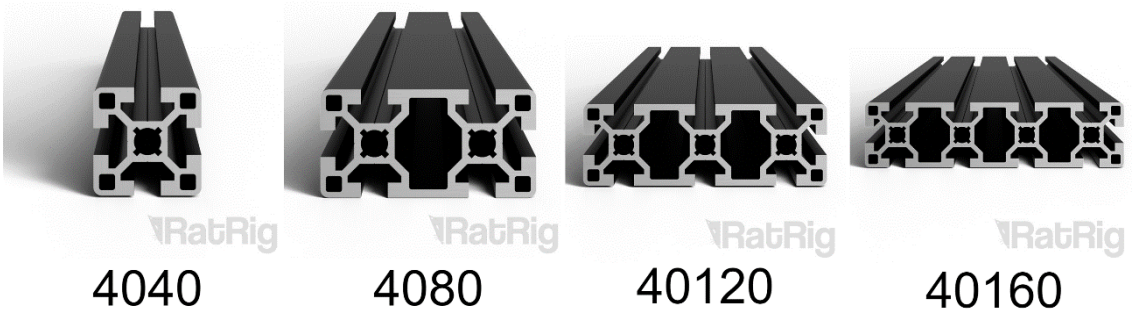

Fig. 16 Rat Rig 40 series T-Slot extrusion profiles

All axes will be easily resized according to the extrusion lengths. The Mill frame will be based on the Openbuilds mini mill machine concept, using a 40120 T-slot extrusion for the Y and Z axis

numbered 1 and 5 respectively in Fig. 17, the X axis will use a 40160 extrusion(2) to provide the mill with a wide work area in the Y axis (160mm as set in the machine specifications), and two 4080 extrusions(3) for the Z tower, lastly there will be two 40120 extrusions(4) to give the spindle enough clearance when moving the Y axis. This frame is a concept, all extrusions can be later modified if needed. Fig. 18 helps visualise the 3 moving axes in the frame.

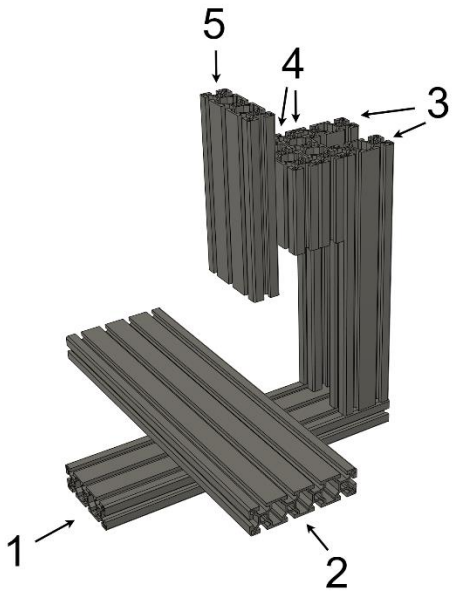

Fig. 17 Mill extrusion frame. 1- Y-axis extrusion; 2- X axis extrusion; 3- Z tower extrusions; 4- Z tower extension extrusions; 5- Z-axis extrusion.

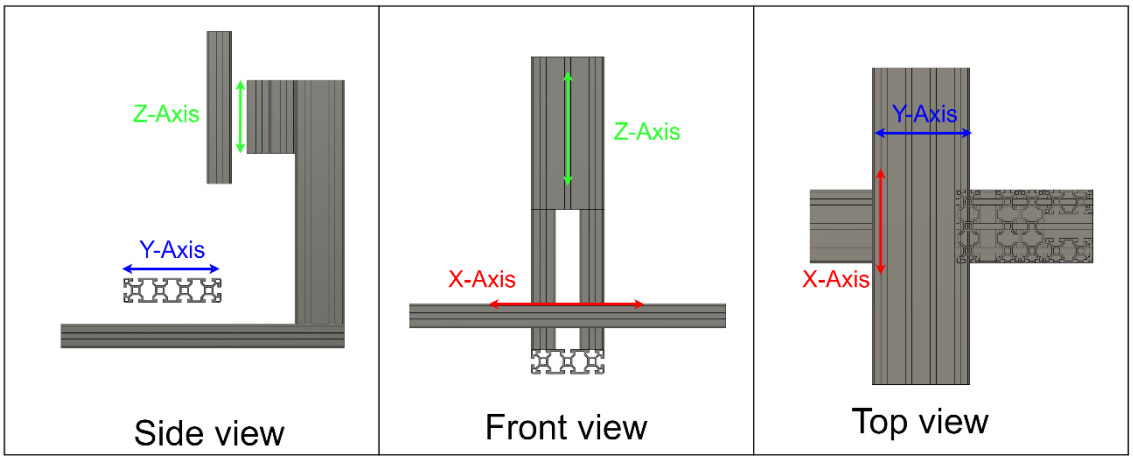

Fig. 18 Mill frame mock-up, first concept using T-Slot extrusions, side, front and top view along with the axis's directions.

T-Slot alone isn't enough to make a machine structure, mounting hardware is required like screws, t-nuts and joining plates. Rat Rig mostly uses 6061-T6 aluminium for the joining plates, this alloy is one of the most versatile and widely used in the industry. It is known for its excellent mechanical properties, good weldability, and high corrosion resistance. The T6 temper indicates that the alloy has been solution heat-treated and artificially aged to achieve its desired mechanical properties. It has a tensile strength of approximately 290 MPa and a Yield strength of

approximately 240 MPa. It also has excellent corrosion resistance when exposed to atmospheric conditions, making it less prone to stress corrosion cracking compared to other high-strength aluminium alloys. 6061-T6 has good machinability, allowing it to be easily cut, drilled, and milled, which is essential for Rat Rig to make custom features for each machine structure. Another great selling point is the fact that it can be anodized to improve corrosion resistance and wear resistance, as well as to add aesthetic finishes. Wear resistance is crucial since this will be a DIY kit and users are prone to scratching the plates while assembling the kit. Lastly, this aluminium is fully recyclable without losing its properties, making it an environmentally friendly material. While this alloy isn't the cheapest, especially when compared to steel that offers exceptional mechanical properties for a machine such as the Mill, it has many benefits stated above that make it an obvious choice over regular grade steel. Having the T-Slot extrusions and the joining plates, we fasteners to complete the assembly. Rat Rig has a variety of fasteners to choose from Fig. 19, all the way from cap head screws, low head screws, countersink screws, button head screws, set screws, t-nuts, nylon locking nuts, just to name a few.

Fig. 19 Fasteners from the Rat Rig CAD repository 1- Cap Head screw, 2- Button head screw, 3 - Low head screw, 4 - Countersink screw, 5 - Nylon locking nut, 6 - Set screw, 7 - Drop-in T-nut, 8 – Washer

All screws are made from 12.9 grade steel due to the specific mechanical properties and performance characteristics required for high-strength applications. These fasteners have a minimum tensile strength of 1,200 MPa, which means they can withstand very high levels of stress without breaking, this is mandatory to ensure they handle the required torque for structural stability. Since Rat Rig sells DIY kits, fasteners are prone to repeated use, since the user might assemble the kit incorrectly and need to disassemble and re-assemble it all, 12.9 grade steel offers superior fatigue resistance, reducing the risk of failure over time. Unfortunately, 12.9 grade steel isn't the best at handling corrosion when exposed to atmospheric environments. To prevent rust, Rat Rig usually supplies all screws with a thin oil coat, providing some extra protection during shipping.

The assembly will require mounting plates for all axes and interconnecting them. These plates will be mounted to the linear rails and extrusions of the machine, the main objectives for these plates are ease of assembly, alignment flexibility and rigidity. Ease of assembly means the plates

must be intuitive to orient and not require any major assembly dependencies, for example, the Milo1.5 previously introduced in this document requires the user to remove the linear rail carriages from the linear rails in order to complete the assembly, this is a major downside as the user can easily loose the bearing balls inside the carriage while removing them, making the linear rails useless. There are ways to avoid this simple user/assembly mistake, nonetheless, the goal should always be to keep the assembly as simple as possible and remove mistake opportunities. These interfacing plates will be a crucial point of alignment for the machine's squareness and tramming, the user must be able to easily adjust these factors in a matter of minutes. Lastly, these plates must provide a solid and rigid mounting surface for all axes. Rat Rig mostly uses 6mm thick 6061-T6 for machined plates, leading this project to prioritize this aluminium variant first. If there cannot be a compromise between the plate's objectives above with this alloy, we will need to dive deeper into material alternatives. Starting with the XY plates, the X extrusion is a 40160 T-Slot extrusion while the Y extrusion is a 40120 T-Slot extrusion, resulting in a non-square interface between them, as Fig. 20 demonstrates.

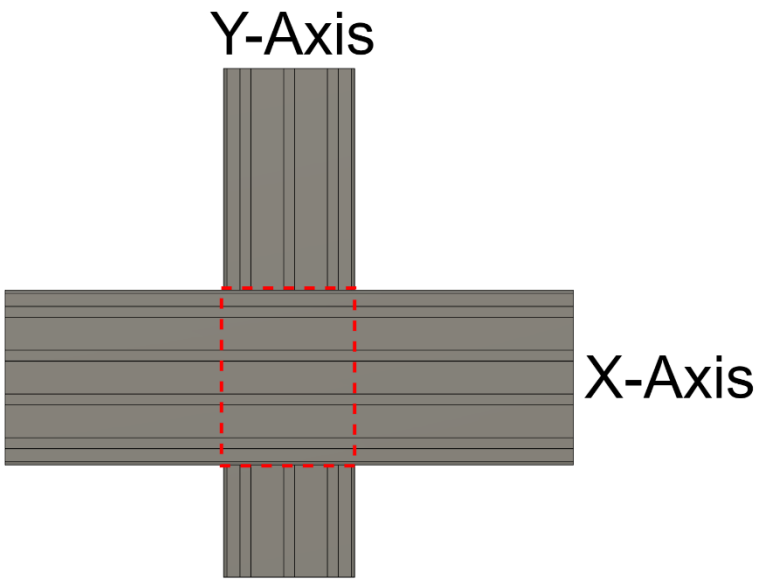

Fig. 20 XY T-Slot extrusion interface surface, non-square shape

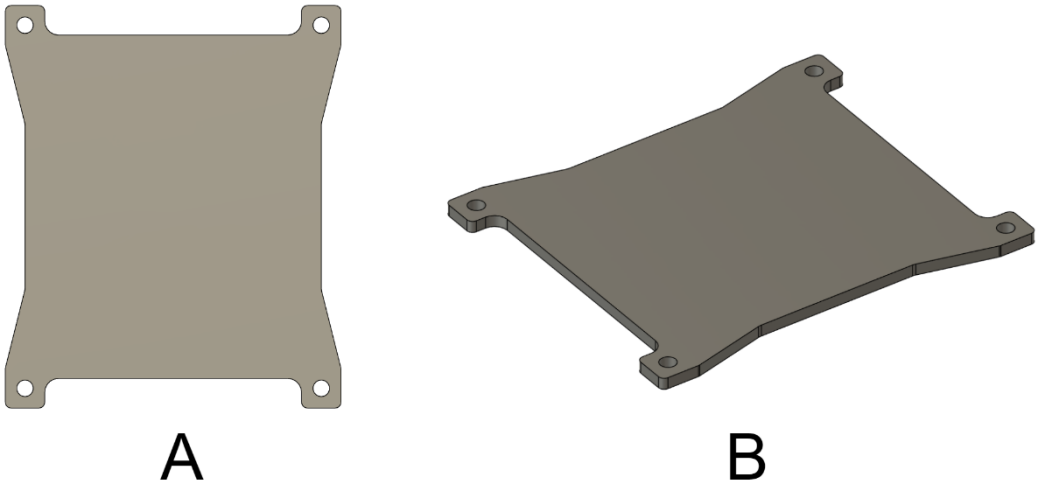

Fig. 21 First XY plate concept, 6mm thick 6061-T6 aluminium, with four mounting points to connect them together.

Fig. 21 illustrates the first concept of the XY plates, having 4 holes one on each corner allows the user to easily insert a screw from the top and use a hex nut along with a wrench to secure the assembly. These holes must not interfere with the T-Slot extrusions, meaning the extrusions cannot restrict access to said fasteners at any time, this is accomplished by positioning the joining screws as Fig. 22 shows:

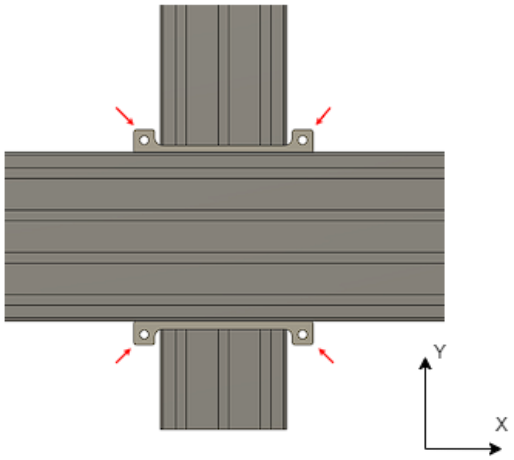

Fig. 22 XY joining plate and joining fasteners location, showing how these are never covered by the T-Slot extrusions.

The interface between the Z axis and the Mill frame will be similar to the XY plates, except that it will connect a moving axis to the frame instead of two moving axis together. Fig. 23 enlightens how the first concept was born, keeping the same principle of always having the joining fasteners accessible at all times.

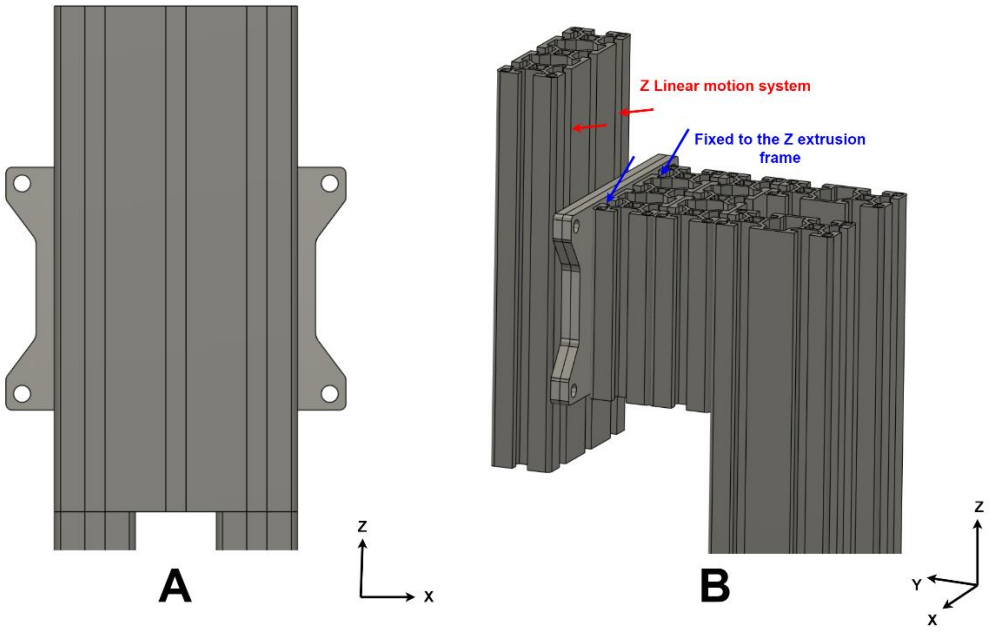

Fig. 23 A- Front view of the machine concept, showing the accessibility to the four corner mounting fasteners. B - Rear right view of the machine, demonstrating how the two plates will be independently assembled to the frame and Z-axis and later interconnected.

The large empty faces on the plates will allow for greater flexibility when choosing the linear motion hardware, as hole patterns can be easily iterated.

The frame Z tower will be assembled using two large Z tower plates, using the same 6mm thick 6061-T6 aluminium. Fig. 24 shows the development of the Z tower plate, starting from the first shape sketch (A) then the first model (B) and lastly the side plate on the frame (C) , with mounting holes. The mounting holes were spaced 40mm in the plane, this spacing was decided based on the 4040 T-Slot pattern, since the extrusion grooves are spaced 40mm, M8 fasteners were chosen mostly based on looks, to hopefully give it a robust and “tank” like feel, we will later determine all forces and inspect if these fasteners are sufficient to withstand the machine’s requirements. The technical drawing for this plate can be found in the attachments section, Fig. 82.

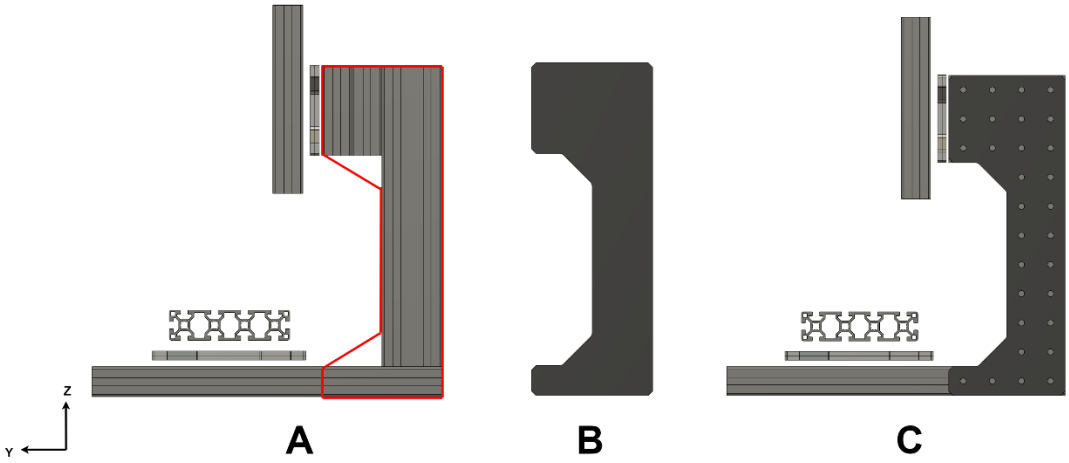

Fig. 24 A- Z tower plate sketch along the current frame iteration; B - First Z tower plate concept; C - Z tower plate filled with 40mm spacing M8 holes for mounting fasteners.

4.2.2 Motion system

The motion system will use a linear motion component along with a transmission system to provide a sturdy and smooth movement.

The selection of the appropriate linear motion system depends on the specific requirements of the application, including forces, moments, speed, precision, cost, and maintenance frequency, since the Mill is an assembly kit, assembly complexity is also heavily taken into account. Linear rails, also known as linear guideways or linear slides, are mechanical components designed to provide smooth and precise linear motion. They consist of a rail and a carriage (or slider) that moves along the rail, usually with the help of rolling elements like balls or rollers.

When selecting the appropriate linear motion device for a specific application, it's crucial to consider several key factors:

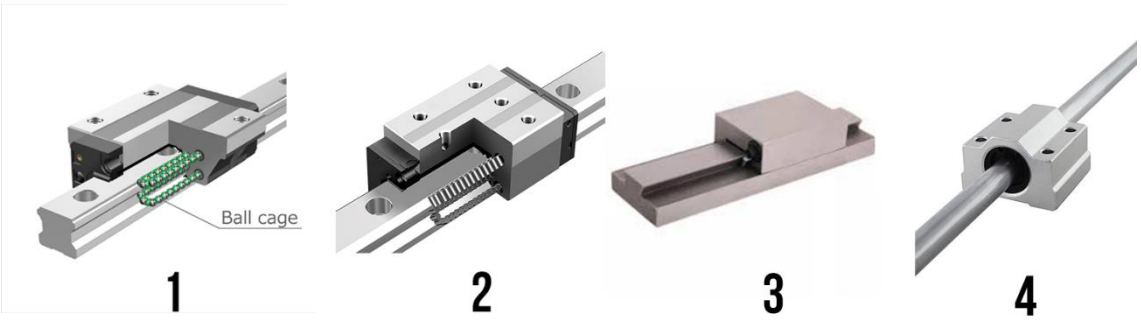

Fig. 25 Examples of the most used linear motion components: 1 - ball bearing linear rail + carriage, 2 - roller bearing linear rail + carriage, 3 - dovetail slides, 4 - linear shaft

The first variant found in Fig. 25 position 1, is a ball-bearing linear rail plus carriage, it consists of a rail with a profiled cross-section and a carriage containing recirculating ball bearings. It provides high precision and load capacity, and low friction, these can be found in 3D printers,

CNC machines and some medical devices. The second variant in Fig. 25 position 2 is very similar but it uses cylindrical rollers instead of balls, these provide a much larger contact interface between the carriage and a rail, resulting in a stiffer assembly capable of handling higher loads. Next in Fig. 25 position 3, a dovetail slicer can be observed, it gets its name from the trapezoidal dovetail shape which provides a smooth and precise movement. This linear motion mechanism relies on the precision and roughness of the contact surfaces, requiring them to be extremely well-maintained to avoid creating and increasing friction. Lastly in position 4, a linear shaft can be observed, these have a better load performance than linear rails due to the larger contact surface in between the bearings, in all axes when compared to the linear rails, but are considerably harder to install and align. Over the years, based on company experience, linear rails have been the best solution for all Rat Rig products, due to their ease of assembly, cost and low volume, allowing for better packaging for the end user, these factors led Rat Rig to stock only linear rails, this paper will focus the research on the different parameters between the variants.

The choice between linear ball bearings, and linear roller bearings, depends on how these factors align with the demands of the machine. Each type of linear rail handles forces differently. Ball-bearing linear rails can handle significant loads in applications requiring smooth, high speed. The rigidity and stiffness of linear motion devices impact their ability to handle moments or torques. Linear roller bearings provide exceptional stiffness, minimising deflection and making them ideal for applications with significant off-centre loads or moments.

Accurately determining the forces acting on a linear rail system with ball-bearing carriages is a complex challenge due to the numerous variables involved and the behaviour of ball bearings under load. The magnitude, direction, and point of application of loads significantly impact the forces experienced by the rail and carriages, as well as all dynamic forces generated during rapid movement that introduce additional loads and affect the distribution of forces. The alignment of the whole assembly is also crucial as even slight misalignments during installation can lead to uneven force distribution, increasing wear and reducing the system's lifespan. The ball bearings within the carriage respond to loads by deforming slightly, which changes the contact points between the balls and the linear rails. Ideally, the load is distributed evenly across all the balls, but in reality, due to manufacturing tolerances, misalignments, or uneven loading, some balls may carry more load than others. This uneven load distribution can lead to premature wear or failure of the bearings. The forces on individual balls are also influenced by the rigidity of the rail and carriage, the quality of the lubrication, and the precision of the ball tracks. Given these complexities, the most reliable method for selecting an appropriate linear rail system is to utilise the manufacturer's datasheet and online calculation tools. These resources incorporate empirical data, material properties, and sophisticated algorithms to help predict system behaviour under various conditions. They account for the many variables and help ensure that the system will perform reliably. Using the Hiwin online calculator tool (Hiwin, n.d.), the user is met with an initial page to select the kinematics combination as shown in Fig. 26. This can vary from a single rail with a single carriage to a double rail with one or multiple carriages. The mill will use a combination of double rails with two carriages in each rail, for all axis. This setup provides more flexibility in the assembly and design of components, as various mills on the market have proven.

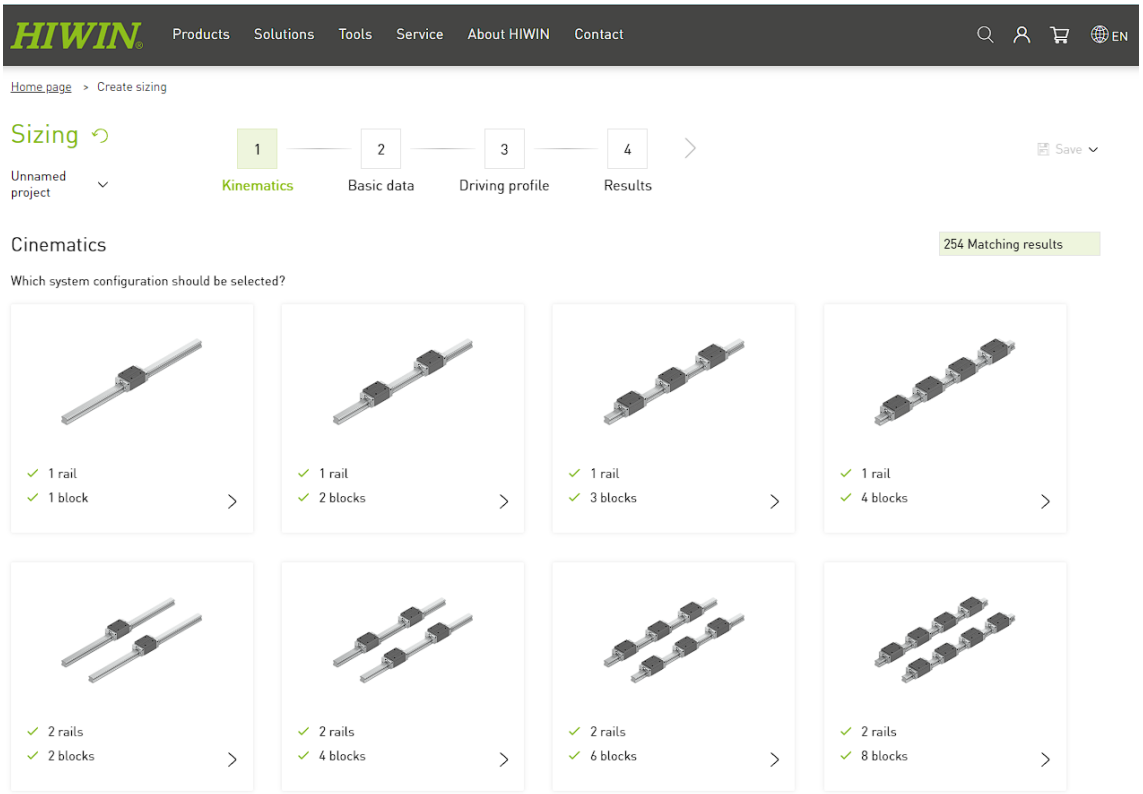

Fig. 26 Hiwin online calculator tool- Step 1 Selecting the kinematics

After selecting the kinematics model, the engineer must insert all the basic data shown in Fig. 27 such as Stroke length referring to the maximum travel distance of the system, Rail distance referring to the total length of the linear rails, and the angle of the rails in space A and B, used to reference the coordinates of the system, following with the Block distance or carriage distance, set by the mounting plate, rail- drive distance which represents the distance from the top of the linear rail carriages to the lead screw centre in the Z-axis and the Y-axis. After all the compulsory details are inserted, the moving masses must be prompted, and their offsets in space. Next, all forces are required, these fields will accommodate the maximum cutting forces to which the mill is subject when machining. Lastly, HIWIN asks if the project has a product and block type preference, for a

company such as Rat Rig this means selecting the most used and stocked linear rails, to hopefully get a better cost opportunity.

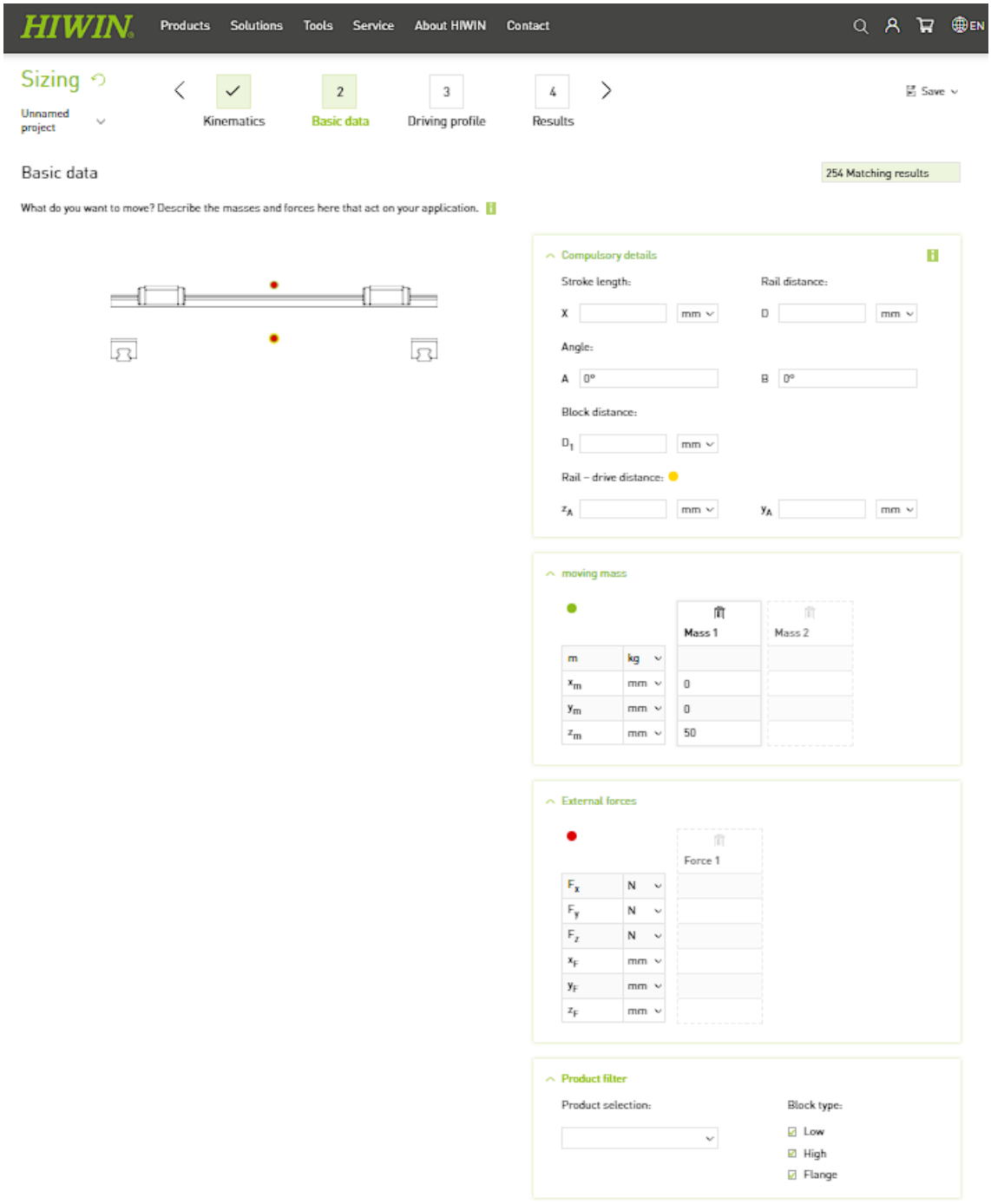

Fig. 27 Hiwin online calculator tool - Step 2 Basic data prompt

The speed at which a linear motion device can operate is critical in many applications. Linear roller bearings can operate at moderate to high speeds, though not as high as ball bearings due to slightly higher friction. Ball-bearing linear guides are designed for high-speed applications, providing low friction and smooth motion ideal for dynamic systems.

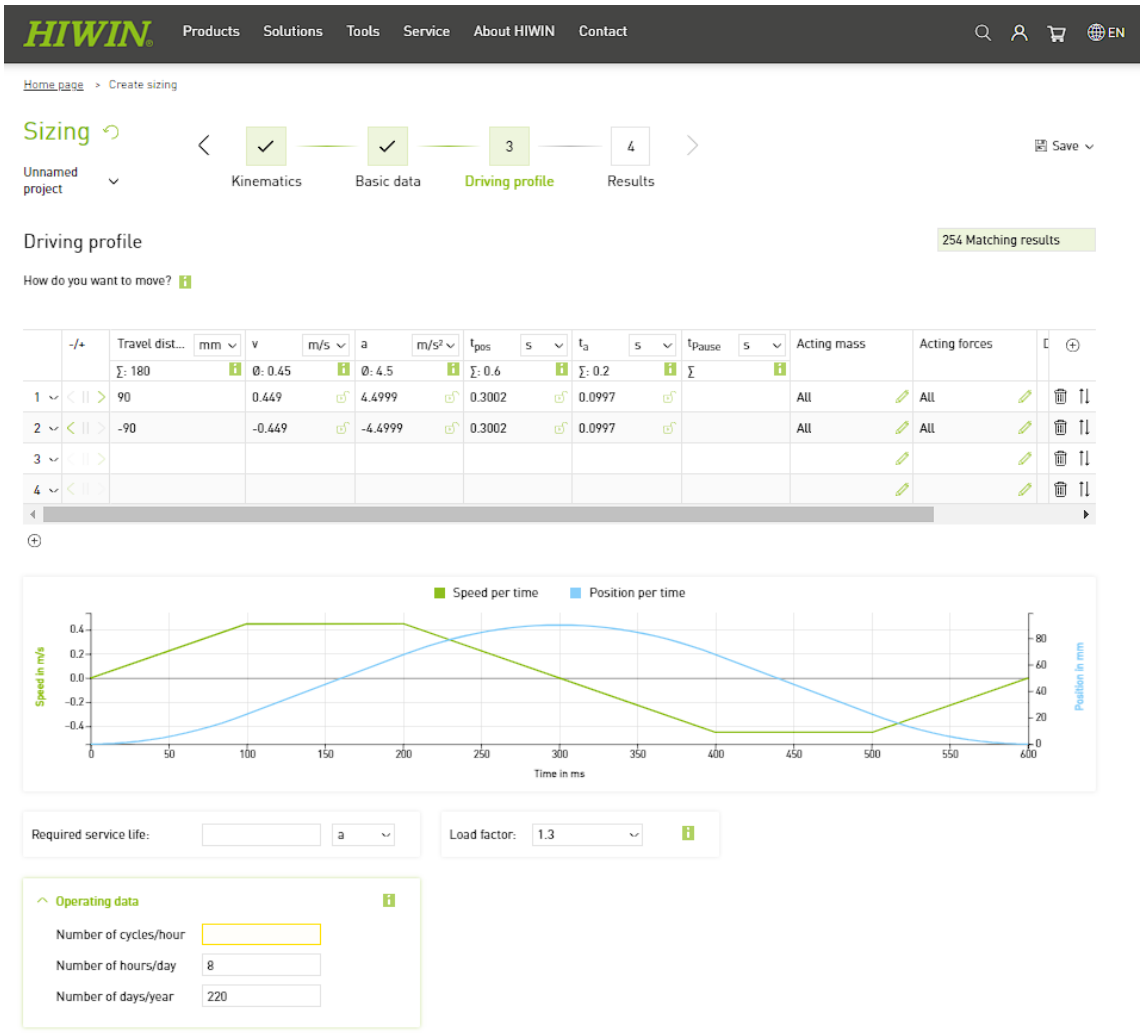

Fig. 28 Hiwin online calculator tool - Step 3 Sizing

Fig. 28 shows what parameters must be taken into consideration when sizing a linear rail, the travel distance, its velocity, acceleration, t_{pos} which refers to the time required for the movement per single travel run, t_a for the time required per single travel run for acceleration and t_{pause} for the pause corresponds to the time in which the system blocks do not move during a single travel run. e.g. wait times. Lastly on the table, the user must input what forces are acting when the axis is moving. A very important factor is the required service life, which can be inputted in kilometres, years or cycles, as well as the load factor, varying from 1 to 3, 1 being for systems with no shock and vibrations, 1,5 for normal load systems, 2 for small shocks and 3 for an assembly subject to vibrations and shocks such as the Mill.

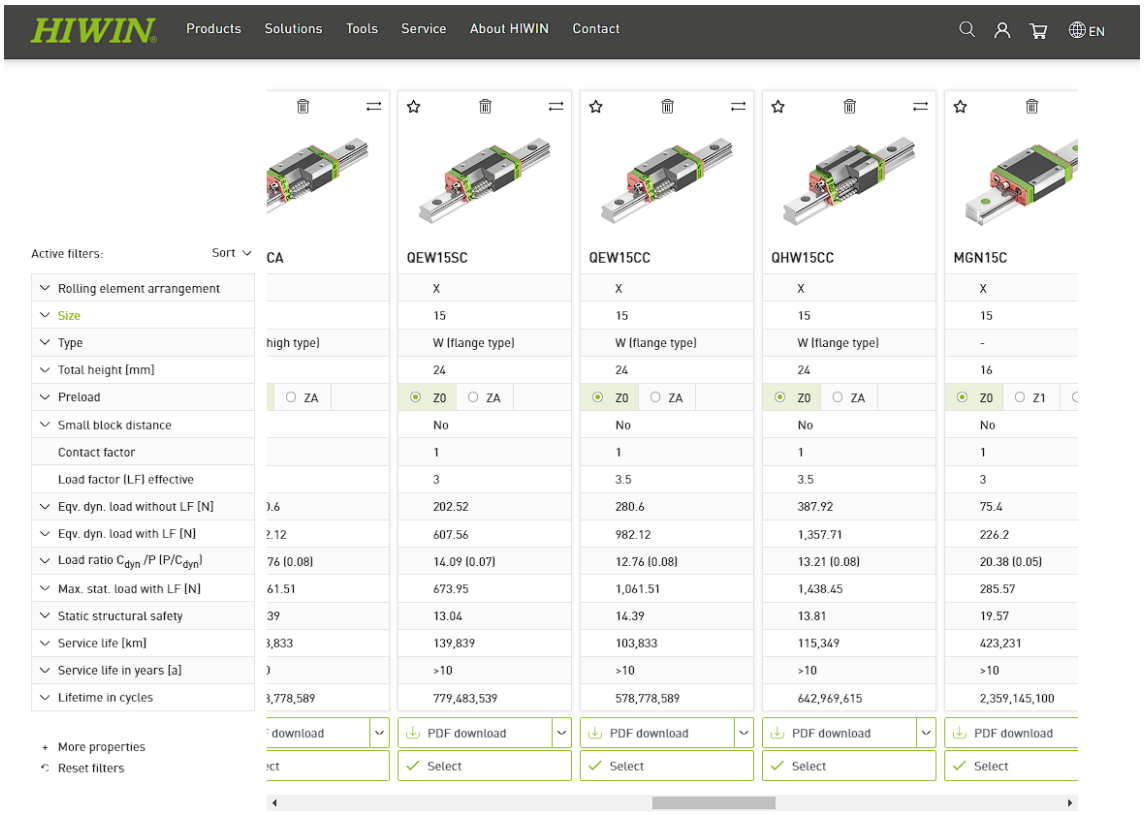

Fig. 29 Hiwin online calculator tool - step 4 Results

In this last step, Hiwin provides a comprehensive list of all their products that can suit the inputted requirements, ranging from the smaller cheaper rails to the more robust and expensive solution, pivoting through all sorts of carriages and mounting solutions. All the details are displayed in the table represented in Fig. 29, like the size of the rail, preload option, contact factor, load factor, dynamic loads with and without the load factor, load ratio, static structural safety and service life.

4.2.2.1 X-Axis and Y-Axis linear rails

The linear rails for the X-axis and Y-axis will be mounted onto the XY plates on the carriages, while the rail bodies will be secured to the extrusions using T-nuts and cap head screws. Selecting the appropriate linear rail model for this assembly may involve a process of trial and error, and multiple iterations may be necessary to achieve a configuration that integrates components such as lead screws and stepper motors. That being said, the initial iteration will use MGN15H rails, as these are currently available from Rat Rig, facilitating prototyping and testing if the parameters below can be verified.

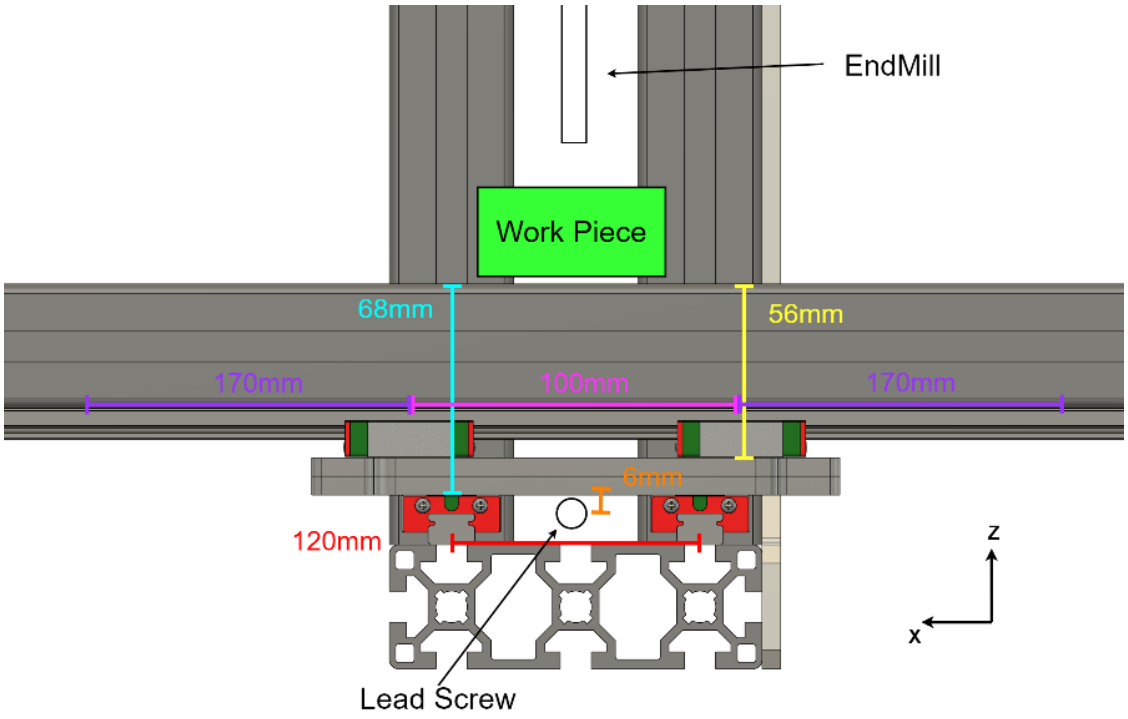

Fig. 30 Front view of the machine, where both X and Y axis are equipped with MNG15H linear rail assemblies. All distances and measurements can be easily identified and prompted into the linear rail configurator tool.

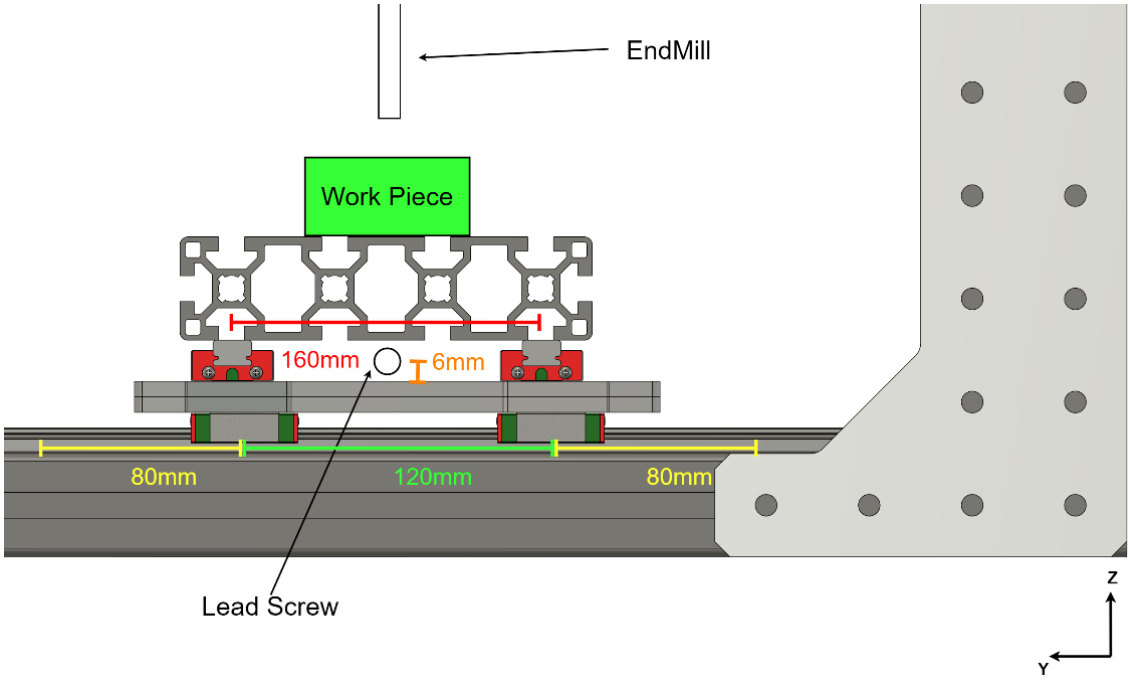

Fig. 31 Side view of the machine, where both X and Y axis are equipped with MNG15H linear rail assemblies. All distances and measurements can be easily identified and prompted into the linear rail configurator tool.

Starting with the Y-axis linear rail, Fig. 30 shows the distance between the two rails (D) as 120mm, defined by the aluminium extrusion slot distance, as well as the rail-to-drive distance (Za), it also shows the distance to the workpiece, this value will be used as the force point of application, more specifically Xf Yf and Zf. These offsets vary greatly with the size of the workpiece and its position

when machining, considering a workpiece with 30mm, we can set Zf as 68+15=83mm, Yf as 0 mm and Xf as 0 mm. The applied cutting force will be in X Y and Z, all with the same magnitude as the total cutting force 134,669N ≈ 135N (for simplicity), as mentioned in chapter 3.3. The total mass carried on these rails is a combination of the X extrusion, estimated at 2970 g in the CAD, X linear rails, estimated at 1000 g each in the CAD and the two 6mm aluminium plates, estimated at 445 g each in the CAD, generating a total weight of 5863 g in total, with the centre of mass 25,81 mm higher than the top of the Y linear rail carriages. Setting Xm and Ym to zero and Zm to 25,81 mm. Looking at Fig. 31 we can extract the rail stroke (X) as 80 mm to each side, so a total of 160mm, and a set carriage distance (D1) of 120 mm.

Variable	X	D	A	B	D1	Za	m	Xm	Ym	Zm	Fx	Fy	Fz	Xf	Yf	Zf
Unit	mm	mm	º	º	mm	mm	Kg	mm	mm	mm	N	N	N	mm	Mm	Mm
Value	80	120	0	0	120	-6	5,86	0	0	25,81	135	135	135	0	0	83

Table 2. Y rail requirements, used in the Hiwin online tool, all measurements were taken in Fig. 30 and Fig. 32.

Using a velocity of 50mm/s and an acceleration of 500mm/s² for the movement limits, the required number of cycles of 200 000 000 and a load factor of 3, the Hiwin online tool gave the results in Fig. 32. A filter for size MGN15 was used to check if the Rat Rig stock was capable of sustaining the application. In fact, both MGN15C and MGN15H are capable of handling the Mill loads, although the MGN15H has double the service life in KM and cycles. For this reason, MGN15H will be used in the Mill Y-axis.

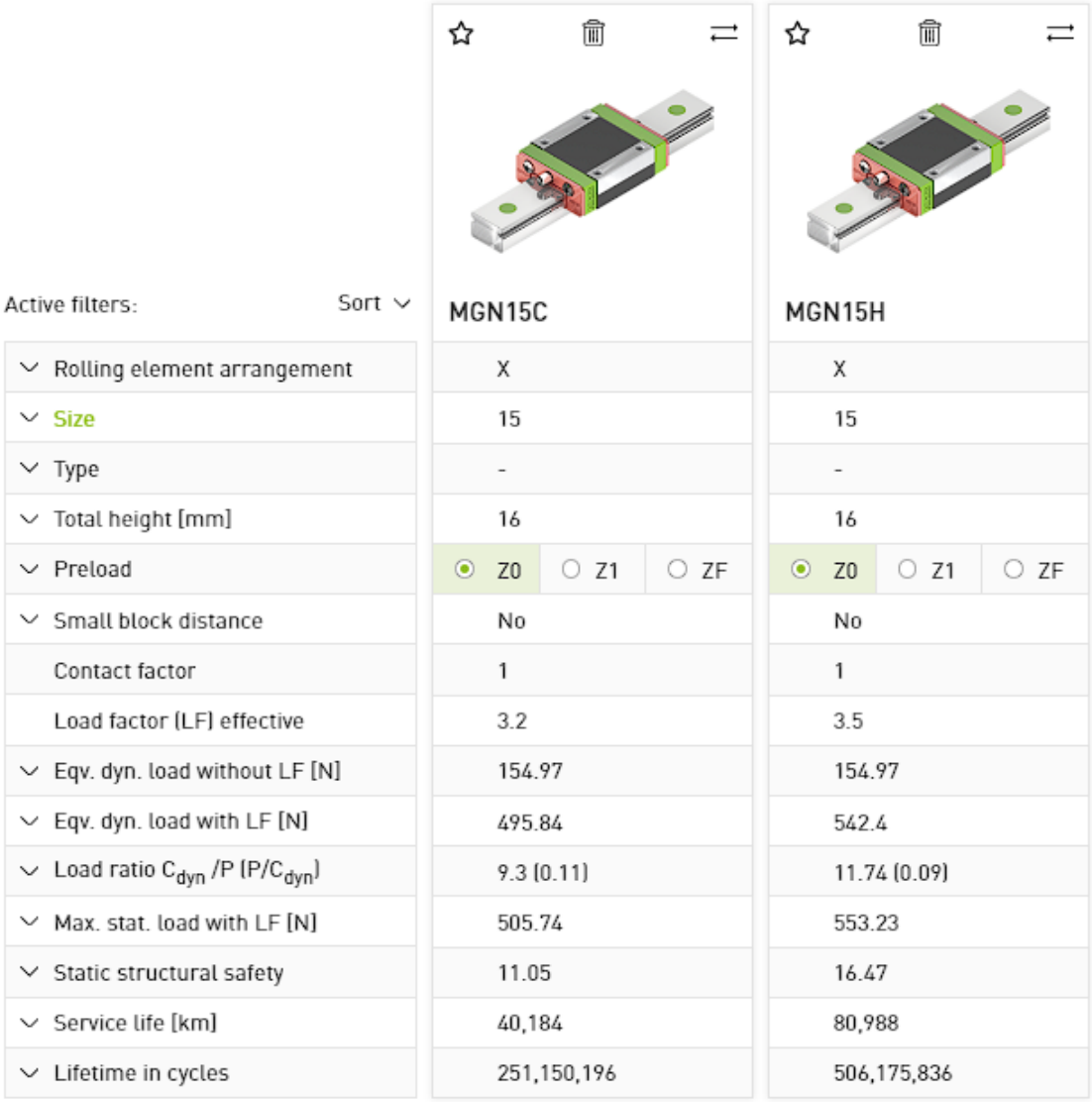

Fig. 32 Hiwin online tool results for the Y rails, according to the prompted data and size 15MGN filter.

Following the same workflow as for the Y linear rails, table 4 represents the input parameters for the X linear rails

Variable	X	D	A	B	D1	Za	m	Xm	Ym	Zm	Fx	Fy	Fz	Xf	Yf	Zf
Unit	mm	mm	º	º	mm	mm	Kg	mm	mm	mm	N	N	N	mm	Mm	Mm
Value	170	160	0	0	100	-6	3.89	0	0	-24.1	135	135	135	0	0	-71

Table 3. X rail requirements, used in the Hiwin online tool, all measurements were taken in Fig. 30 and Fig. 31.

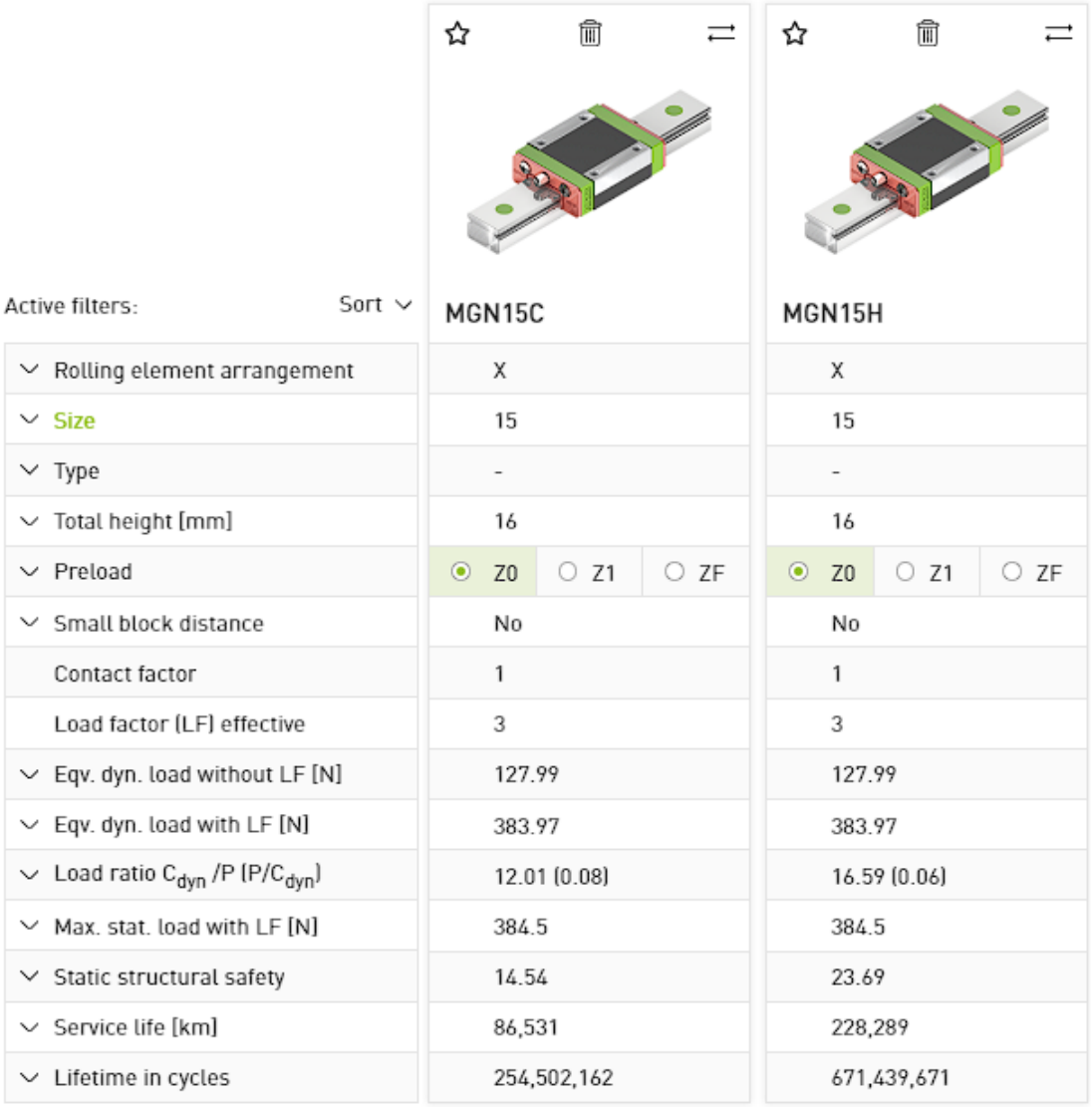

Active filters: Sort	MGN15C	MGN15H
Rolling element arrangement	X	X
Size	15	15
Type	-	-
Total height [mm]	16	16
Preload	Z0 / Z1 / ZF	Z0 / Z1 / ZF
Small block distance	No	No
Contact factor	1	1
Load factor (LF) effective	3	3
Eqv. dyn. load without LF [N]	127.99	127.99
Eqv. dyn. load with LF [N]	383.97	383.97
Load ratio C_{dyn} /P [P/C_{dyn}]	12.01 (0.08)	16.59 (0.06)
Max. stat. load with LF [N]	384.5	384.5
Static structural safety	14.54	23.69
Service life [km]	86,531	228,289
Lifetime in cycles	254,502,162	671,439,671

Fig. 33 Hiwin online tool results for the X rails, according to the prompted data and size 15MGN filter.

Fig. 33 shows the results from the hiwin online tool for the X-axis linear rails, where MGN15H was the chosen candidate, keeping it consistent with the Y rails.

4.2.2.2 Z-Axis linear rails

The Z-axis linear rails will be mounted to the Z plate and the Z-axis extrusion (extrusion nº 5 in Fig. 17) within the T-slots, using t-nuts. As most commonly found on milling machines, a four-carriage configuration will be used, fixating the four carriages to the Z plate and the linear rail body to the extrusions.

Fig. 34 shows the distance between the two rails (D) as 120mm, defined by the aluminium extrusion slot distance, as well as the rail-to-drive distance (Za), it also shows the distance to the workpiece, this value will be used as the force point of application, more specifically Xf at 0mm Yf at 120mm (Fig. 34) and Zf at 271+15=286mm (Fig. 35) These offsets vary greatly with the size of the workpiece and its position when machining, considering a workpiece with 30mm, we can

set Zf as 271+15=286mm (Fig. 35), Yf as 120mm (Fig. 34) and Xf as 0mm. The applied cutting force will be in X Y and Z, all with the same magnitude as the total cutting force 134,669N ≈ 135N (for simplicity), as mentioned in chapter 3.3. The total mass carried on these rails is a combination of the Z extrusion, estimated at 1098 g in the CAD, Z linear rails, estimated at 500 g each in the CAD and the spindle, estimated at 5300 g in the CAD, generating a total weight of 7398 g in total, with the centre of mass 25,81 mm higher than the top of the Y linear rail carriages. Setting Xm and Ym to 29.74mm and Zm to 0mm. Looking at Fig. 35 we can extract the rail stroke (X) as 65 mm to each side, so a total of 130mm, and a set carriage distance (D1) of 80 mm.

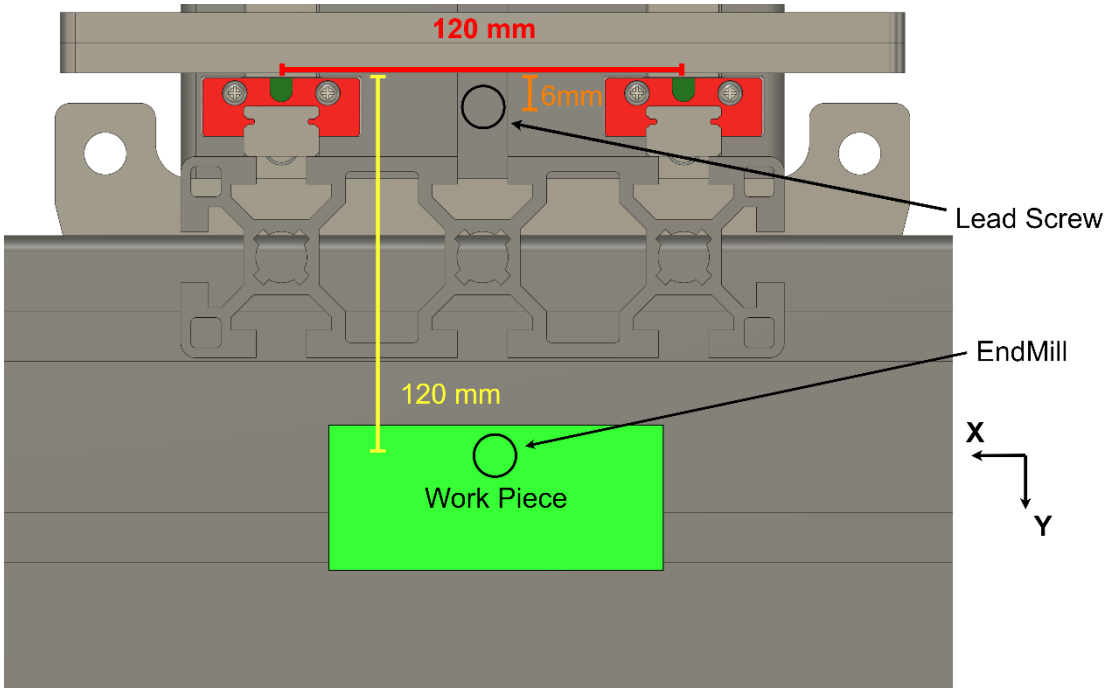

Fig. 34 Z rail top view of the machine, where the axis is equipped with MNG15H linear rail assemblies. All distances and measurements can be easily identified and prompted into the linear rail configurator tool.

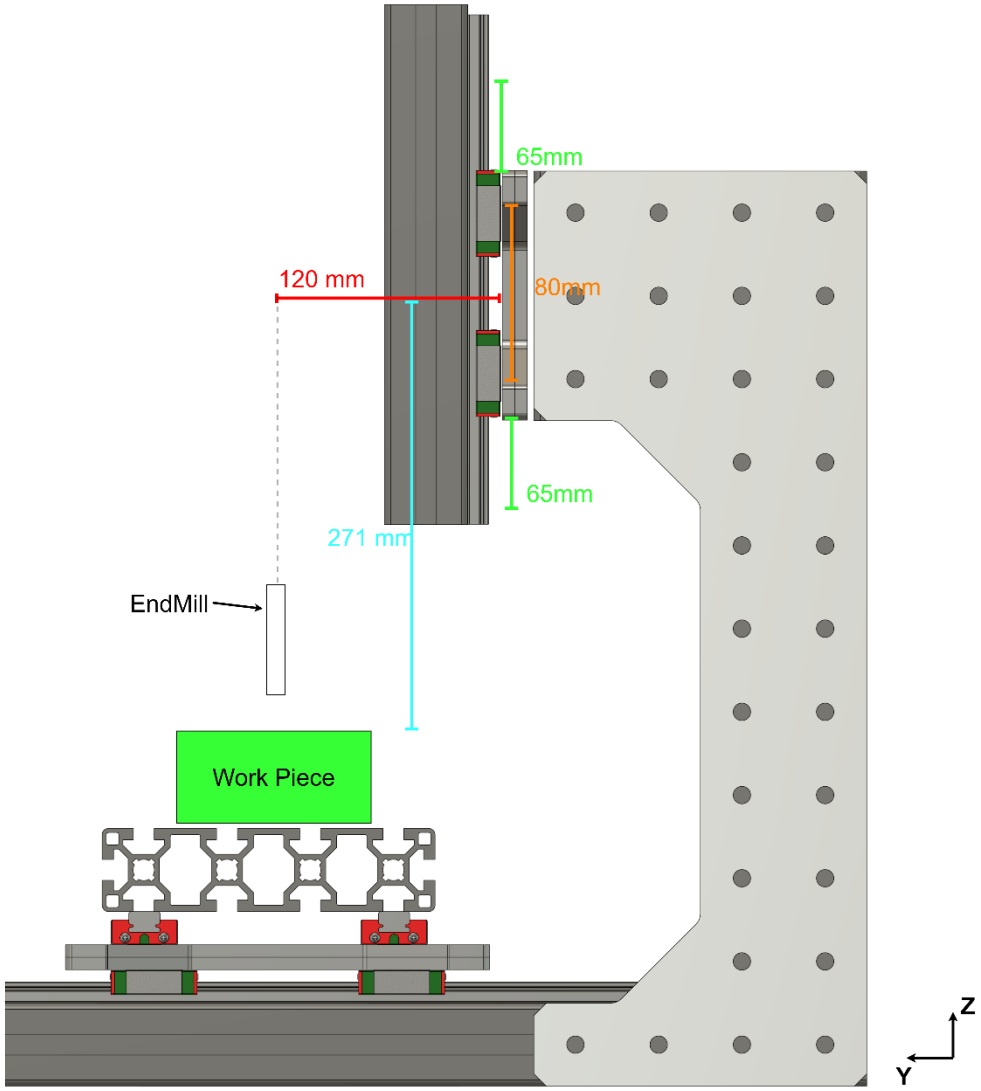

Fig. 35 Z rail side view of the machine, where the axis is equipped with MNG15H linear rail assemblies. All distances and measurements can be easily identified and prompted into the linear rail configurator tool.

Variable	X	D	A	B	D1	Za	m	Xm	Ym	Zm	Fx	Fy	Fz	Xf	Yf	Zf
Unit	mm	mm	º	º	mm	mm	Kg	mm	mm	mm	N	N	N	mm	Mm	Mm
Value	130	120	0	0	80	0	7.4	0	29.74	0	135	135	135	0	120	0

Table 4. Z rail requirements, used in the Hiwin online tool, all measurements were taken in Fig. 34 and Fig. 35.

Using a velocity of 50mm/s and an acceleration of 500mm/s² for the movement limits, the required number of cycles of 200 000 000 and a load factor of 3, the Hiwin online tool gave the results in Fig. 36. A filter for size MGN15 was used to check if the Rat Rig stock was capable of sustaining the application. In fact, both MGN15C and MGN15H are capable of handling the Mill loads, although the MGN15H has double the service life in KM and cycles. For this reason,

MGN15H will be used in the Mill Z-axis. The fact that all rails are MGN15H is a big plus for the Mill, as component sourcing is much simpler.

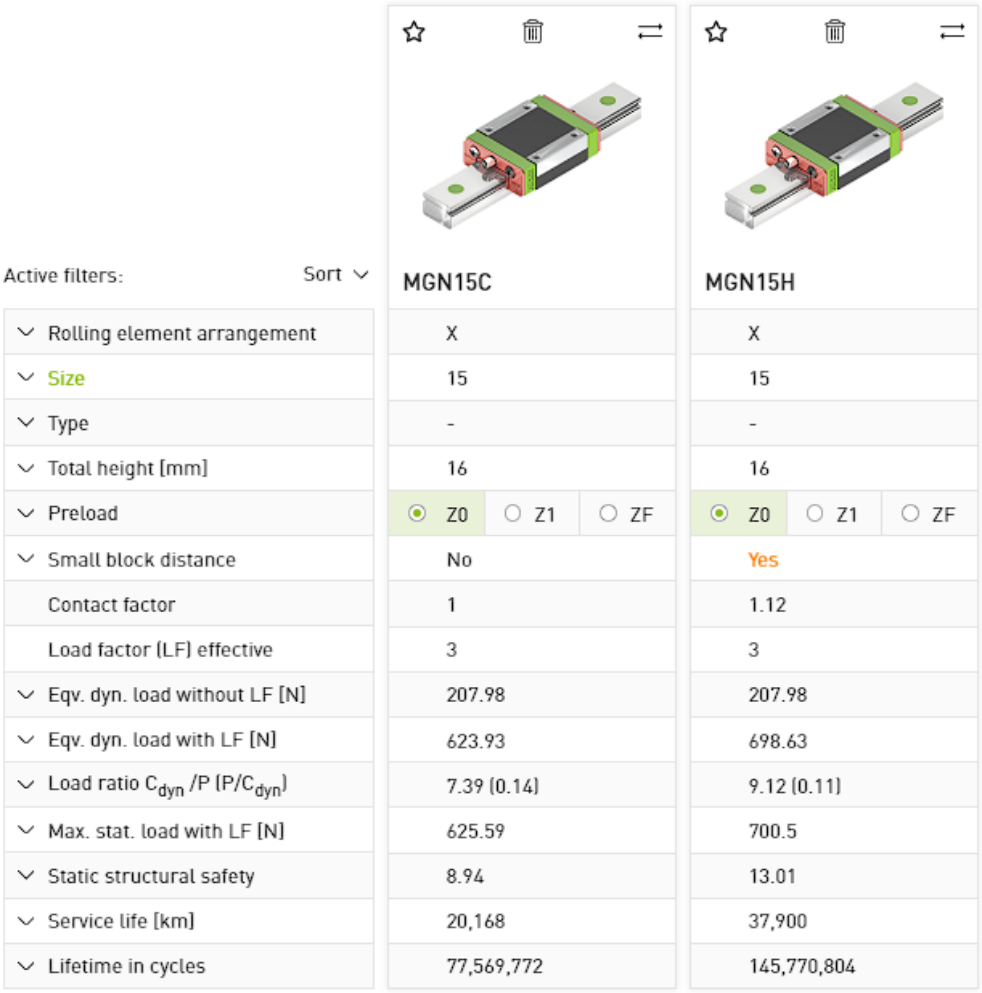

Active filters: Sort	MGN15C	MGN15H
Rolling element arrangement	X	X
Size	15	15
Type	-	-
Total height [mm]	16	16
Preload	Z0 / Z1 / ZF	Z0 / Z1 / ZF
Small block distance	No	Yes
Contact factor	1	1.12
Load factor (LF) effective	3	3
Eqv. dyn. load without LF [N]	207.98	207.98
Eqv. dyn. load with LF [N]	623.93	698.63
Load ratio C_{dyn} /P (P/C_{dyn})	7.39 (0.14)	9.12 (0.11)
Max. stat. load with LF [N]	625.59	700.5
Static structural safety	8.94	13.01
Service life [km]	20,168	37,900
Lifetime in cycles	77,569,772	145,770,804

Fig. 36 Hiwin online tool results for the Z rails, according to the prompted data and size 15MGN filter.

4.2.2.3 Lead screws

The goal is to choose a lead screw that balances resolution, load capacity, speed, precision and works below its critical speed. The Mill machine requires a resolution of 0.1mm with an error tolerance of 0.05mm, a load capacity of 135N, and a linear speed of 50mm/s. There are two main approaches for lead screws, ball screws and ACME screws, ball screws are definitely more precise and long-lasting but costly and less space-efficient while ACME lead screws are cheaper, easier to maintain and space efficient. For these reasons, ACME lead screws will be considered the main preference for the next steps. The most commonly found lead screws are 8mm, as used in most 3D printers, Rat Rig has a big stock of TR8x4 and TR8x8 lead screws, the main difference between these is the pitch, the first being 4mm and 8mm for the second. The pitch of the lead screw defines how much linear travel there is for a full rotation of the screw, this parameter is crucial for precision, as a lower-pitch screw has the potential to be more precise. Although there is a price to pay for more precision, increased rotation on the stepper motor which leads to less torque

available. A generic nema 17 or 23 stepper motor has 200 steps in a full rotation, the linear movement of a lead screw per step can be easily determined by dividing the pitch for the 200 steps, resulting in 0.02mm for the TR8x4 lead screw and 0.04mm for the TR8x8 lead screw. Microstepping can also further increase the precision of this movement, which will be discussed in the next chapter. As shown previously, both lead screws can easily achieve a resolution of 0.1mm as required. Both lead screw options have an 8mm lead, so their axial force handling capability is the same and must be verified. To calculate the maximum axial load a lead screw can handle, there are two primary factors to consider: the compressive strength and the tensile strength of the lead screw material. These factors depend on the lead screw's dimensions, material properties, and the way it is supported. The critical compressive strength is the maximum axial load that the lead screw can withstand before it starts to buckle. This load is influenced by the lead screw's length, diameter, and end support configuration. The formula used to calculate the critical buckling load P_{cr} is based on Euler's Buckling Theory, visible in equation 16:

$$P_{cr} = \frac{\pi^2 \times E \times I}{(K \times L)^2} \ (16)$$

Where E is the modulus of elasticity of the material, I is the second momentum of inertia given by the cross-section, K is the end condition factor, based on how both ends are constrained and L is the length of the lead screw between supports. The modulus of elasticity is 193x10^9 MPa for stainless steel. The second momentum of inertia is given by equation 17 for a solid circular cross-section.

$$I = \frac{\pi \times d^4}{64} = \frac{\pi \times (0.0065)^4}{64} = 8.76 \times 10^{-11}\ m^4 \ (17)$$

The K factor depends on the boundary conditions of the assembly, the lead screw will be coupled to the stepper motor on one end and supported on the other, so K=1.0. The biggest possible lead screw length is on the X-axis, with a maximum possible length of 600mm. That being said, equation 18 translated the critical bucking load:

$$P_{cr} = \frac{\pi^2 \times (193 \times 10^9) \times (8.76 \times 10^{-11})}{(1.0 \times 0.6)^2} = 463.51\ KN \ (18)$$

The tensile strength of the lead screw can also be a limiting factor, particularly if the lead screw is subjected to pulling loads. The maximum axial load based on tensile strength is given by equation 19:

$$P_{tensile} = \sigma_t \times A \ (19)$$

Where σ_t is the tensile strength of the material, 520x10^6 MPa in the case of stainless steel, and A is the cross-section area of the lead screw, given by equation 20:

$$A = \frac{\pi \times d^2}{4} = \frac{\pi \times 0.0065^2}{4} = 3.32 \times 10^{-5}\ m^2 \ (20)$$

$$P_{tensile} = 520 \times 10^6 \times 3.32 \times 10^{-5} = 17.2\ KN \ (21)$$

Equation 21 shows the maximum tensile strength of the lead screw of 17.2 KN, both tensile strength and critical bucking load are way below what the lead screws will be subject to, on the Mill machine.

Pivoting now to the last lead screw parameter that must be accounted for, critical speed. The critical speed of a lead screw is the speed at which the screw begins to vibrate excessively due to resonance. Exceeding this speed can cause excessive vibration, leading to poor performance or even damage to the screw and machine components. The critical speed depends on the lead screw's length, diameter, end support configuration, and material properties. Equation 22 shows how to calculate the critical speed for a lead screw:

$$n_{critical} = \frac{C \times 4.76 \times 10^6 \times d}{L^2} \ (22)$$

Where C is the support configuration factor, d is the lead screw diameter, L is the unsupported lead screw length and $4.76x10^6$ is a conversion factor to RPM. Considering that the lead screw will be attached to the stepper motor on one end and constrained by the drive component on the other end, it can be considered to be supported on both ends, so C = 4. Following the same criteria as the last calculations, a maximum length of 600mm will be considered for the x-axis, so L=300mm since the lead screw is supported in the middle by the drive component and d is 6.5mm not accounting for the thread height. The critical speed will be determined in equation 23:

$$n_{critical} = \frac{4 \times 4.76 \times 10^6 \times 6.5}{300^2} = 1375\ RPM \ (23)$$

Considering that the Mill must achieve a linear speed of 50mm/s, the RPM of the lead screw highly depends on the pitch of it. At this stage, both 4mm pitch and 8mm pitch are capable of working on the Mill. To ensure a speed of 50mm/s the lead screw must rotate at a speed of 750 RPM with a 4mm pitch and 375 RPM with an 8mm pitch lead screw, both values are far from their critical rotation value. A lower RPM is preferred for the Mill, as any stepper motor has higher torque at lower speeds, that being said, the TR8x8 provides the required movement speed plus the required precision at lower RPMs leading to more torque available by the stepper motor, when compared to the TR8x4 Lead screw, for this reason, the Mill will use TR8x8 ACME lead screws.

4.2.2.4 Stepper motors

Selecting the right stepper motor for the linear movement assembly at this stage requires looking into numerous parameters, such as stepper angle/resolution, torque, speed, current and voltage. Stepper angle/resolution determines the precision of the motor, common stepper motor angles are 1.8º and 0.9º, this angle refers to the angle between stepper motor steps, meaning a 1.8º stepper has 360º per rotation divided into 1.8º segments, leading to a total of 200 steps per revolution, while 0.9º steppers have double the steps per revolution, at 400. Rat Rig only stores 1.8º steppers as those are the most commonly used in the industry and provide enough precision for the application. A 1.8º stepper combined with a TR8x8 lead screw can achieve a linear precision of 0.04mm, which is within the Mill specifications. Torque and speed are super important as they define if the machine can perform as expected or stall under load. As speed increases, torque decreases as torque VS speed curves demonstrate, it's important to ensure the motor provides enough torque at the desired operating speed. The Mill will operate in the range of 0 RPM to 375 RPM, it is important that the stepper can provide enough torque at that speed range, to satisfy the machine's requirements set in chapter 4.1, 135N of linear force must be achieved. The linear force can be converted into the required torque using equation 24:

$$T = \frac{F \times Lead}{2 \times \pi \times n} \quad (24)$$

Where T is the required stepper motor torque, lead is the "pitch" of the lead screw, 8mm for a TR8x8 lead screw, and n is the lead screw efficiency, ACME lead screws have a typical efficiency of 30% to 50%, depending on the used nut. If a brass nut is used, the efficiency is closer to 30% while with a POM (Polyoxymethylene) nut efficiency rises closer to 50%. Considering the big impact this component has on linear motion efficiency, the Mill will use POM nuts similar to Fig. 37.

Fig. 37 POM nut block, chosen for the Mill machine, due to its low friction and low profile.

Torque requirement can now be calculated for the stepper motor, equation 25:

$$T = \frac{135 \times 8}{2 \times \pi \times 0.5} = 344.8\ Nmm = 34.5\ Ncm \quad (25)$$

The most commonly used nema 17 stepper motors have a maximum torque of 30 to 35 N.cm, Fig. 38 shows the power torque curve of a nema 17 1.8º 42x42x48mm 17HS19-0406S from stepper online.

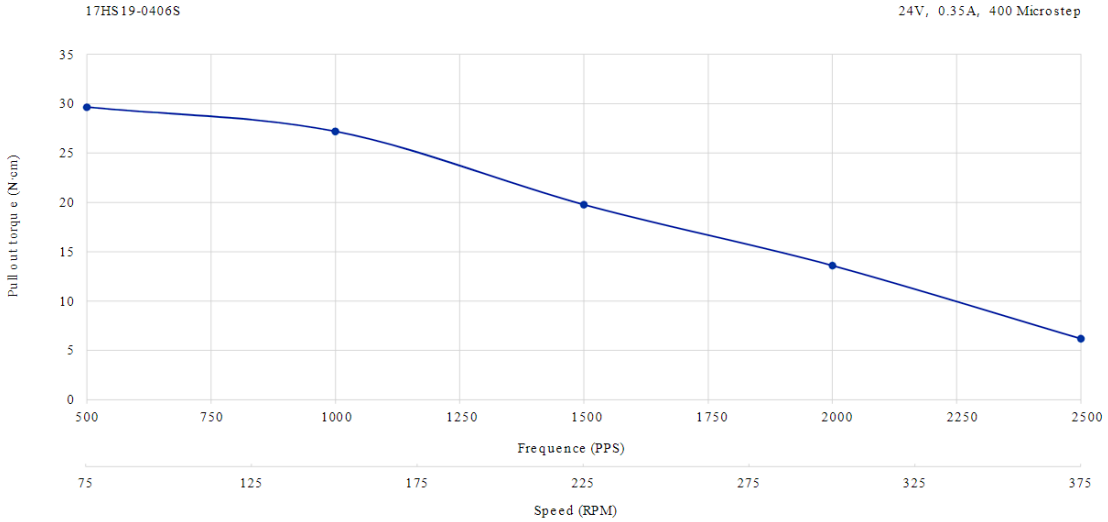

Fig. 38 Nema 17 17HS19-0406S Stepper motor, torque versus speed curve where a maximum of 30N.cm can be observed at 75RPMs, as speed further increases the torque drastically decreases.

A maximum 30 N.cm torque can be observed at 500 RPMs but decreases as speed increases, at 375 RPM the torque is unusable for the Mill machine. A more powerful stepper motor is required, two different models of nema 23 will be analysed next. Below we can see two speed vs torque curves, for a nema 23 57mmm and a nema 23 86mm, both from StepperOnline, these are not the stepper motors used on the Mill as Rat Rig currently only stocks LDO motors, unfortunately, LDO doesn't provide speed vs torque curves, so an equivalent stepper motor model will be used for data. It's important to note that these curves do not represent the behaviour of the LDO stepper motors but can provide a baseline for the selection decision. Fig. 39 shows the speed VS torque curve of the nema 23 57mm from stepper online, where torque is constant at around 85 N.cm in the range of 0 to 150 RPMs, then quickly drops. Although during the entire speed range of the Mill, which is 0 RPM to 375 RPM, the stepper motor is capable of outputting the minimum 34.5 N.cm as calculated above.

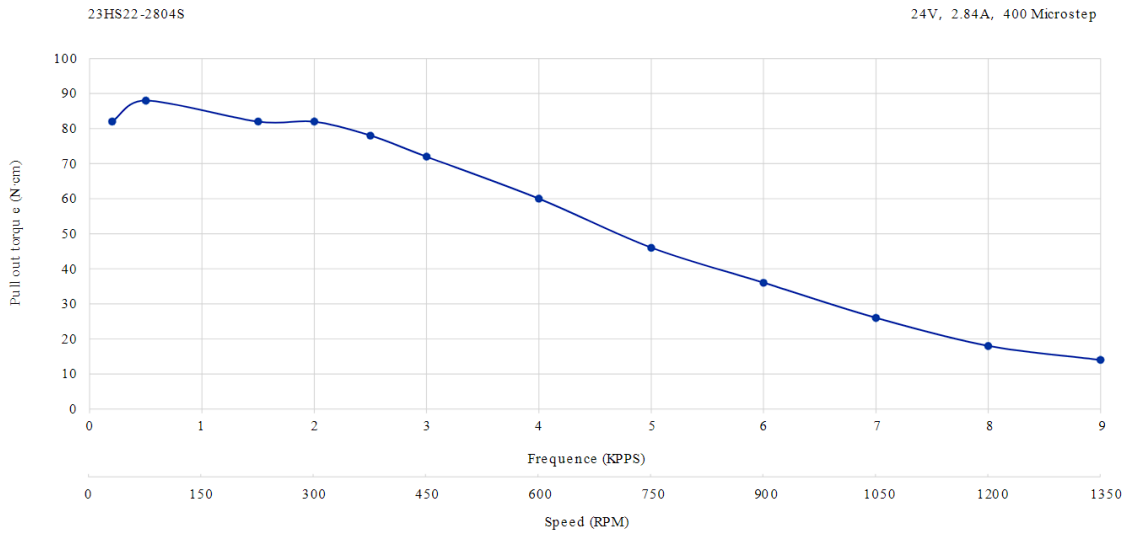

Fig. 39 Nema 23 57mm from Stepper Online, Speed VS Torque curve, torque is held constant in the range of 0 to 300 RPMs then quickly decreases.

Looking now at the nema 23 86mm from stepper online in Fig. 40. It's clear that it has a lot more torque at lower speeds than the nema 23 57mm, more than double. Its speed range is much closer to the Mill operating range. Torque is much higher at lower speeds (60 RPM to 150 RPM), then drops to around 50 N.cm closer to 300 RPM, it is still above the 34.5 N.cm calculated above. Although the graph doesn't show the 375 RPM, it seems to be lower than the nema 23 57mm at that speed.

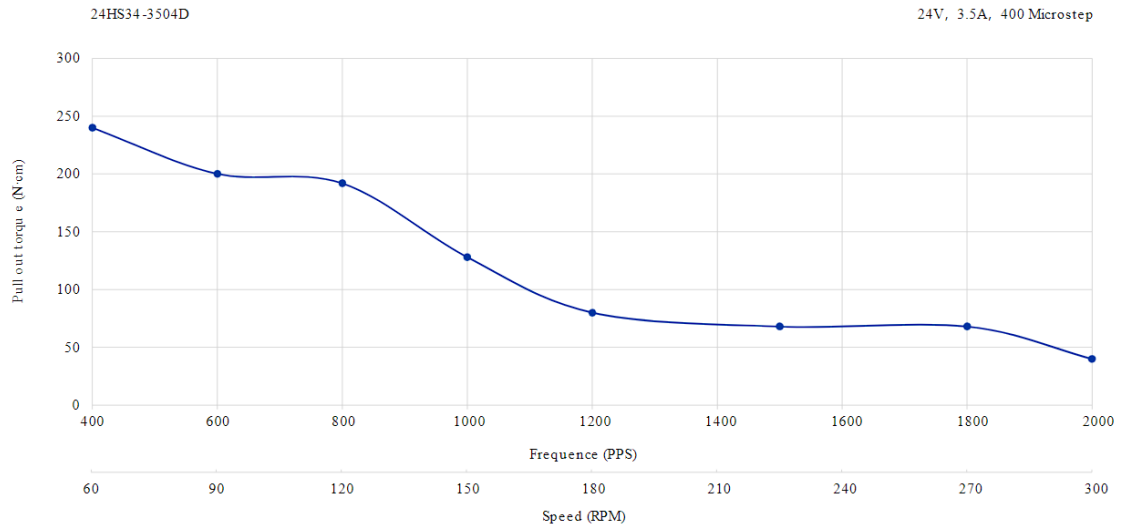

Fig. 40 Nema 23 86mm from Stepper Online, Speed versus Torque curve, Torque is much higher in lower speeds (60 RPM to 150 RPM), then drops to around 50 N.cm closer to the 300 RPM.

Looking at both curves, the nema 23 57mm seems to be the more accurate decision to fulfil the Mill specifications, but the nema 23 86mm has more than double the torque at lower speeds, this ensures the machine has more than enough power at lower speeds for every use, with a safety

factor of 5.79 when comparing a maximum torque of 250 N.cm with the 34.5 N.cm, while the nema 23 57mm only has a safety factor of 2.6 when comparing the maximum torque of 90 N.cm with the baseline of 34.5 N.cm. The higher safety margin ensures the user always has enough power at lower speeds, while the nema 23 57mmm may struggle at lower speeds if the user is experienced with milling and wants to push the machine further. Both Steppers are capable of accomplishing the Mill requirements since they have the same footprint and shaft diameter, as shown in Fig. 41, the assembly can easily swap between stepper motors, offering the user more flexibility with his set-up.

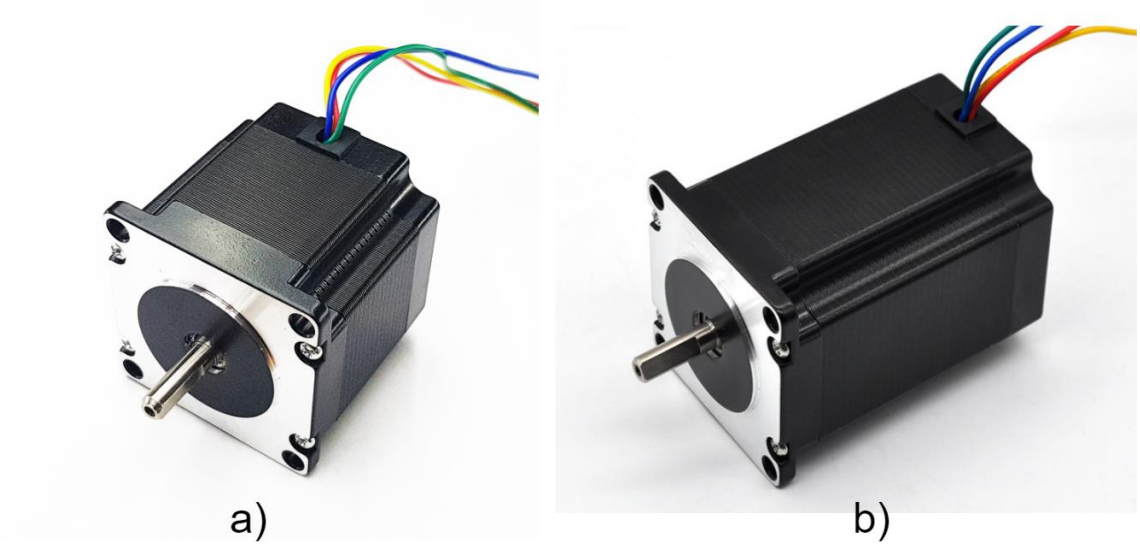

Fig. 41 a) Nema 23 57mm from LDO. b) Nema 23 86mm from LDO. Both images are from the Rat Rig online store.

4.2.2.5 Bearings and Couplers

Up to this stage, all the linear motion components have been selected, linear rails, lead screws, driving nuts and stepper motors, leaving the assembly in need of structural support. For this purpose, Rat Rig has a vast selection of bearings in stock. The linear motion assembly already has the linear rails as a structural component, they do not only provide a smooth linear motion but also constrain the entire gantry assembly, leaving the lead screws as the only component without proper constraints. The lead screw will need axial and radial support, Fig. 42 illustrates the forces to which the lead screws are subject:

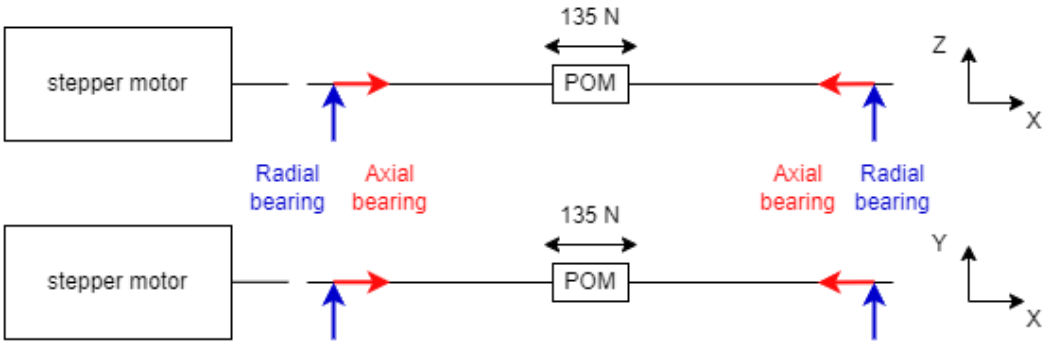

Fig. 42 X and Y lead screw forces when milling, from the ZX and YX planes, with a visual representation of the cutting force and proposed bearing positions.

The axial bearing must be rated higher than the 135 N of cutting force and the inner diameter must be larger than the lead screw another important factor is the maximum rated speed of the bearing, it must be higher than 375 RPM as specified for the Mill, Rat Rig has a bearing dedicated to this purpose, the FM8-16M, shown in Fig. 43:

Fig. 43 Axial bearing FM8-16M , composed of two outer rings and an inner ring with 9 spheres hosted inside.

The FM8-16 bearing doesn't have any type of seal, so its location must be protected from milling debris as they can fall inside the sphere's groove raceways and stop them from rotating freely, Fig. 44 shows the dimensions for this bearing. As stated by the manufacturer, this bearing can withstand a dynamic load of 2499.9 N, meaning it will operate under an 18.5 safety factor, ensuring a long lifetime with the proper lubrication. Its maximum rated speed is 4000 RPM, while the Mill is designed to go up to 375 RPM, so rotation speed is not an issue for this bearing model. Diving further into the bearing lifetime, following the L10h rule, where 90% of the bearings will still be operational, in equation 25:

$$L_{10h} = \frac{1000000}{60 \times n} \times \left(\frac{C}{P}\right)^3 \quad (25)$$

Where L_{10h} if the bearing lifetime in hours, where 90% of the bearings will still be operational, C is the dynamic load rating of the bearing, P is the equivalent load on the bearing, n is the rotation speed, considering the data above we can calculate the bearing expected lifetime, in equation 26:

$$L_{10h} = \frac{1000000}{60 \times 375} \times \left(\frac{2499.9}{135}\right)^3 = 2.8 \times 10^5 \; hours \; (26)$$

For better rigour, L5h life should be taken into account, where a 0.62 factor should be multiplied by L10h, resulting in approximately 20 years of operation.

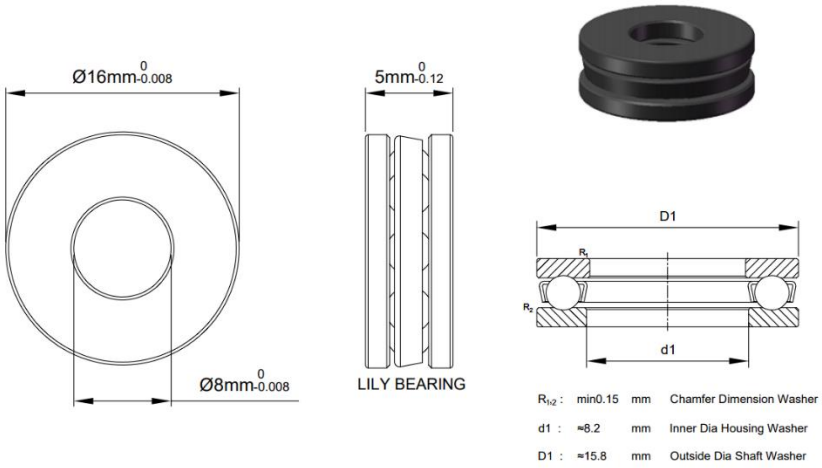

Fig. 44 Dimensions of the F8-16M axial bearing by the manufacturer LiLy (LILY, n.d.-b)

Regarding the radial bearings, although the lead screws are not directly subject to any radial forces, there are a couple of benefits to using radial bearings, such as preventing lateral movement created by vibrations or misalignments in the assembly, reducing lead screw wobble in case they are not perfectly straight from the manufacturer. Both these motives can improve accuracy and precision in motion while reducing noise, Rat Rig has in stock the ball bearing 688ZZ a fairly inexpensive solution illustrated in Fig. 45:

Fig. 45 Radial ball-bearing 688ZZ from the Rat Rig web store.

The 688zz bearing has a shielded seal and doesn't require any maintenance from the user, it is rated for a maximum speed of 36000 RPM way below the Mill operation range. Assuming all the radial load is handled by the axial F8-16M bearings and the radial load is almost non-existent, the

supplier has a web tool to calculate the expected lifetime in hours, in its current application it will last 28305564571 hours. Fig. 46 shows the dimensions of the 688ZZ.

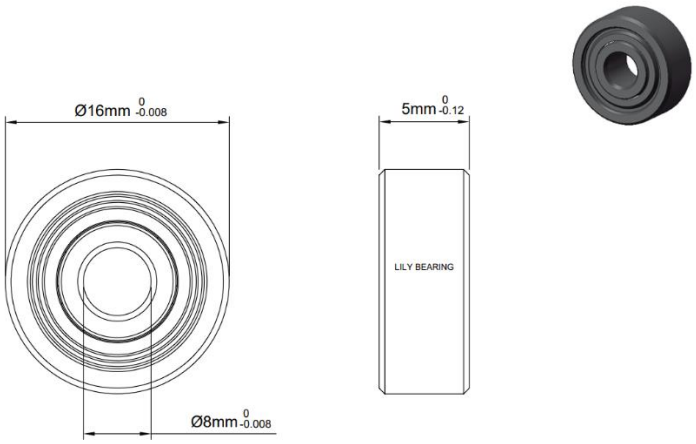

Fig. 46 Dimensions of the 688zz axial bearing by the manufacturer Lily (LILY, n.d.-a)

Pivoting not to the couplers, there are many options on the market to connect the stepper motor shaft to the lead screw. The couplers are responsible for transmitting the mechanical power from the stepper to the lead screw as well as allowing the assembly to be misaligned, this is inevitable due to manufacturing tolerances, for example, the stepper motor mounting component, stepper motor shaft eccentricity, lead screw runout and bearing mounting component. A few important parameters when choosing a coupler include maximum allowed speed, maximum torque and backlash. Rat Rig has a coupler with the right shaft diameters on both ends, 8mm for the lead screw side and 6.35mm or 1/4" for the stepper motor shaft side, the DCSK 16-8MM-1/4"-A coupler. The maximum speed operating speed of the mill machine is 375 RPM, so the coupler must be able to support that comfortably, this coupler can operate at speeds up to 10000 RPM. The maximum torque defined in chapter 4.1.2.4 was 34.5 N.cm, the coupler can handle a dynamic torque reversing of 140N.cm and 280N.cm of non-reversing dynamic torque, the first representing a sudden change in direction without stopping and the second a change in direction with a proper deceleration and acceleration. While operating, the Mill will change directions without stopping very often, for this reason, 140N.cm is used as the rated torque for the coupler, equation 27 determines the coupler safety factor:

$$SF_{coupler} = \frac{140}{34.5} = 4.06 \ (27)$$

The manufacturer indicates this is a zero-backlash coupler, this parameter is important to ensure there is no mechanical lag in the system, meaning the coupler could absorb the rotation of the stepper motor and take a split second to deliver that same rotation to the lead screw. The coupler is made of aluminium and uses two screws on each end to clamp itself to the shafts, its outer dimensions are 26mm in diameter by 26mm in length.

4.2.3 Machine design

After choosing all the main components for the Mill, the best assembly process must be considered when designing the mounting components. Starting with the linear rails, the four plates shown in Fig. 21, Fig. 22 and Fig. 23, need to have screw holes to connect them with the linear rail carriages. Since the plates are facing each other, the carriage screws need to be flush with the plates, so they can be properly assembled, a counterbore hole will be used as shown in Fig. 47.

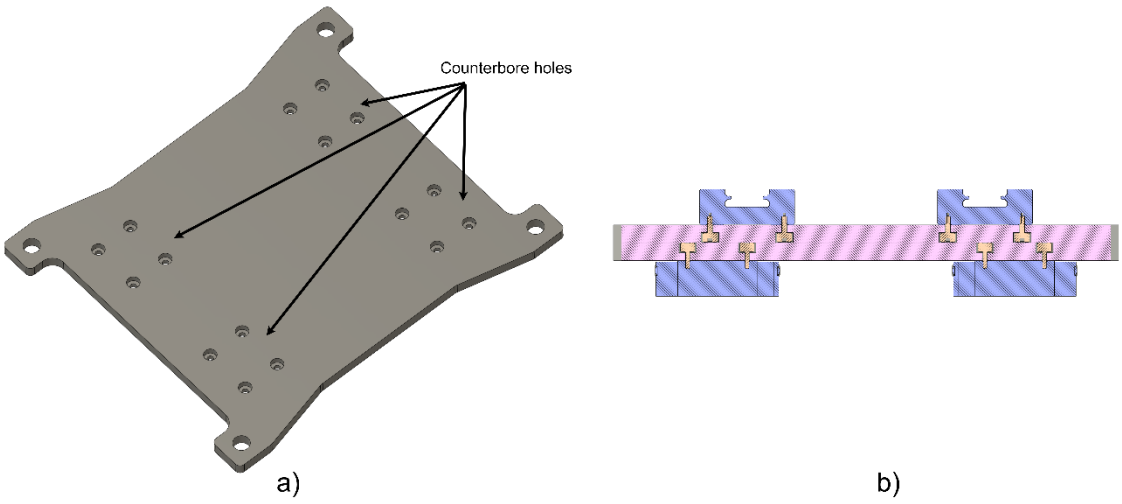

Fig. 47 a) XY gantry plate with the marked linear rail carriage holes, where counterbore holes will be machined, b) Section view of the plate with the linear rail carriages mounted with M3 screw embedded in the plates.

To secure the carriages, M3x6mm Cap Head Screws will be used, as they allow the full usage of the carriage's M3 thread. Furthermore, the POM nuts will be assembled to the plates, allowing the lead screw to drive the axis, accordingly to Rat Rig experience, these nuts have significant backlash meaning there needs to be two of them per axis to prevent the backlash. This can be accomplished by adjusting the nut's distance although having them synchronised with the lead screw pitch is crucial. If they are not perfectly aligned with the lead screw pitch, the POM nut can create excessive drag and even binding. It's nearly impossible to set the perfect distance between two POM nuts that always ensures correct pitch alignment due to plate milling tolerances and POM manufacturing tolerances, these can vary significantly from user to user, thankfully Rat Rig solved this in a clever way, by having one POM nut fixed and one adjusted by the user. This assembly process allows every machine to be adjusted to the lowest friction possible, increasing linear motion efficiency, Fig. 48 clearly shows the POM nuts installed along with the M5x16mm low head screws and M5 nylon locking nuts.

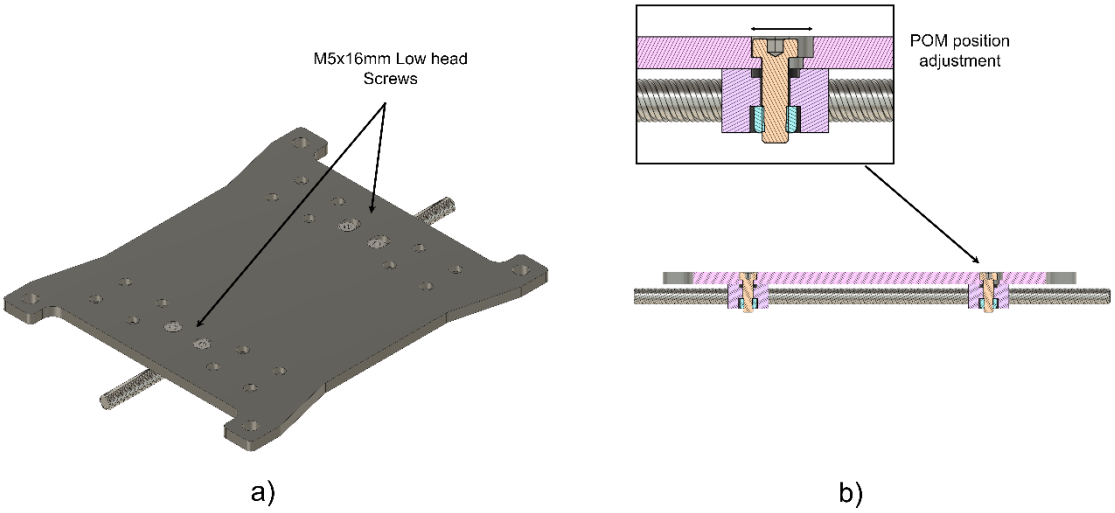

Fig. 48 a) Top isometric view of the XY gantry plate with the M5x15mm Low Head Screws with adjustment, b) Side section view of the XY gantry plate where the adjustment of the POM pitch can be made.

The four corners of the plates can be connected using M8x25mm Cap Head Screws, with M8 washers and M8 Locking Nylon nut to prevent it from becoming loose with machine vibrations. This "sandwich" system allows all the axes to be assembled individually, making it much easier for the user to align every component and move the assembly around if needed, as this is a very heavy assembly. Fig. 49 shows the XY gantry plates assembled, with all the required components. Furthermore, additional M3x0.5 threaded holes have been added in the top plate, allowing Rat Rig to mount accessories later, if needed, like a bellow cover. The technical drawing for these plates can be found in the attachments section, Fig. 83 and Fig. 84.

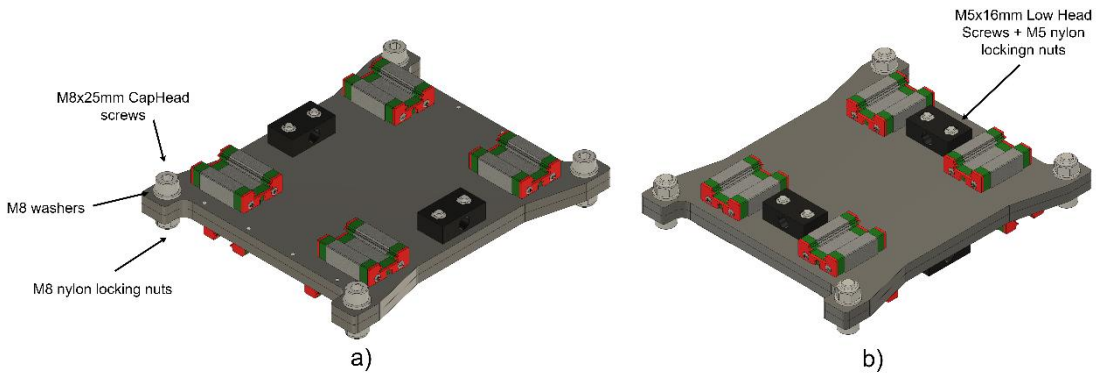

Fig. 49 a) Top isometric view of the XY gantry plate with the M8x25mm Cap Head screws + M8 washer + M8 nylon Locking nuts installed. b) Bottom isometric view of the XY plates with the POM nuts installed with M5x16mm Low head screws + M5 nylon locking nuts.

Mounting the stepper motors to the assembly can be done easily with an aluminium plate, that is installed in each extrusion and has tapped holes, by using an aluminium spacer between the plate and the stepper motor, the coupler and axial bearing can be fit in between the two, providing a sturdy assembly.

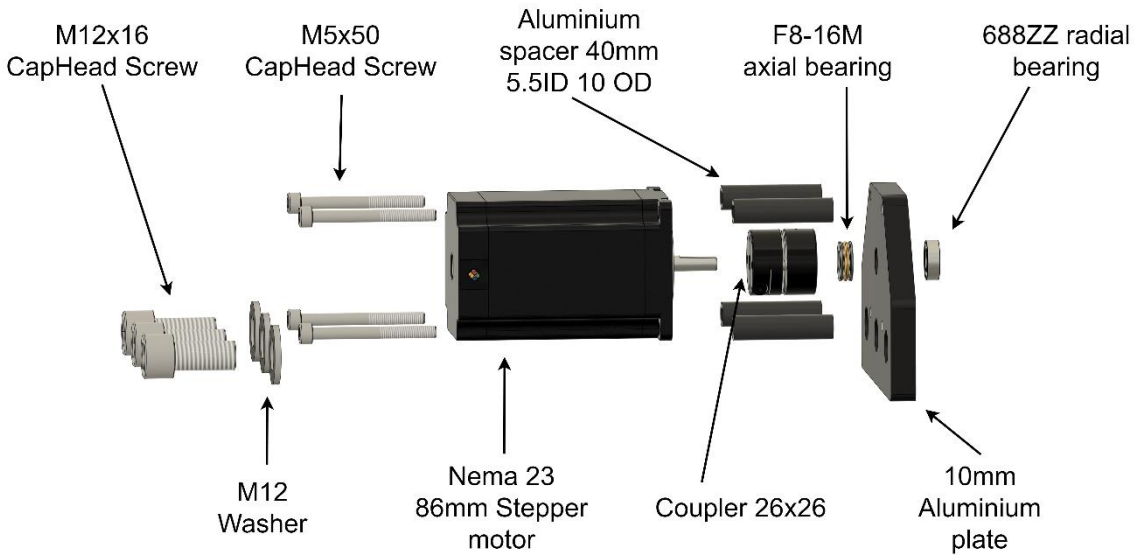

Fig. 50 Stepper motor mount assembly, where all components can be observed as well as the assembly order.

As for the fitting of the 688ZZ ball bearing, a 16.1mm hole is used to hold the bearing with friction, this has been a standard at Rat Rig as it provides a perfect fit between their bearings and their plate manufacturer as Fig. 51 shows.

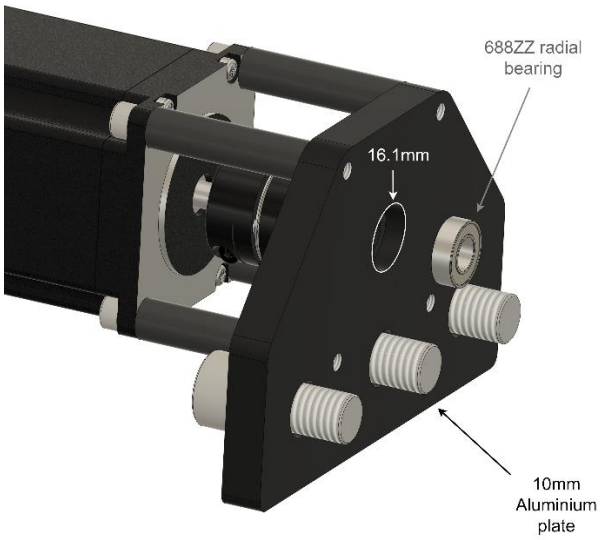

Fig. 51 Stepper motor plate mounting, illustrating the 688ZZ radial bearing hole at 16.1mm, where the bearing is press fitted.

The rear of the Y axis is now fully constrained, the front of the axis will have a similar set-up, excluding the stepper motor. A 10mm aluminium plate will be mounted in the front of the Y extrusion, but using countersink screws instead of cap head, as this plate is the front of the machine and countersink screws have a cleaner look. The technical drawing for this plate can be found in the attachments section, Fig. 85. This plate will also support the front of the lead screw

with a 688ZZ radial bearing. Most milling machines have jog wells, allowing the users to easily move the axes when the machine is powered off or idle. Both X and Y axis will have jog wheels, It will be installed at the end of the lead screw, the jog wheel is installed in the lead screw with two set screws, another axial bearing will be included between the jog wheel and the aluminium plate, providing extra support for the lead screw loads but most important making it impossible for the user to install the jog wheel right against the aluminium plate, this could cause drag, excessive wear and even complete binding of the axis. Fig. 52 shows the Y-axis fully assembled with all the components described above.

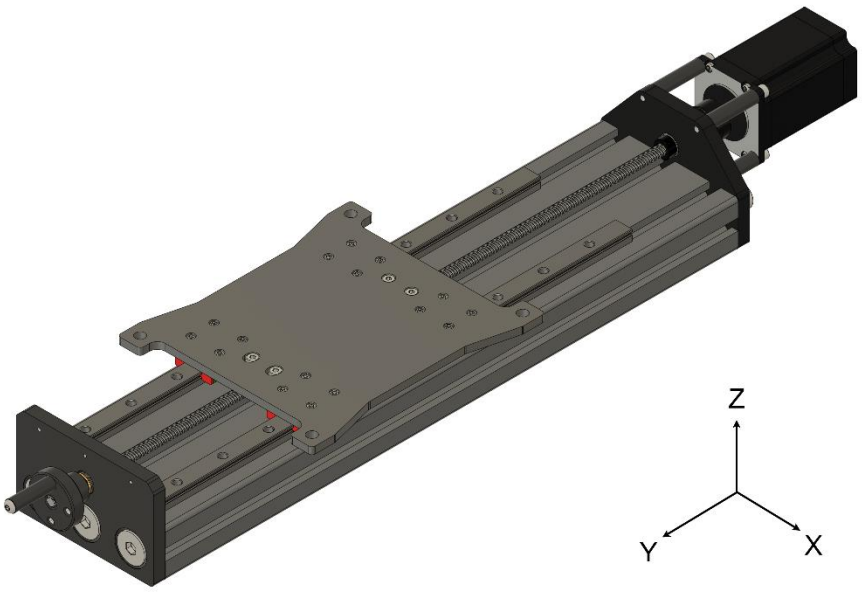

Fig. 52 Y axis assembly, linear rails, Y gantry plate, stepper motor assembly on the back with all the bearings and front plate plus jog wheel.

The X-axis follows the same design approach as the Y-axis, except the extrusion is a 40160, adjusting the plate dimensions is required. Fig. 53 shows both plates for the X-axis as well as the assembly order. The technical drawing for these plates can be found in the attachments section, Fig. 86 and Fig. 87.

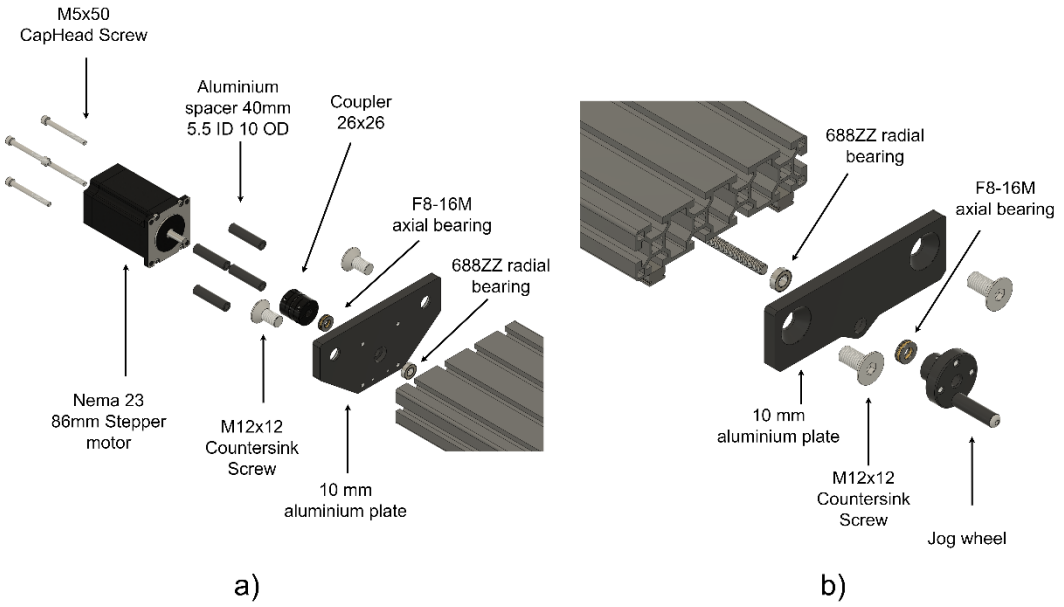

Fig. 53 a) Left side of the X-axis, illustrating the assembly order and components of the stepper motor mount. b) Right side of the X-axis assembly, illustrating the end plate assembly and jog wheel.

Having both axes assembled, they can be joined with the four M8x25mm cap head screws, M8 nylon locking nuts and M8 washers as shown in Fig. 49. The full XY motion system is complete as shown in Fig. 54.

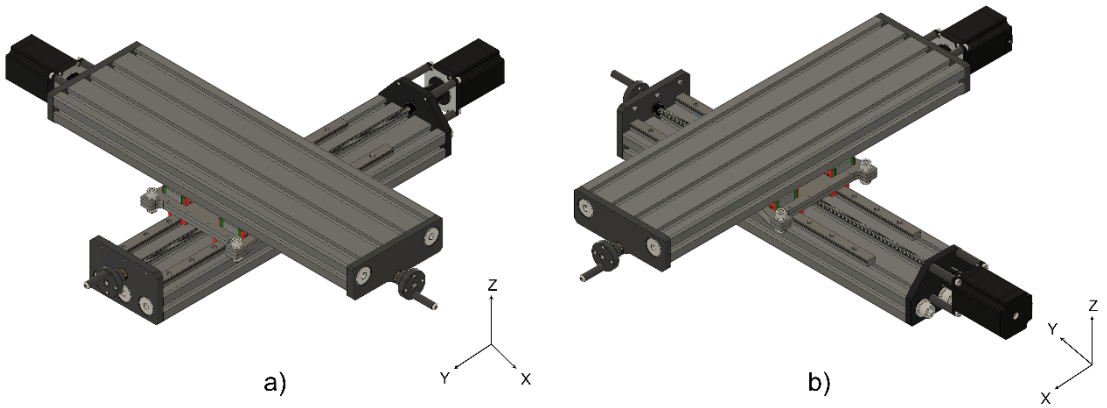

Fig. 54 a) Isometric front view of the X and Y axis assembled, b) Isometric rear view of the XY axis assembled.

The Z axis follows the same concept as the X and Y axes, just at a smaller scale, Fig. 55 illustrates the assembly of the Z axis. This is the only axis that doesn't have a jog wheel, making the assembly simpler.

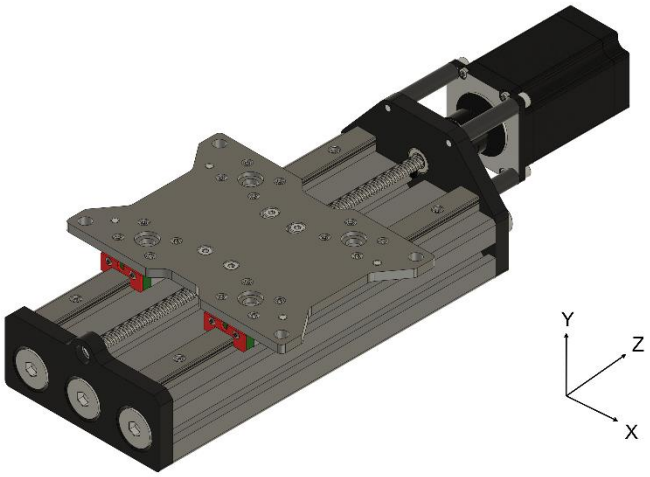

Fig. 55 Z-Axis full assembly

The main difference between the X and Y axes and the Z axis is the fact that the Z axis is connected to a fixed extrusion, the Z tower assembly. For this reason, the mounting plate must suffer some design changes, it must allow the user to independently assemble the Z axis and install it on the Z tower with the same sandwich method as the XY plates. The assembly will use two similar plates. By using the same design, Rat Rig can reduce manufacturing costs, simplify the bill of materials and simplify the user experience. These plates allow the mgn15h carriages to be mounted with M3x8 cap head screws, like the X Y plates as well as the same POM nut mounting assembly, the assembly of the two plates is done via the M8x25 cap head screws plus M8 washers and M8 nylon locking nut. To mount the plate to the 40120 Z tower extrusion, four M8x12 low-head screws will be used, these have a low profile of 5mm allowing them to be hosted in between the 6mm plates and still have 3.3mm of plate thickness below the screw heads. Combining the M8 low head screws with M8 4040 T-nuts, one of the two Z plates can be secured to the Z tower. Fig. 56 illustrates the Z plates assembly described above. The technical drawing for this plate can be found in the attachments section, Fig. 88.

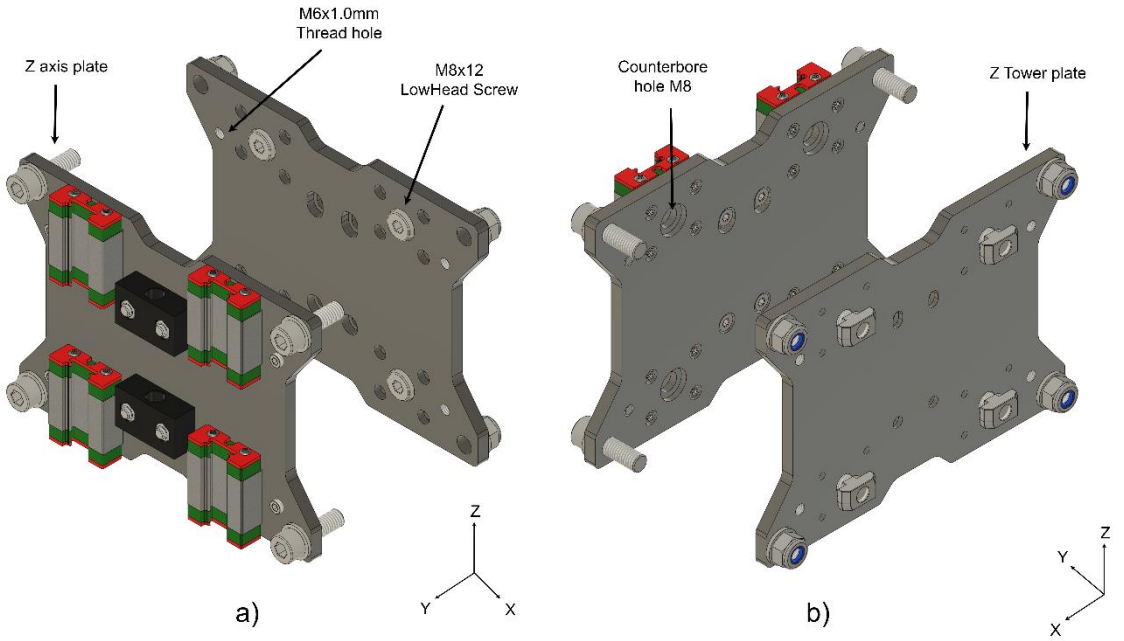

Fig. 56 Z plates assembly, illustrating the Z axis plate side and the Z tower plate side. a) isometric front view of the Z plates assembly, b) isometric rear view of the Z plates assembly.

At this stage, Rat Rig decided to include four M6x1.0mm threaded holes in the plates, these are offset from the centre so that they do not match when the plates are aligned. These threaded holes are meant for M6 set-screws that assist the user in tramming the machine, meaning they provide an extra degree of adjustability to the Z-axis assembly, this is required to ensure the Z-axis is perfectly perpendicular to the Y and X axes. Fig. 57 shows the Z-axis assembly of the Z tower, as well as the freedom the four screws provide when assembling the machine.

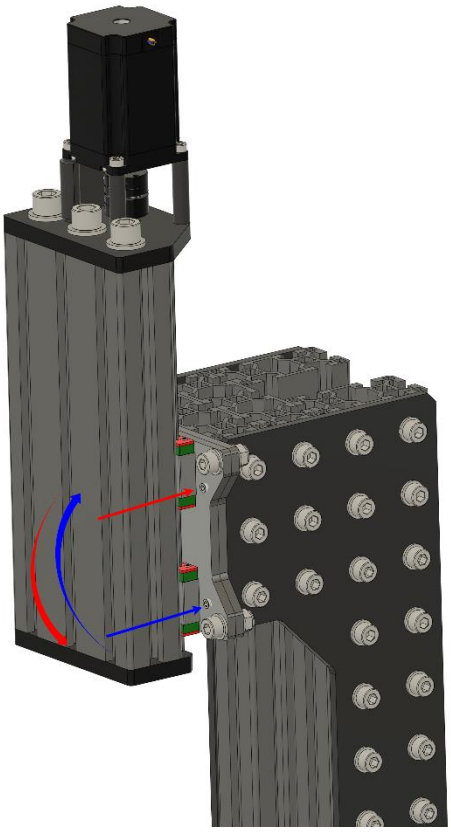

Fig. 57 Z-axis adjustment freedom. Tightening the red screw means the axis rotates counterclockwise in the X axis and the blue screw allows the rotation clockwise in the X axis.

Merging the Z axis and Z tower with the X and Y axes assemblies shown in Fig. 54, the Mill starts to gain shape. The two large assemblies can be connected together with the side Z tower plates. The assembly design described above allows any user to assemble and align each axis individually without having to move or rotate the fully assembled machine. Fig. 58 demonstrates how the machine is assembled together. At this stage, the basic mechanical assembly is finished, and all the project's initial requirements are met.

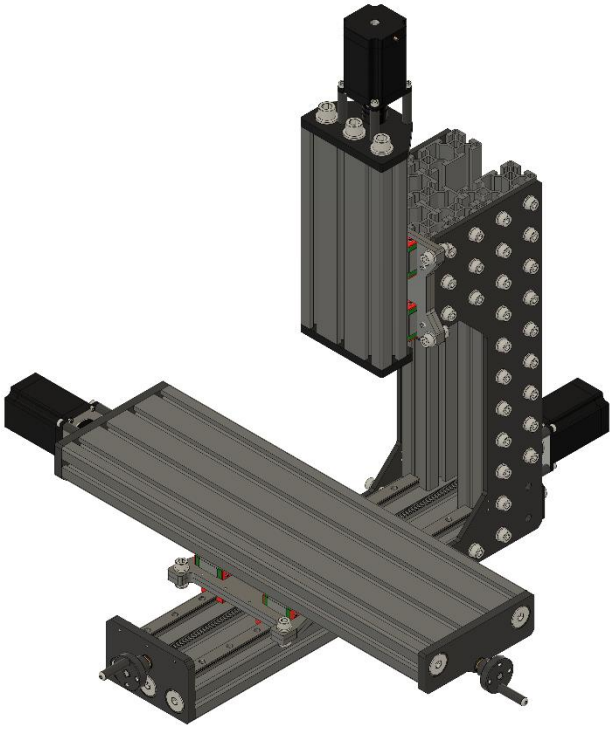

Fig. 58 Mill assembly, combining the X Y and Z axes assemblies.

4.2.4 Mechanical validation

A short mechanical validation must be done to ensure the structure can handle the required loads. A static force simulation will validate if the Z tower frame deflects in a significant way that compromises the performance of the machine, while the weakest bolted joints will be calculated.

A static stress simulation was conducted using the Ansys software. In order to reduce simulation complexity and mesh calculation, the assembly was reduced to the bare minimum. Fig. 59 shows the imported Step assembly of the Z tower of the Mill to Ansys, where all the materials were attributed to each component.

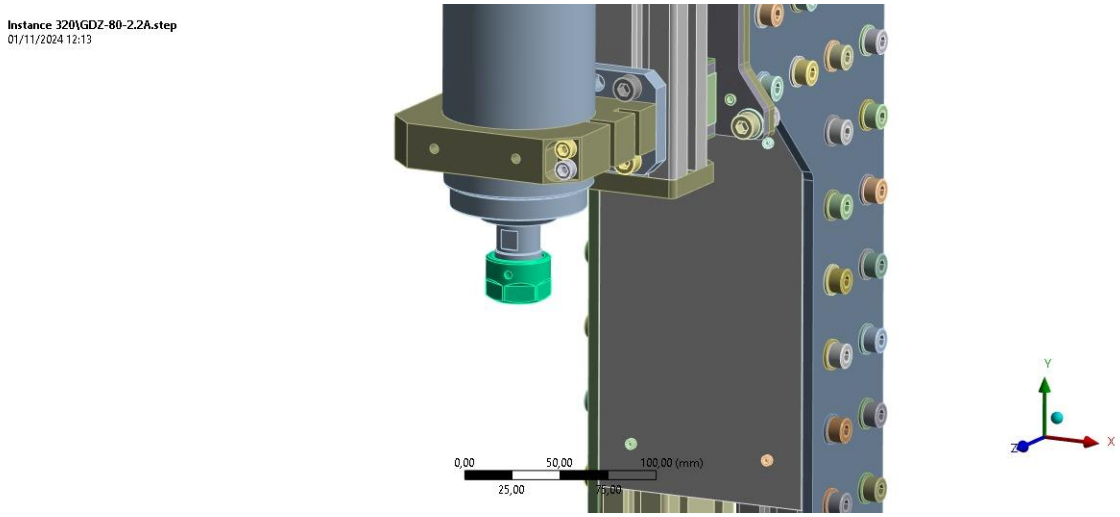

Fig. 59 Mill Step assembly imported to Ansys software.

A simulation for equivalent stress was conducted using the Von-Mises criterion, where a maximum of 47,068MPa can be observed in Fig. 60, on the spindle collet piece.

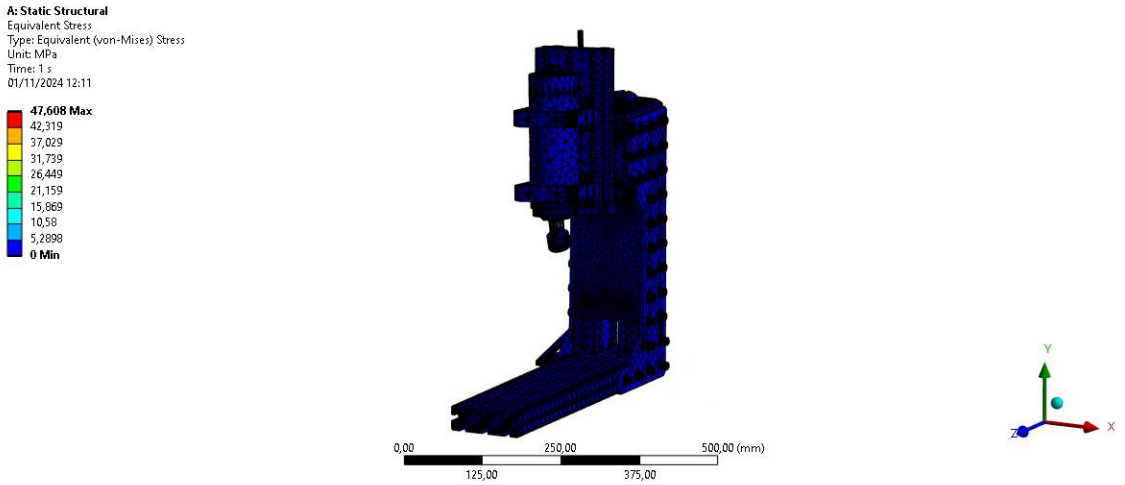

Fig. 60 Simulation for equivalent stress was conducted on the Ansys software, where only the Z tower was analysed.

The spindle collet is the component subject to the largest stress, given the fact that this component is made out of 12.9 steel, it has a maximum yield strength of 1,200 MPa, making it capable of handling the maximum operating loads of the machine as Fig. 61 shows.

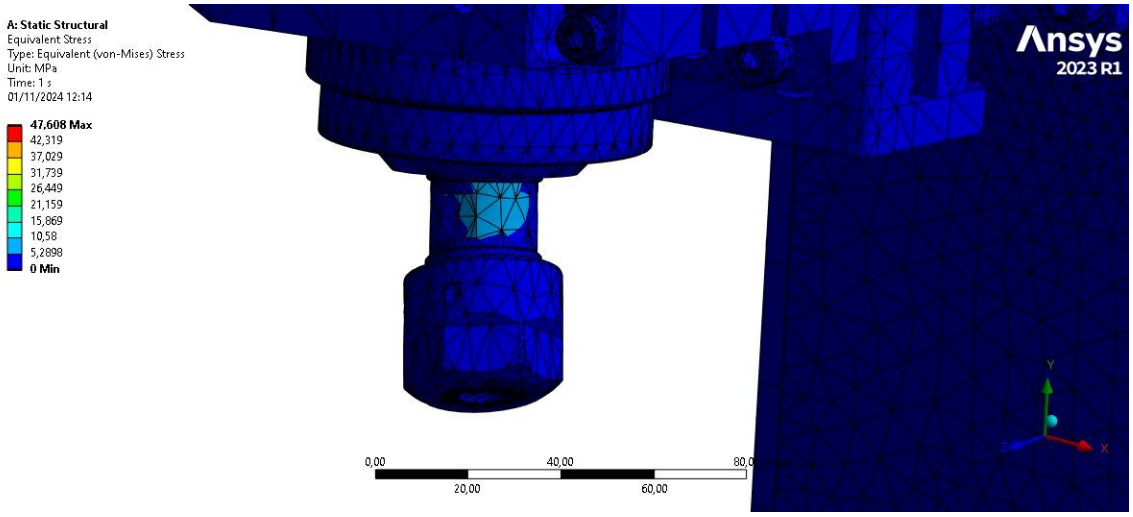

Fig. 61 Closed look at the most critical component of the Mill assembly, when subject to maximum operating forces.

Furthermore, a deformation study was conducted in Ansys, to better understand what impact the stresses previously demonstrated has on the assembly rigidity. Deformation is a critical subject for milling machines, especially diy machines and kits. If deformation is big enough, it will affect the machine's precision on high loads. Fig. 62 shows the overall deformation of the Z tower assembly, where the spindle and its support suffer the largest displacement while the Z tower it self hasn't any visible deformation, making the bolter joint on the Z tower plates subject to a lot of stress. Fig. 63 gives an up-close view of the spindle nut, where the largest deformation of 0.011mm can be observed, considering the endmill doesn't have any deformation on its own, this small deflection will generate a milling error twice as big as itself. 0.022mm of error will be introduced if milling at the maximum load the machine was projected for.

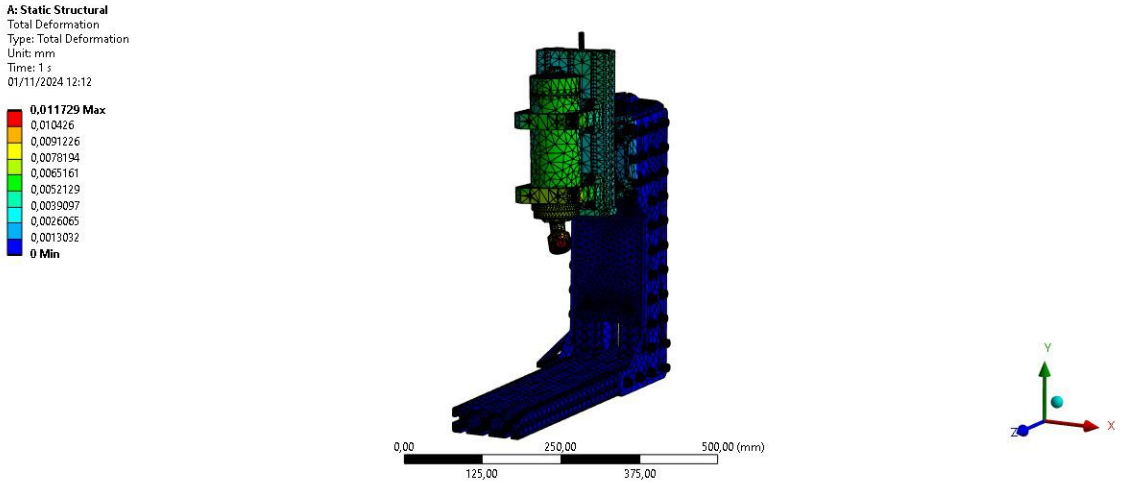

Fig. 62 Static structural deformation in mm for the Z tower assembly of the Mill machine.

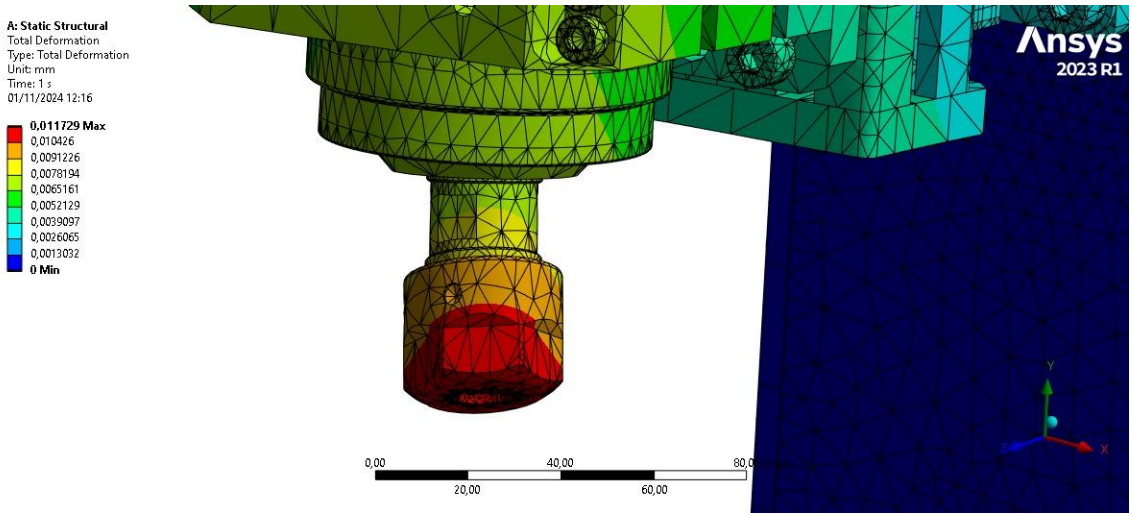

Fig. 63 Static structural deformation in mm for the Z tower assembly of the Mill machine. Focused on the most critical point, with a maximum deformation of 0.011mm.

The weakest bolted joints are the Z tower plates and the XY gantry plates, where four M8 cap head screws handle the full load of the machine, for this reason, those screws must be validated. Fig. 64 shows the Z tower plate analysis from the XY plane, while Fig. 65 shows the XZ plane.

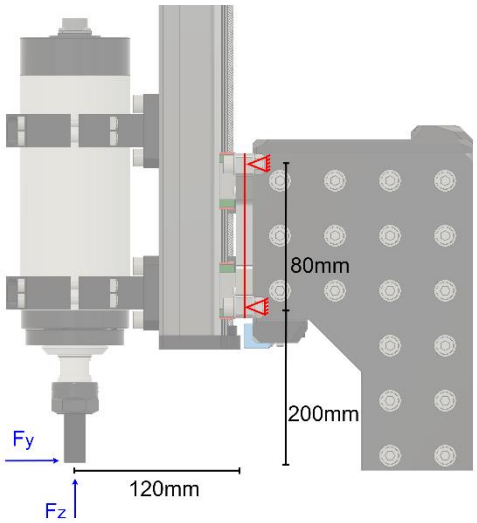

Fig. 64 XY plane of the machine, where the Z tower plate can be observed. Both Y and Z forces are represented along with their offsets to the mounting screws.

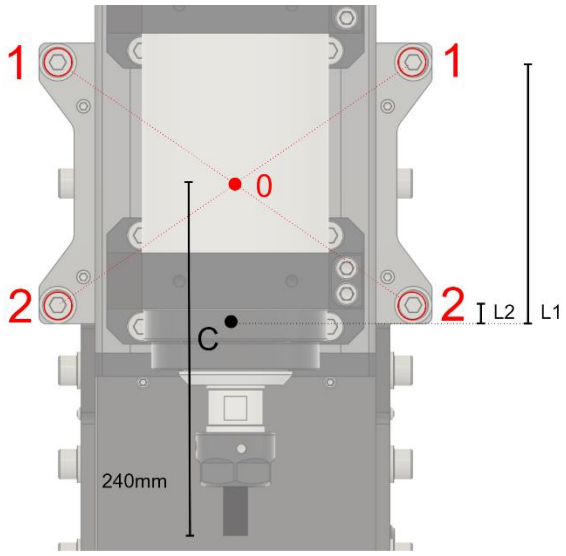

Fig. 65 XZ plane of the machine, where the Z tower can be observed. The M8 screws being analysed are represented and numbered, as well as all the necessary offsets for the validation.

Since all the screws are symmetrical, there is no need to determine the centroid 0. Starting with the primary cut, equation 28 represents it, while equation 29 shows the pulling force fraction supported by each screw, then equations 30 and 31 determine the exact pulling force per screw connection.

$$F1' = F2' = \frac{Fz}{4} = \frac{135}{4} = 33{,}75\ N \quad (28)$$

$$C = \frac{Fz \times e_z + Fy \times e_y}{2(l1^2 + l2^2)} = \frac{135 \times 120 + 135 \times 240}{2(88^2 + 8^2)} = 3{,}11\ N/mm \quad (29)$$

$$F1'' = C \times l1 = 273{,}68\ N \quad (30)$$

$$F2'' = C \times l2 = 24{,}88\ N \quad (31)$$

Since the screws numbered 1 are the ones subject to the highest pulling force, we must verify their safety factor, ensuring the machine can operate without any mechanical compromises. Following the Tresca criteria, equation 32 verifies the safety factor for the 8mm screws, considering 70MPa as its ultimate tensile strength.

$$SF = \frac{70}{\sqrt{\frac{\left(\frac{273{,}68}{\pi \times 8^2}\right)^2}{4} + \frac{\left(\frac{33{,}75}{\pi \times 8^2}\right)^2}{4}}} = 99{,}86 \quad (32)$$

As shown above, the safety factor for these screws is very high at 99,86 guaranteeing the machine won't have structural issues.
After validating both the static stress and deformation simulations, as well as the safety factor for the Z tower plate bolted joint, we can confirm that the machine is structurally capable of operating within the initially projected load limits. Should the machine exceed these limits, the spindle will lack sufficient power to continue operating, resulting in a complete stall of the spindle motor. This will automatically trigger the control board, initiating an emergency stop and preventing any potential damage to the components.

4.2.5 Miscellaneous components

The current state of the Mill is very barebones, there is a lot of room to make the user experience better, adding accessories is a simple way to make the product much more reliable and user-friendly. A major problem with any milling machine is the debris generated during operation, the workpiece chips can quickly make a mess and even cause axis binding if they fall inside the lead screw threads or linear rail paths. This issue is most concerning in the X-axis where the motion components are facing up unprotected, fortunately, it can be solved with bellows. Simply adding four M3x0.5mm threaded holes in the X gantry plate provides the mounting point required for a bellow solution. Fig. 66 illustrates the four threaded holes along with a small printed part design for this use case its technical draw can be found in Fig. 98. Adding M3 threaded heat inserts to the printed part, the user can easily remove the bellows for maintenance.

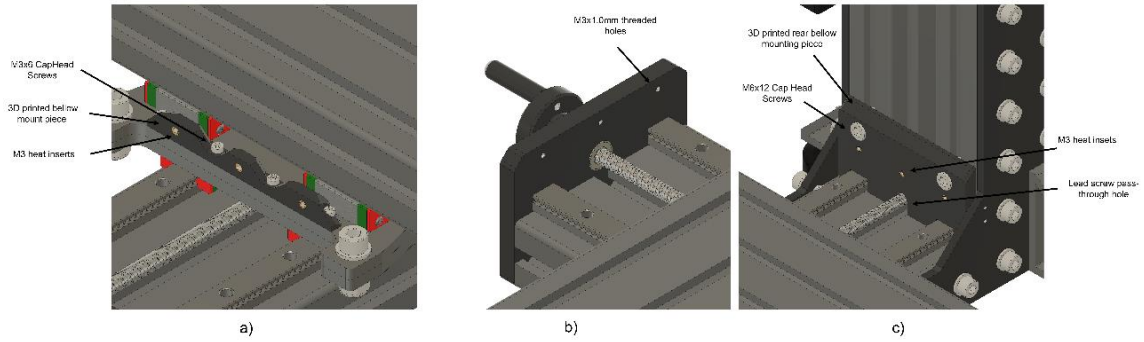

Fig. 66 a) XY Gantry plate 3D printed part for mounting the bellows, M3x1.0 threaded holes were added to the plates to secure the printed part, then by adding M3 threaded heat inserts to the printed part, the user can easily remove the bellows for maintenance. b) Front Y plate with the added M3x0.5 threaded holes to mount the bellow in the front. c) Z tower printed part to secure the bellows in the Z tower while clearing the lead screw and having the M3 heat inserts.

Adding four threaded holes in the front Y plate allows the bellows to be mounted directly to it as demonstrated in Fig. 66. The same concept can be used in the Z tower assembly, a small printed part was designed to secure the bellow, while clearing the lead screw, as shown in Fig. 66 c), its technical draw can be found in Fig. 99. This printed part also used the M3 threaded heat inserts and is secured to the Z tower with M6x12 cap head screws. Fig. 67 shows the bellow pieces off the machine and installed in the Y axis.

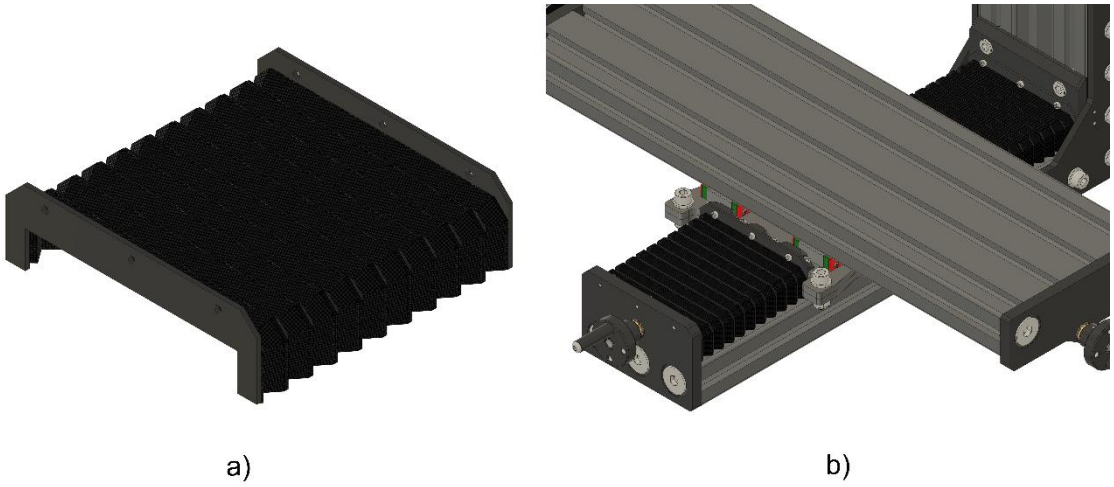

Fig. 67 a) Bellow component. b) front and rear bellow installed to the Y-axis, covering the linear motion components from chips and other debris.

There is still one problematic spot for chips to fall, in between the two Z tower 4080 extrusions, the chips could quickly accumulate there and cause the Y axis to malfunction. To prevent this, an acrylic shield plate will be laser cut and secured to the Z tower assembly, completely sealing the machine from chips. Fig. 68 shows the acrylic plate installed with four M3x16mm Cap Head Screws and 40 series M3 T-nuts. On another note, this machine is subject to high forces and possibly vibrations if not handled correctly, for this reason, it is important that the machine is firmly secured to the workbench. Four brackets will be added to the Y-axis extrusion, providing

the user with mounting options. Since the machine is heavier on the back, 4080 tall brackets will be installed there, while the front will use only 4040 brackets. Fig. 68 shows the brackets installed and the optional rubber feet, in case the user doesn't want to bolt the machine to the workbench. A top cover was designed and 3D printed for the top of the Z tower extrusions, using four M12x12 countersink screws to fix it to the extrusions. The M12x12 Countersink screws are obviously over-dimensioned for the application, but since the 40 series extrusions have an M12 thread inside, it's only logical to use that as a fixation method. Lastly, a fixture plate was designed to provide the user with a flat surface to mount the workpiece, this fixture plate has multiple threaded M6x1.0mm holes to cover a large amount of fixation solutions. Made out of a 10mm aluminium plate, the fixture plate has enough thickness to accommodate the mounting screws, and M6x12 cap head screws that secure it to the X-axis extrusion. This plate was requested with a fine machining resurface to ensure it is flat. Fig. 68 shows the top z tower cover part installed as well as the fixture plate. The technical drawing for this plate can be found in the attachments section, Fig. 89, and the technical drawing for the Z tower cover in Fig. 100.

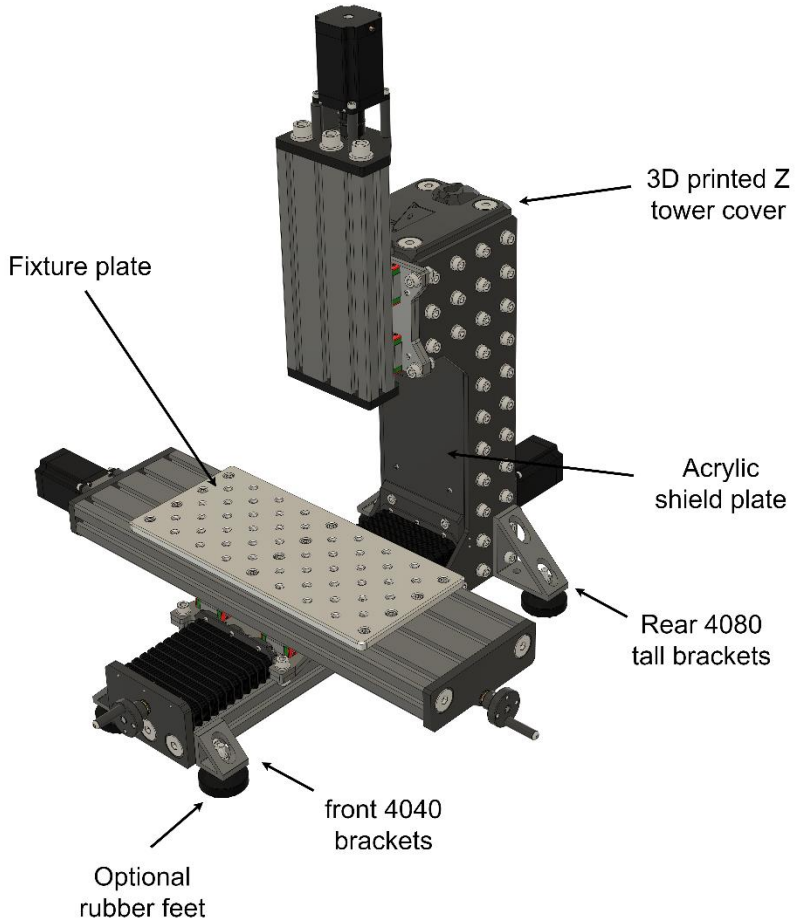

Fig. 68 Mechanical assembly of the Mill machine with the fixture plate, front and rear support brackets, acrylic shield panel, z tower printed part and optional rubber feet.

4.3 Electronics

4.3.1 Controller board

The controller board is responsible for running the firmware and continuously controlling all the electronic components of the machine, such as stepper motors and sensors. Rat Rig is known for its open-source approach, meaning all the projects and firmware are fully open and anyone can experiment with it. Before deciding on a board, it is crucial to choose firmware as it defines the required board microcontroller, one of the easiest out there is FluidNC, an open-source, free-to-download and use firmware. It is also easy to install and set up and even has a web interface, all these topics are enormous selling points as the majority of the users are scared of the firmware and programming languages. Most boards on the market that are easy to set up are a few hundred euros, which is way out of the price tag of this machine kit. For this reason, RatRig was left in a tight spot, going for an off the shelf easy to use and expensive solution, or a cheap but hard to set-up controller board. For these reasons, Bigtreetech was contacted, to develop a custom control board for the Mill. This new board must have an ESP32 processor, allowing it to run FluidNC and GrblHal, two free-to-use and easy to set-up firmware, use a driver capable of extracting the full potential of the nema 23 86mm stepper motors, have at least 5 optical endstop inputs, a probe input, spindle control functions, customisable outputs, display port, microSD card reader, USB, and variable power input, Fig. 69 is a representation of the flow chart of objectives for the new controller board.

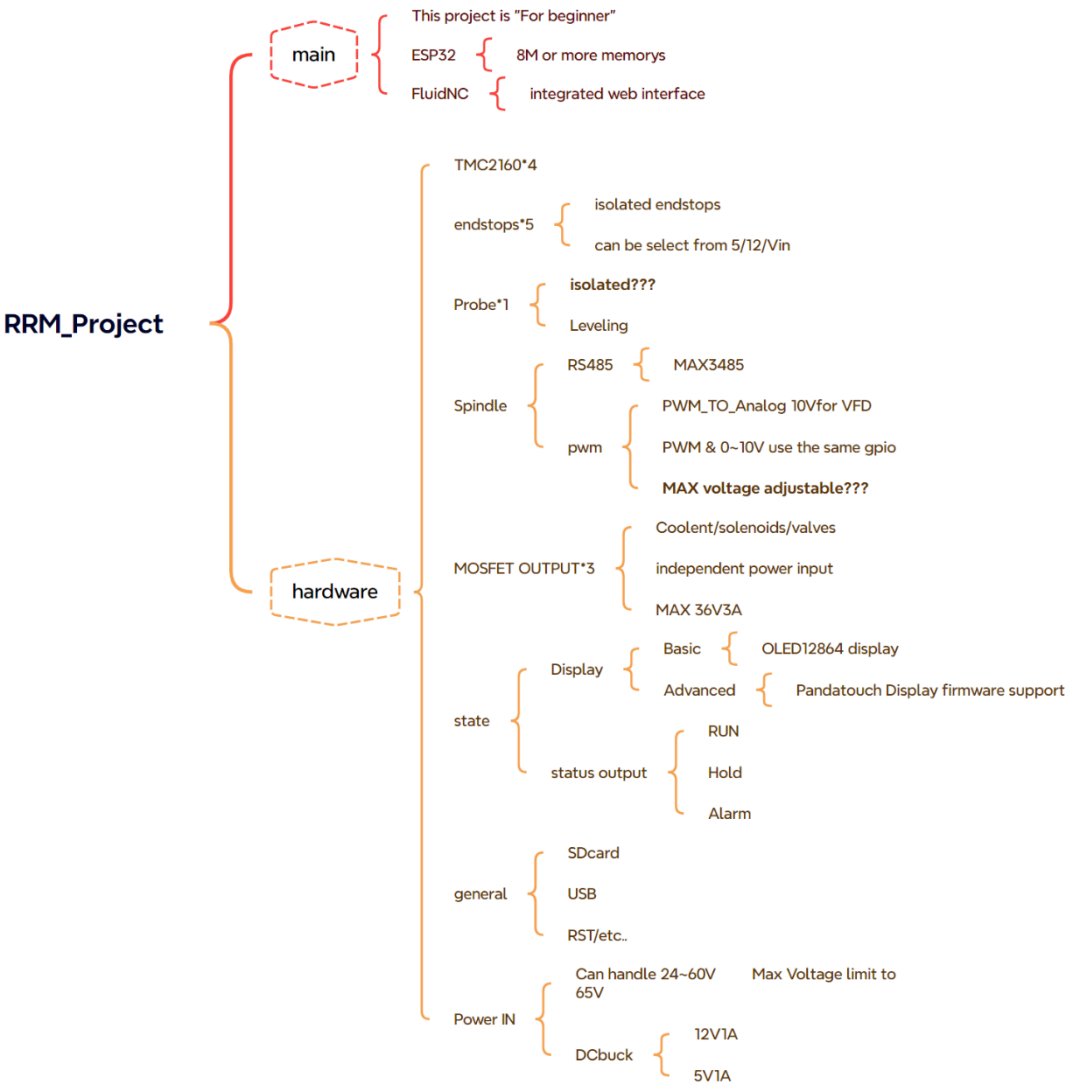

Fig. 69 Flowchart for the Mill controller board requirements, called Rat Rig Mill project at the time, short for RRM project

This board was soon named RodentZ, with the focus of easy set-up for all user levels, meaning it must be beginner-friendly. The first decision was to use the EPS32 processor allowing the board to run on FluidNC with a web interface. Second was the stepper motor drivers, as the powerful nema 23 86mm is rated for 3A, most common stepper drivers such as the TMC2209 can output up to 2A, at first the TMC5160 seemed like the best choice, but they are very complex and have multiple control options that are unavailable on fluidNC like motion planner, this would mean a higher cost for functionality that couldn't be used. Bightreetech then suggested using the TMC2160. The TMC2160 have a step/dir interface with micro-stepping interpolations, allowing for very precise control of the motor, it has a voltage range from 8 to 60V, a serial peripheral interface (SPI) which refers to the use of the SPI communication protocol to control and interface with a stepper motor driver. SPI is a high-speed, synchronous communication protocol that allows data exchange between a master device (like a microcontroller) and one or more slave

devices (such as stepper motor drivers). When stepper motors are controlled via SPI, the motor driver uses this communication channel to receive commands from the master device allowing the microcontroller to set parameters such as current limit and microstepping in real time. Regarding the endstops, inductive proximity endstops will be used on the Mill machine as these sensors don't have mechanical parts to ear or get damaged with milling debris, making them more durable and reliable in the long run. These endstops don't require any type of maintenance, reducing the failure opportunity of the Mill. Rat Rig has the SN04 inductive endstops in stock as illustrated in Fig. 70.

Fig. 70 SN04 inductive endstop.

This endstop has one core disadvantage versus a common mechanical endstop, it is very sensitive to electrical noise if its wires are close to high-power electrical devices such as the stepper motor , stepper motor wires and power supply. These interferences can distort the sensor signal leading to a false trigger or missed detection. To solve this problem, optical isolated endstop inputs were implemented in the RodentZ, by optically isolating the endstop ports, the signal is transferred is not directly connected between the sensor and the control board. This isolates the controller board from any electrical noise, spikes, or ground loops that might be introduced by the sensor's wiring or environment. Electrical noise such as switching noise from motors or power supplies, that could otherwise travel through the signal wiring is blocked by the optical isolator, which only transfers the optically encoded signal to the controller, preventing false triggering or misreading. Moving to the probe input, like any other CNC mill machine, a touch probe is essential to correctly position the workpiece and set the work coordinates for the specific job, illustrated in Fig. 71.

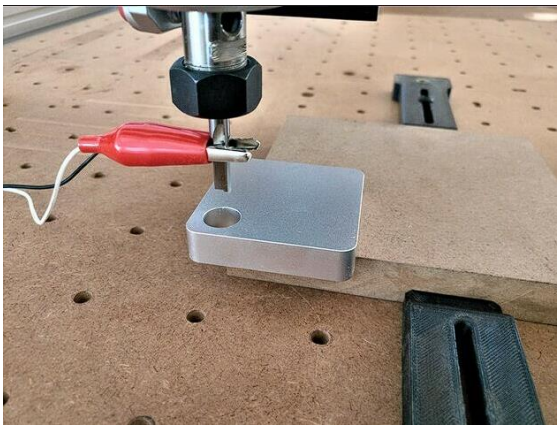

Fig. 71 CNC touch probe to define the work coordinates, using an alligator clip to close the circuit between the probe body and the endmill (3DPrintronics, n.d.)

These probes work by closing an electronic contact between the probe body and the endmill, which is connected to the same signal via a generic alligator clip or a magnet. Regarding the spindle control, The RodentZ must have a 0-10V PWM output, allowing it to externally control the speed of the spindle, additionally, a RS485 port was added to enable a more advanced user to take advantage of the variable frequency driver (VFD) spindle controller, as this communication protocol allows the feedback of information such as actual spindle speed, status messages and error communication. This control protocol has numerous benefits against the simple PWM 0-10V spindle control, although the PMW method is much simpler to set up and use, making it ideal for a beginner user. A VFD plus 2.2KW spindle combo can be observed in Fig. 72 a), in Fig. 72 b) the AMB router with PWM spindle speed control can be observed, this router doesn't require a VFD and can be controlled via the RodentZ board, Fig. 72 c) shows the Rat Rig router, the cheapest of the three options, it doesn't have electronic speed control, the user must regulate the speed via the mechanical potentiometer in the router itself. The Mill was designed to take full advantage of the 2.2KW spindle plus VFD combination, but offers more options, providing different price points and application requirements.

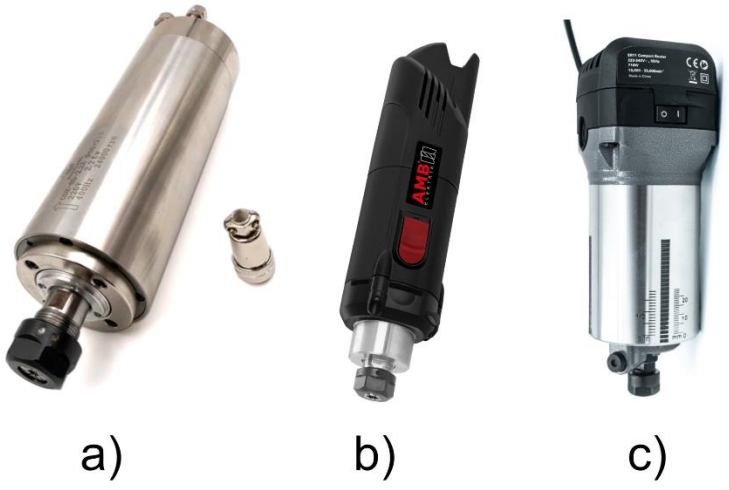

Fig. 72 a) 2.2KW spindle b) AMB router c) Rat Rig router

The RodentZ also has multiple output ports, for coolant, solenoid valves, safety sensors, vacuum, and water pump, at a maximum of 36V 3A, allowing the user to customize their set-ups for the specific job. Additionally, a display port was added, providing an additional layer of convenience for the user, support for a basic OLED 12864 display and the panda touch was added, both options are represented in Fig. 73.

Fig. 73 a) OLED 12864 basic display (Future Electronics, n.d.) b) Panda touch display (3DJake, n.d.)

The RodentZ also has capability for a microSD card, capable of flashing firmware and storing data, as well as a reset button. Pivoting to power input, the Rodent support a power input from 24 to 65V. All the power rails for the board can be individually adjusted by the jumpers on the right lower corner of the board pin-out map in Fig. 74. The pinout map is extremely useful when configuring the firmware, as we can specify inside the config which ports the firmware must access to control a specific component.

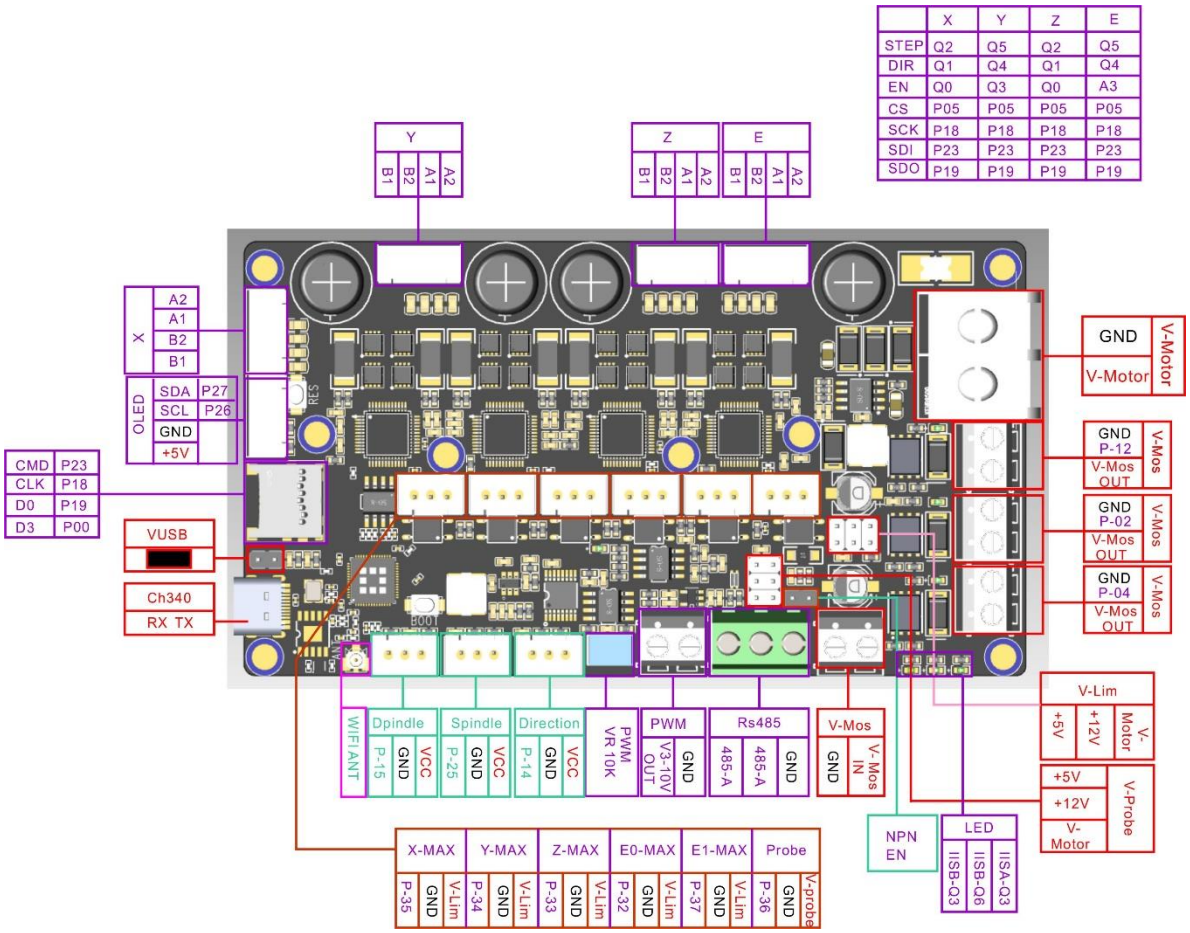

Fig. 74 RodentZ board pinout map, with the specific config ports for each connector and jumper on the board.

4.3.2 Power system

Choosing the right power supply for the machine is crucial to ensure all components have the needed supply to perform with reliability, efficiency and safety. Firstly, the voltage rating, the RodentZ has an input from 24 to 65V, which then gets redistributed to all components. The most commonly used power supply in the 3D printing and CNC Rat Rig products is 24V, for this reason, a 24V power supply will be used. The most demanding components are the stepper motors, at 3A per phase and 3.6V per phase, those steppers work with 2 phases at any given moment, the power per phase can be calculated using Ohm's law in equation 26:

$$P_{per\ phase} = V_{per\ phase} \times I_{per\ phase} = 3.6 \times 3 = 10.8\ W \quad (26)$$

Since the stepper motor operates with two phases, it consumes double the power, at a total of 21.6 W. The mill uses 3 nema 23 86mm, so the total stepper motor power consumption is 64.8 W. Each endstop requires 0.864 W according to the datasheet, while the RodentZ board uses 6.3W according to the manual, making a total power consumption of 73.69 W. Considering an overall system efficiency of 80% to be conservative, the basic set-up without any external accessories

requires at least 88.43 W. The power supply with the least power setting Rat rig has in stock is 75W, not meeting the required power previously determined. The next power supply in line is 200W, ensuring 111.57 W remaining for external accessories. The Mill will use the Meanwell LRS 200W 24V 8.8A exposed in Fig. 75. The wires transmitting the power from the PSU (power supply), to the RodentZ board will carry 24V at a maximum of 8.8A, the recommended wire cross-section of 0.518mm² according to the American wire gauge norms or 20 AWG, for a 20cm copper wire.

Fig. 75 Meanwell LRS 200W 24V power supply used in the Mill.

An IEC will deliver the mains power to the PSU the Meanwell LRS 200W is rated up to 8.8A, the common Rat Rig IEC is rated for 10A of continuous draw, making it the perfect candidate for this application, it also has a 10A built-in fuse to protect the PSU from problems in the mains circuit. The wires transmitting the mains power from the IEC to the PSU will handle 8.8 A at 230V, according to the American wire gauge norms, for a copper wire at 20cm, a 0.518mm² cross-section wire is recommended, or a 20AWG wire.

4.3.4 Electronics enclosure

The electronics enclosure will ensure all components have a proper place to be assembled and work, safely from chips and milling debris. The power supply and RodentZ board will be inside the enclosure, along with an IEC to connect the mains power and a cooling fan. This enclosure must be compact enough to fit on the Mill Z tower assembly, similar to a backpack. The cooling fan was installed on the bottom panel, pushing fresh air in between the control board and the power supply, as well as creating an outward flow in the top panel grill, preventing debris from falling into the enclosure. The panels will be 2.5mm laser-cut acrylic, joined together with 3D printed corners with M3 threaded heat inserts, Fig. 76 shows the open enclosure with all the components inside, while Fig. 77 shows the Mill with the electronics enclosure installed on the Z tower frame. The technical draws for the rear enclosure panel can be found in Fig. 91, the right panel can be found in Fig. 92, the left side panel in Fig. 93, the bottom air intake panel in Fig. 94, the top exhaust panel in Fig. 95 and the cover panel in Fig. 96. The 3D printed corner can also be found in Fig. 97.

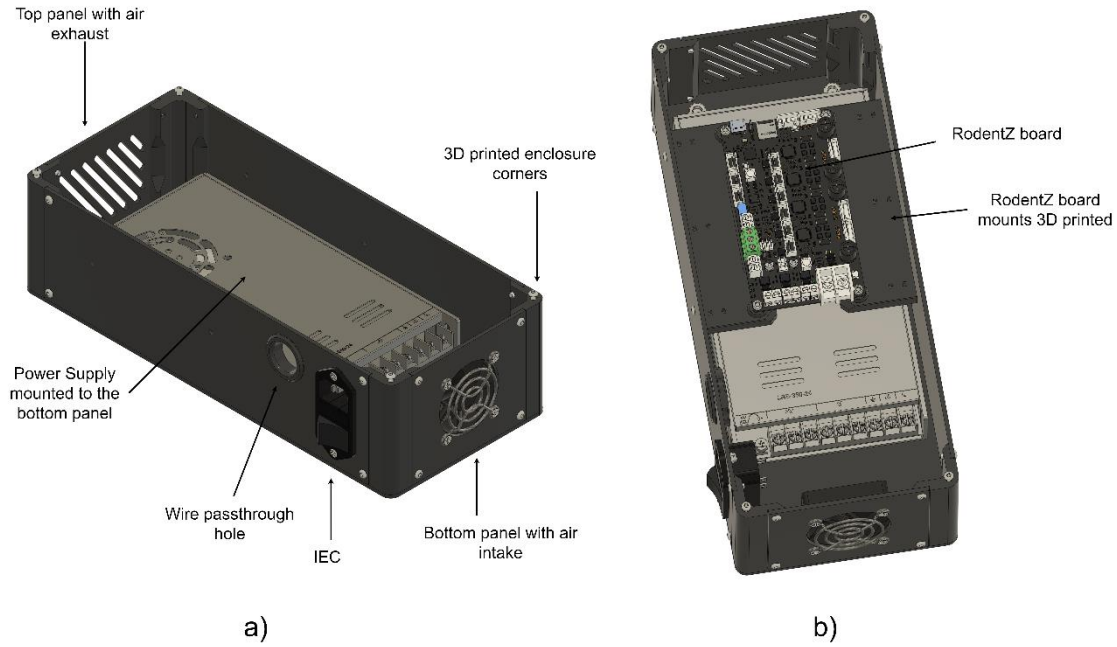

Fig. 76 a) Mill electronics enclosure hosting the power supply, RodentZ board, IEC and cooling fan, made out of acrylic panels and 3D printed corners. b) Mill electronics enclosure with RodentZ control board mounted to its 3D printed mounts, with M3 threaded heat inserts.

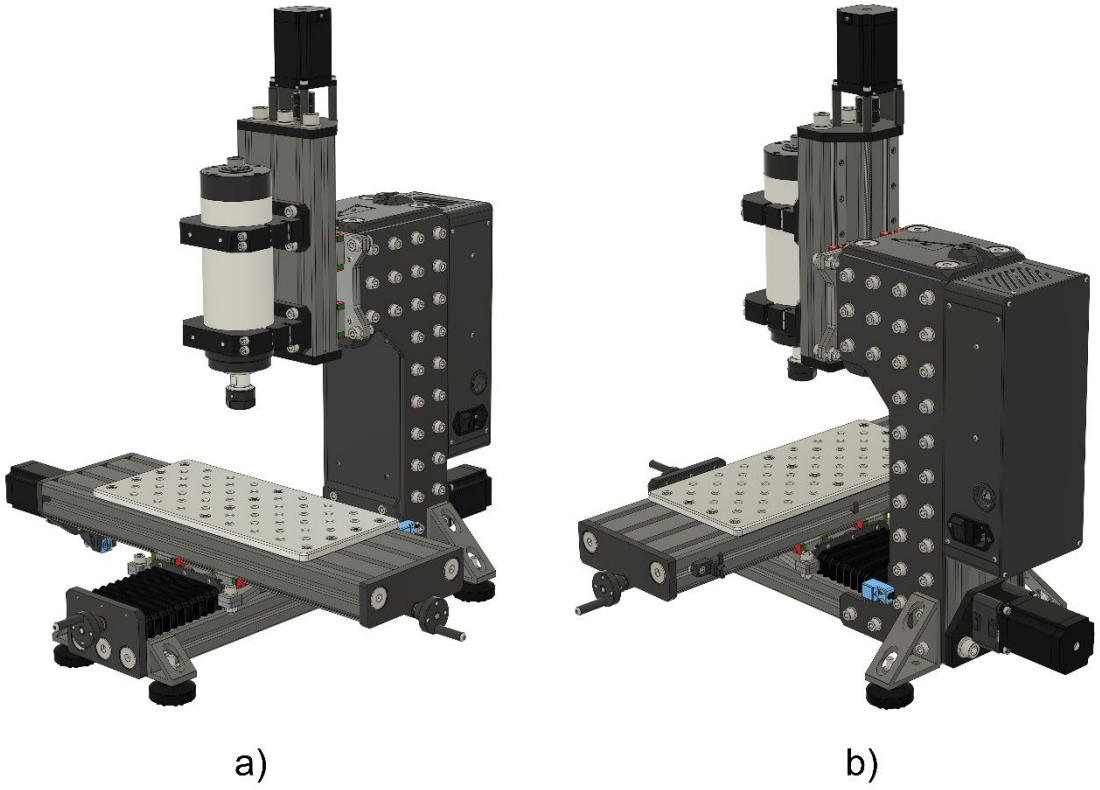

Fig. 77 a) Front isometric view of the Mill with the electronics enclosure installed on the Z tower. b) Rear isometric view of the Mill with the electronics enclosure backpack.

5. Prototype assembly

The assembly of the first prototype presented in Fig. 78, was done with bare aluminium, all aluminium plates and acrylic panels were cut in the Rat Rig workshop as well as the linear rails, lead screws and t-slot extrusions, as the length were custom-made for this machine. This first prototype is essential to ensure all custom parts are accurate and there are no fitment or interference issues before sending all parts to production. Unfortunately, the 2.2KW spindle isn't in stock and the first prototype was assembled with the Rat Rig router. Fig. 79 gives a detailed view of the front Y-axis plate assembly, with the bearings installed and jog wheel, the XY gantry assembly can be also observed along with the 10mm fixture plate on top of the x extrusion. The electronics enclosure fits nicely on the back of the machine as Fig. 80 demonstrates, it can be assembled outside of the machine and only then installed on the back of the Mill. The inside of the electronics enclosure is easily accessible from the back of the machine, allowing the user to perform maintenance or troubleshooting of the connections as Fig. 81 shows.

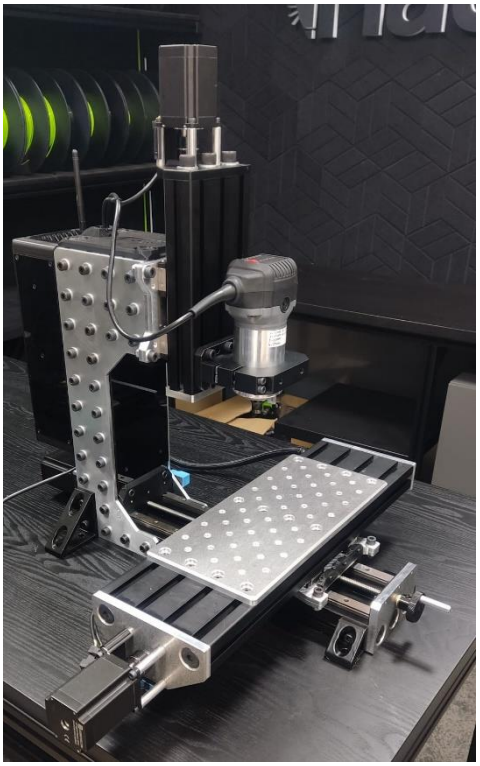

Fig. 78 First Mill machine prototype, made in-house, to test geometries, fitment and tolerances.

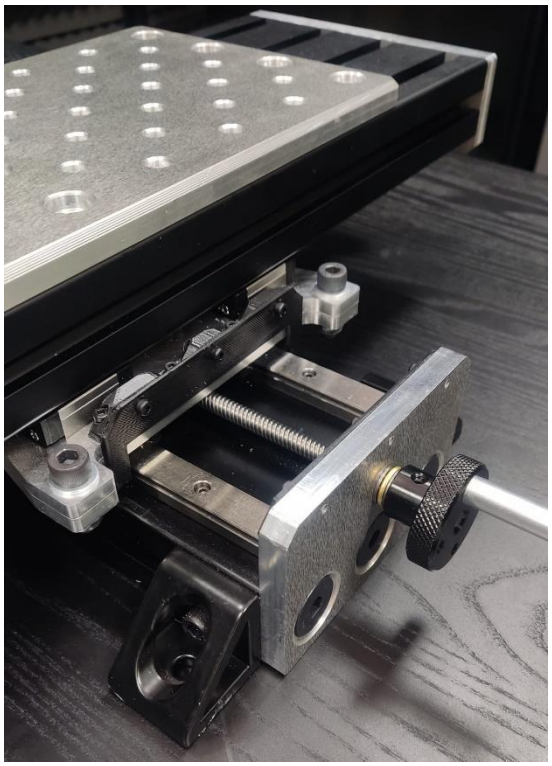

Fig. 79 Front of the Mill, where the Y front plate is installed with the bearings, jog wheel, full gantry plate assembly and fixture plate on top of the X extrusion.

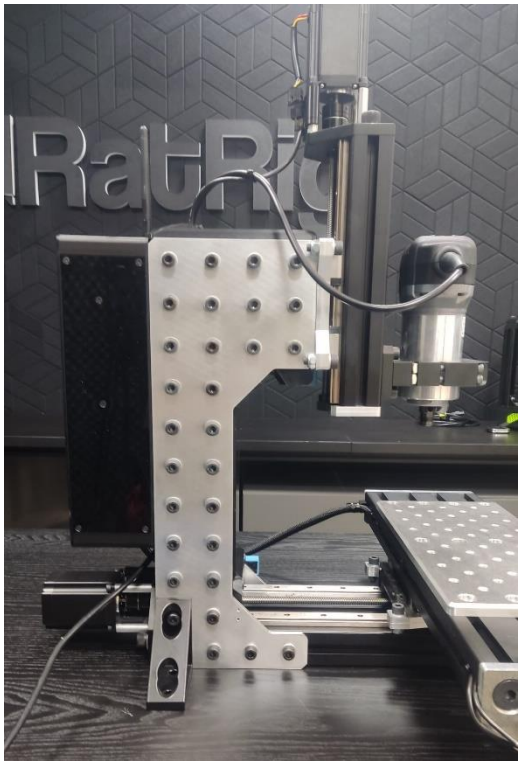

Fig. 80 Side view of the Mill prototype, where the tower Z plates can be observed, along with the electronics enclosure on the back of the assembly

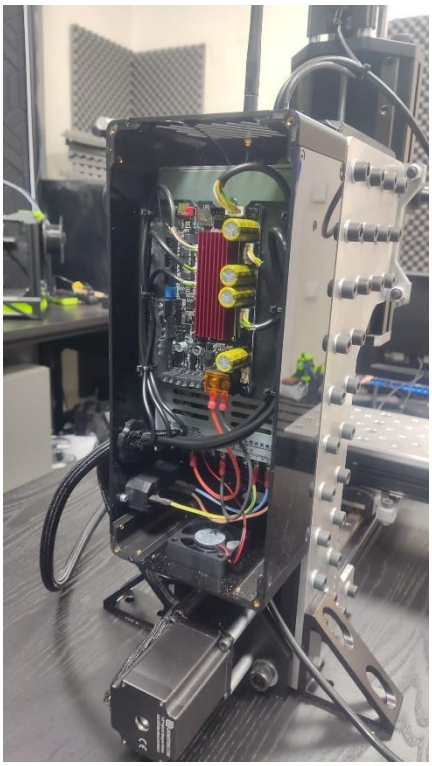

Fig. 81 Electronics enclosure without the cover, allowing the access of the electronics components.

6. Conclusion

In conclusion, this master's thesis presents the complete development of a fully open-source desktop milling machine, including all aspects from mechanical design to component selection and electronics analysis. The project aimed to deliver a high-performance, cost-effective solution, accessible to a wide range of users, from hobbyists to small-scale manufacturers. The mechanical dimensions were calculated and optimised to ensure precision and stability, while the selection of components, including motors, drivers, and control systems, was based on detailed analysis to balance performance, reliability, and affordability. The internal experience gained from working with Rat Rig was incredibly helpful throughout the decision-making process. Their expertise in precision machinery and open-source hardware design guided key decisions in component selection and system integration, which ultimately enhanced the overall performance and versatility of the machine. By sourcing components from Rat Rig, the project ensures that parts are not only high-quality but also readily accessible to the wider maker community. Looking ahead, this project presents significant opportunities for future improvements, particularly in the assembly process. The open-source nature of the machine invites the community to contribute with modifications, upgrades, and optimisations, enhancing mechanical precision, introducing new features, or developing alternative components. This dynamic potential for community-driven innovation promises a vibrant ecosystem around the milling machine, with users tailoring it to their specific needs. This project not only provides a valuable resource for users today but also sets the stage for continuous evolution, driven by the open-source community's collective knowledge and passion for innovation.

6.2 Future work

To facilitate the machine's open-source release, there are remaining documents to be completed, including a detailed assembly guide, wiring guide, and a comprehensive commissioning guide. These documents will ensure that users can easily assemble and configure the machine. Once finalized, this complete kit will allow users to build, customize, and expand upon the design, inspiring further development and creativity within the community.

Bibliography

3DJake. (n.d.). *Panda Touch V1.0*. Retrieved September 20, 2024, from https://www.3djake.pt/bigtreetech/panda-touch-v10

3DPrintronics. (n.d.). *XYZ Corner Finding Touch Probe*. Retrieved September 21, 2024, from https://www.3dprintronics.com/products/xyz-corner-finding-touch-probe

Abd Rahman, Z., Mohamed, S. B., Minhat, M., & Abd Rahman, Z. (2023). Design and development of 3-axis Benchtop CNC milling machine for educational purpose. *International Journal of Integrated Engineering*, *15*(1), 145–160.

Akinnuli, O. B., Balogun, V. A., & Akintayo, T. C. (2015). Design of a Keypad Operated CNC Drilling Router. *International Journal of Engineering Research and General Science*.

Anania, F. D., Pena, A. E., & Canarache, R. M. (2021). Research of design an educational modular 5 axis milling machine. *IOP Conference Series: Materials Science and Engineering*, *1037*(1), 12006.

Avantec. (n.d.). *Face milling cutters and finishing cutters*. Retrieved September 23, 2024, from https://www.avantec.de/products/face-milling-cutters/

Boothroyd, G. (1988). *Fundamentals of metal machining and machine tools* (Vol. 28). Crc Press.

Burek, J., Plodzien, M., Zylka, L., & Sulkowicz, P. (2019). High-performance end milling of aluminum alloy: Influence of different serrated cutting edge tool shapes on the cutting force. *Advances in Production Engineering & Management*, *14*(4), 494–506.

Carlsson, B. (1984). The development and use of machine tools in historical perspective. *Journal of Economic Behavior & Organization*, *5*(1), 91–114. https://doi.org/https://doi.org/10.1016/0167-2681(84)90028-3

Chaoji, P., & Martinsuo, M. (2019). Creation processes for radical manufacturing technology innovations. *Journal of Manufacturing Technology Management*, *30*(7), 1005–1033.

Cheng, X., Yang, X. H., Li, L., & Liu, J. Y. (2014). Design of a three-axis desktop micro milling machine tool. *Key Engineering Materials*, *589*, 735–739.

Future Electronics. (n.d.). *OLED Graphic Display 128x64 Serial I2C 0.96 inch*. Retrieved September 23, 2024, from https://store.fut-electronics.com/products/oled-graphic-display-128x64-serial

Gupta, S., Dangayach, G. S., Singh, A. K., Meena, M. L., & Rao, P. N. (2018). Implementation of sustainable manufacturing practices in Indian manufacturing companies. *Benchmarking: An International Journal*, *25*(7), 2441–2459.

Hiwin. (n.d.). *Sizing project*. Retrieved September 23, 2024, from https://www.hiwin.de/en/projects/newSizingProject/GW

Hoffmann, F., Lee, D. S., & Lemieux, T. (2020). Growing income inequality in the United States and other advanced economies. *Journal of Economic Perspectives*, *34*(4), 52–78.

Koenigsberger, F., & Tlusty, J. (2016). *Machine tool structures*. Elsevier.

Krimpenis, A. A., & Iordanidis, D. M. (2023). Design and analysis of a desktop multi-axis hybrid milling-filament extrusion CNC machine tool for non-metallic materials. *Machines*, *11*(6), 637.

Lee, Y., Resiga, A., Yi, S., & Wern, C. (2020). The optimization of machining parameters for milling operations by using the Nelder–Mead simplex method. *Journal of Manufacturing and Materials Processing*, *4*(3), 66.

Liang, S., Rajora, M., Liu, X., Yue, C., Zou, P., & Wang, L. (2018). Intelligent manufacturing systems: a review. *International Journal of Mechanical Engineering and Robotics Research*, *7*(3), 324–330.

LILY. (n.d.-a). *688zz Metric Standard*. Retrieved September 23, 2024, from https://www.lily-bearing.com/products/688zz/

LILY. (n.d.-b). *F8-16M Miniature Bearing*. Retrieved September 23, 2024, from https://www.lily-bearing.com/products/f8-16m/

Maiyar, L. M., Ramanujam, R., Venkatesan, K., & Jerald, J. (2013). Optimization of machining parameters for end milling of Inconel 718 super alloy using Taguchi based grey relational analysis. *Procedia Engineering*, *64*, 1276–1282.

Mark Carew. (2019, December 13). *OpenBuilds MiniMill*. Build in "CNC ROUTER."

Martins, J. M. Q. (2015). *A Evolução da Arte da Guerra: Da 1ª a 4ª Geração*. XII Curso.

Mekanika. (n.d.). *End Mill Selection Guide*. Retrieved July 24, 2024, from https://www.mekanika.io/blog/learn-1/end-mill-selection-guide-4?srsltid=AfmBOoq0GsjSNrb1V4-hxRcxbPrb6s98S3_UvIBtYhXQbPm4sajTFfEJ

MilleniumMills. (n.d.). *MILO-V1.5*. Retrieved July 4, 2024, from https://github.com/MillenniumMachines/Milo-v1.5

Pitt, C., Park, A., & McCarthy, I. P. (2021). A bibliographic analysis of 20 years of research on innovation and new product development in technology and innovation management (TIM) journals. *Journal of Engineering and Technology Management*, *61*, 101632.

Rat Rig. (n.d.). *T-SLOT 4040 B-Type*. Retrieved September 23, 2024, from https://ratrig.com/aluminium-profiles/t-slot-40-b-type/t-slot-4040-b/t-slot-4040-b-type.html

Ro, S.-K., Jang, S.-K., Kim, B.-S., & Park, J.-K. (2008). Development of a miniature vertical milling machine for automation used in a microfactory. *2008 International Conference on Smart Manufacturing Application*, 186–189.

SEVIC, M., & KELLER, P. (2019). DESIGN OF CNC MILLING MACHINE AS A BASE OF INDUSTRY 4.0 ENTERPRISE. *MM Science Journal*.

Shaw, M. C., & Cookson, J. O. (2005). *Metal cutting principles* (Vol. 2, Issue 3). Oxford university press New York.

Siddhartha, B., Chavan, A. P., HD, G. K., & Subramanya, K. N. (2021). IoT enabled real-time availability and condition monitoring of CNC machines. *2020 IEEE International Conference on Internet of Things and Intelligence System (IoTaIS)*, 78–84.

Speedtiger. (n.d.). *End Mill Size Standards Chart & Introduction*. Retrieved September 23, 2024, from https://www.speedtigertools.com/solution/ins.php?index_id=100

Stephenson, D. A., & Agapiou, J. S. (2018). *Metal cutting theory and practice*. CRC press.

SYIL. (2023, December 28). *Desktop CNC Mill vs. Traditional Milling Machines*.

U.S. Chamber of Commerce. (2022). *Empowering Small Business.The Impact of Technology on U.S. Small Business*.

Usher, A. P. (1961). History of the Milling Machine: A Study in Technical Development by Robert S. Woodbury. *Technology and Culture*, *2*(1), 43–44.

Wang, M., Gao, L., & Zheng, Y. (2014). An examination of the fundamental mechanics of cutting force coefficients. *International Journal of Machine Tools and Manufacture*, *78*, 1–7.

Wayken. (2022, October 21). *What is Helix Angle & How to Choose It in Machining*. https://waykenrm.com/blogs/helix-angle-in-machining/

Attachments

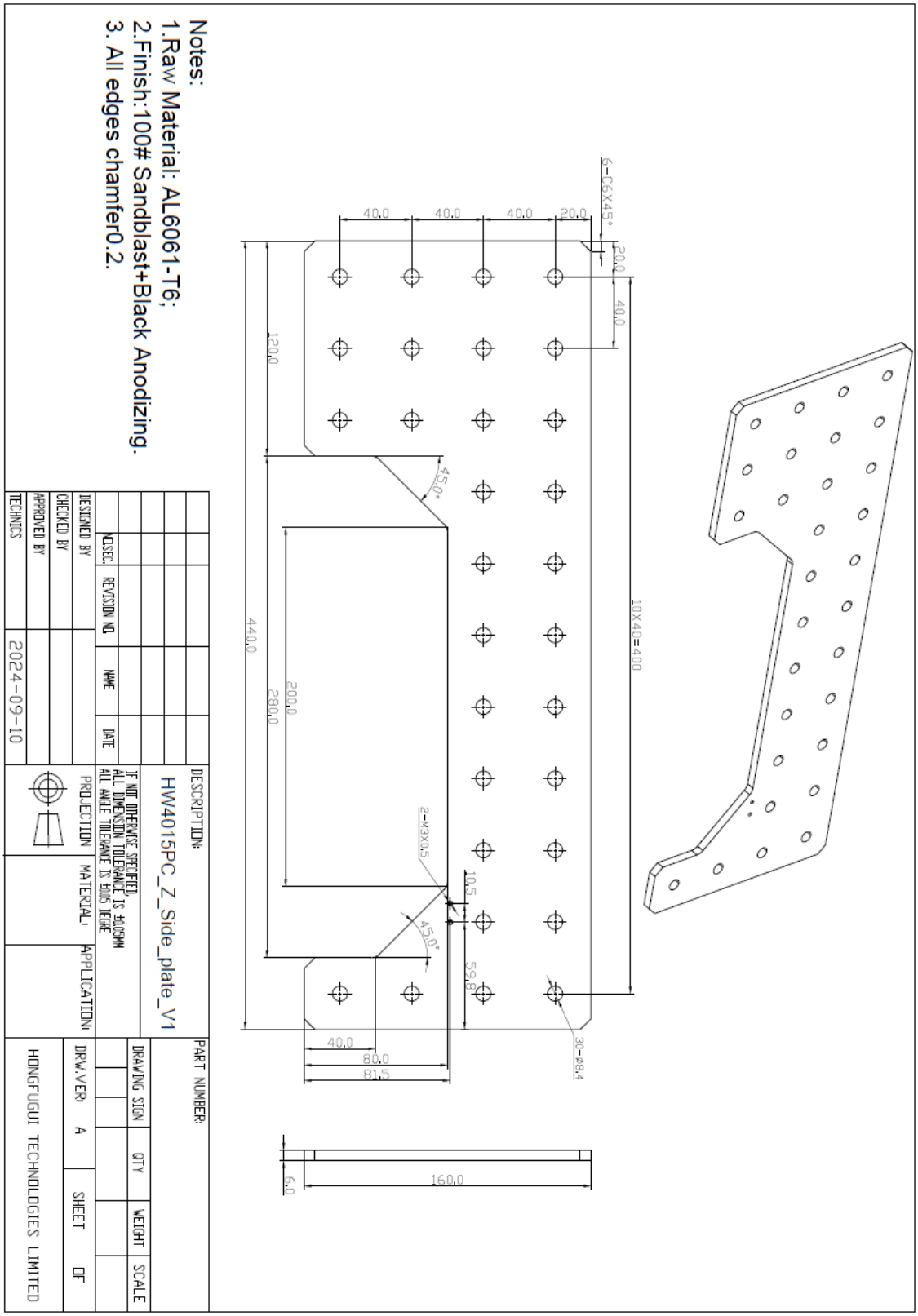

Fig. 82 Z tower plate technical draw by the manufacturer.

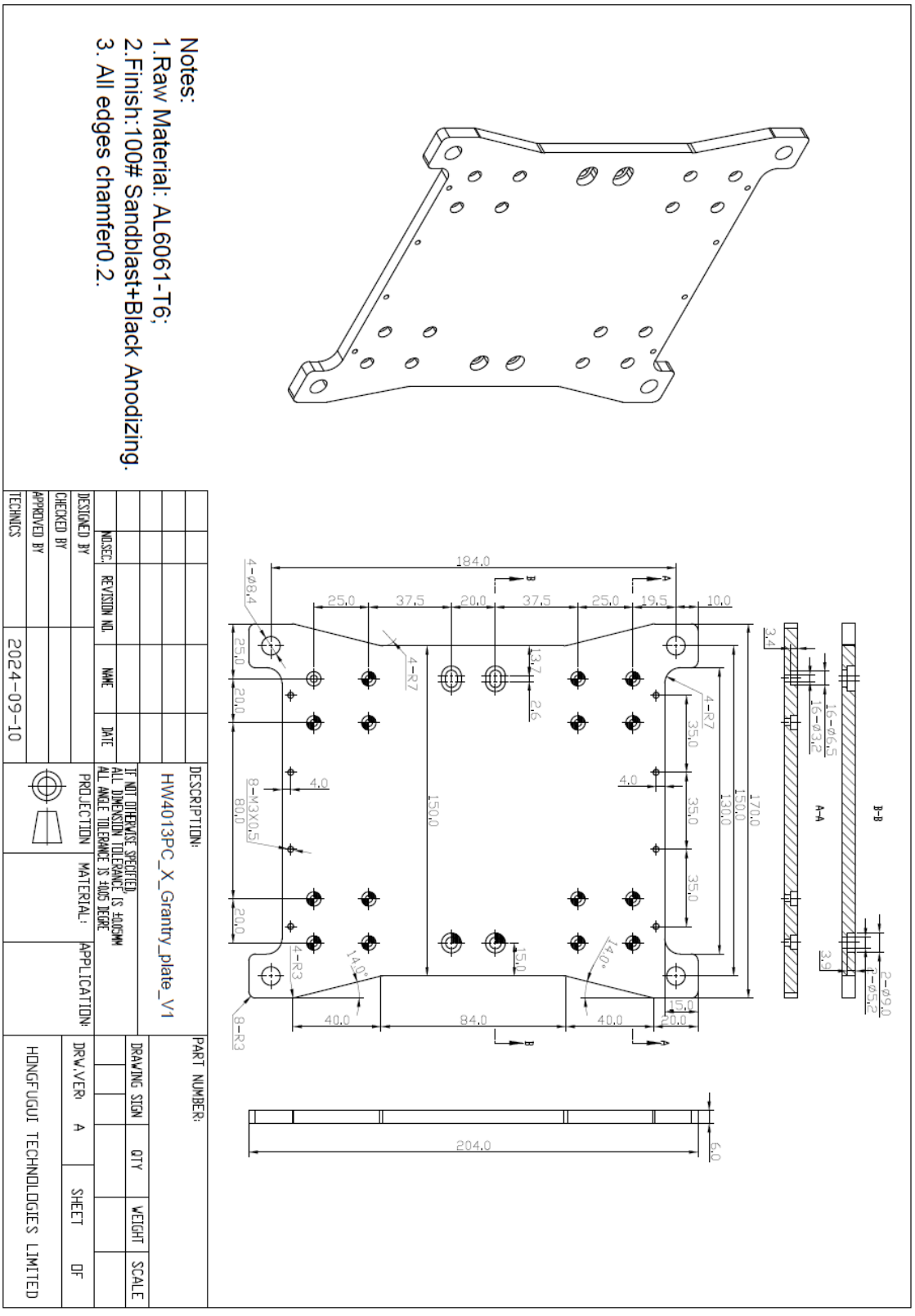

Fig. 83 X gantry plate technical draw by the manufacturer.

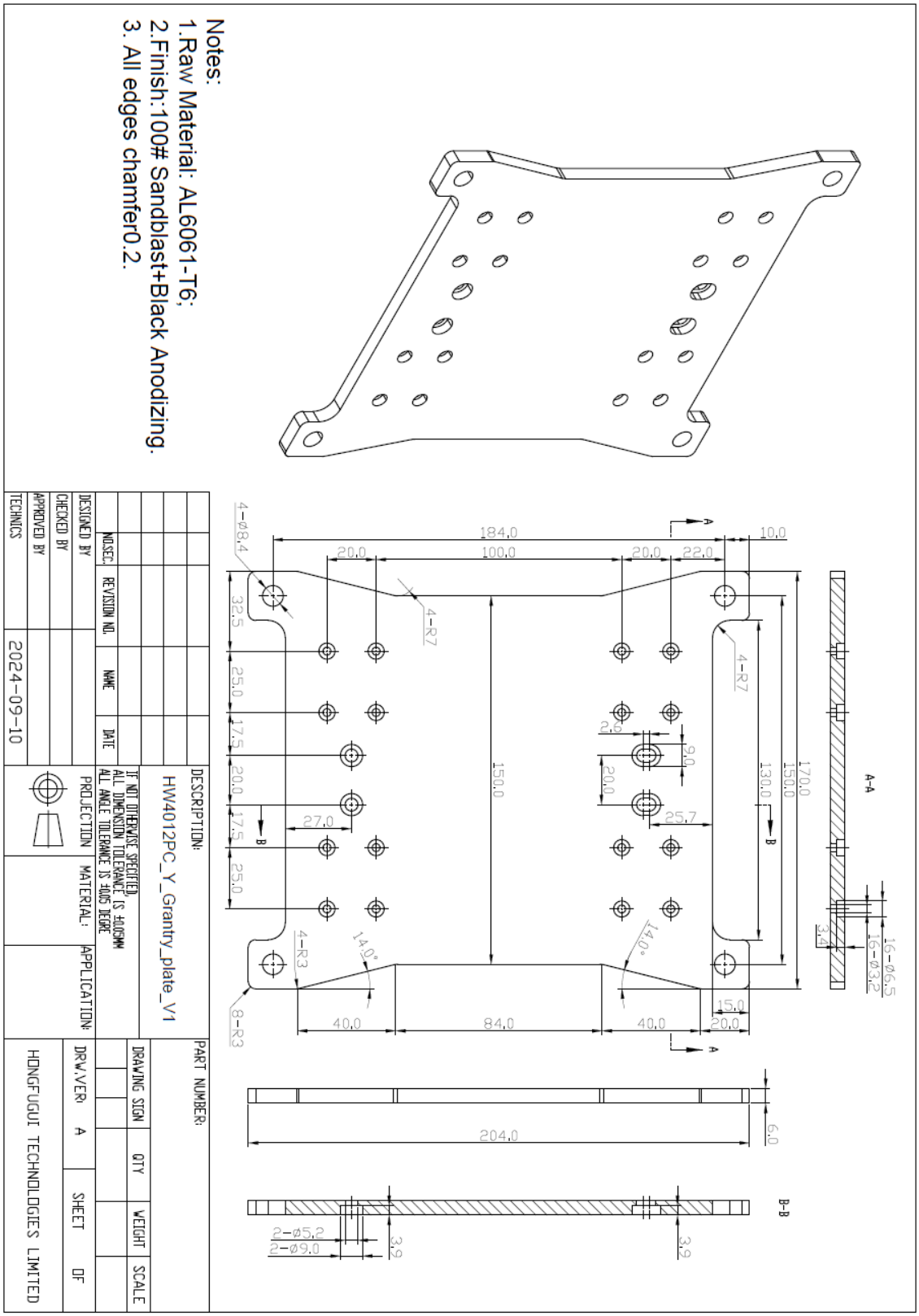

Fig. 84 Y Gantry plate technical draw by the manufacturer.

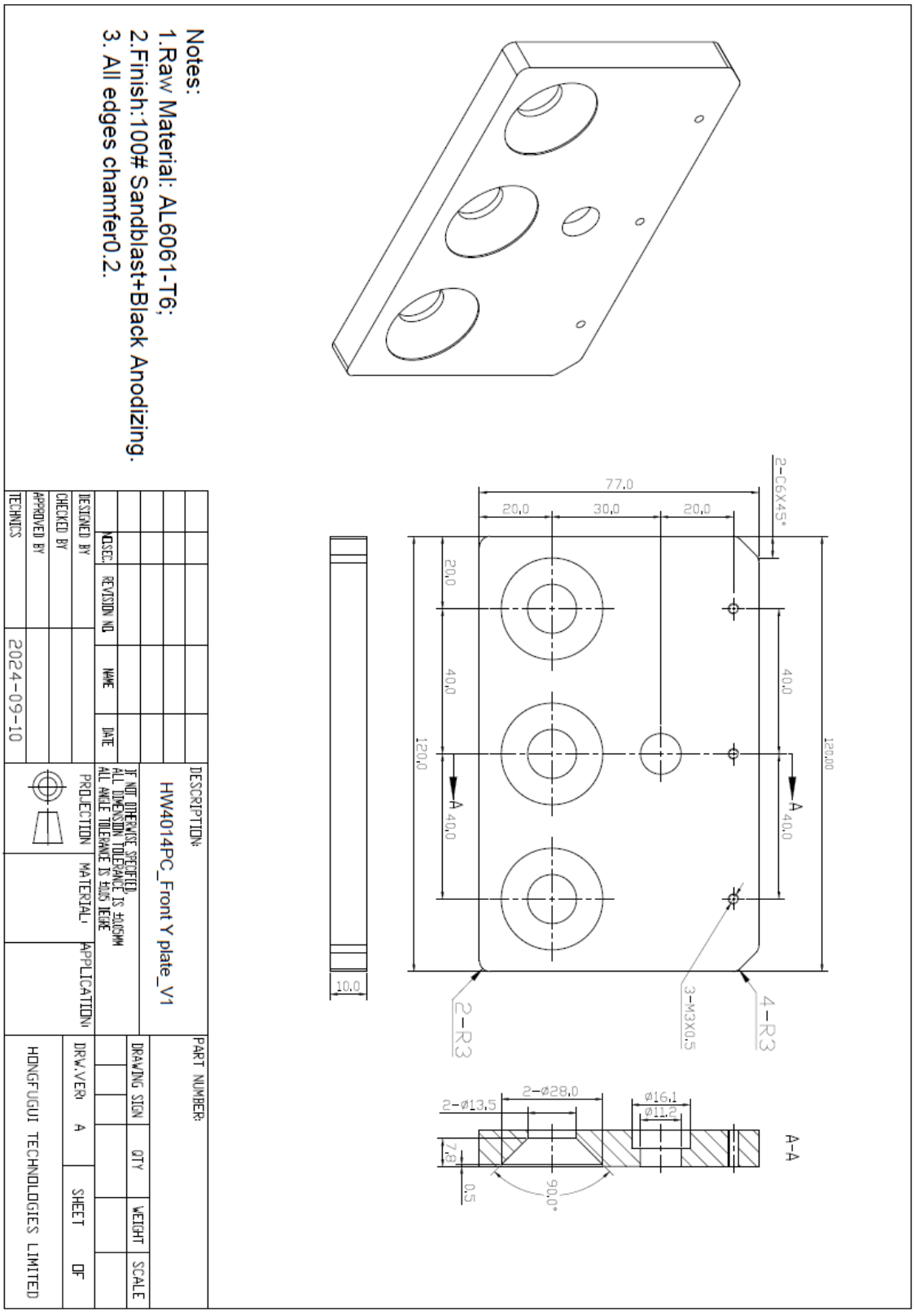

Fig. 85 Y front plate technical draw by the manufacturer.

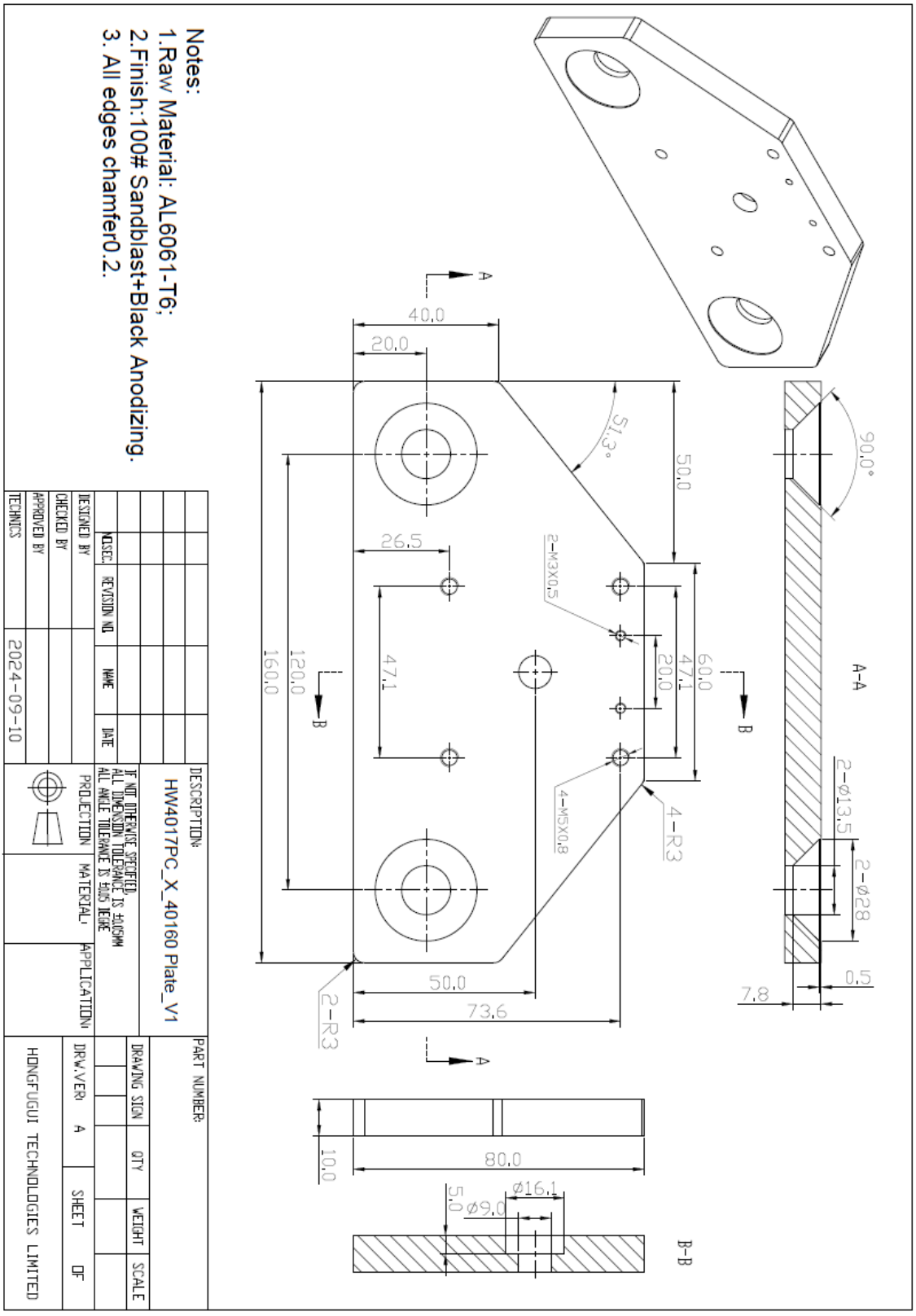

Fig. 86 40160 stepper plate technical draw by the manufacturer.

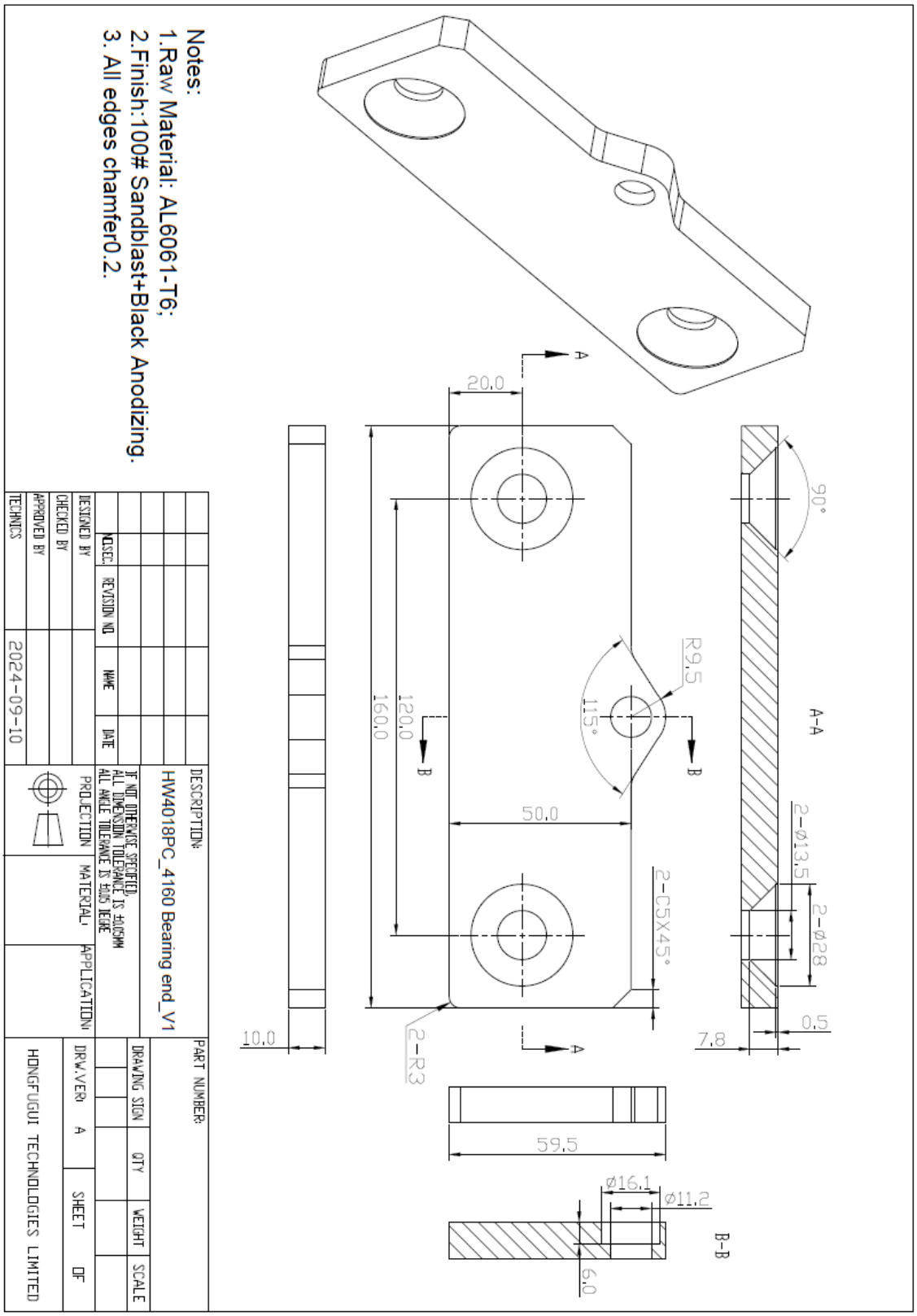

Fig. 87 40160 bearing end plate technical draw by the manufacturer.

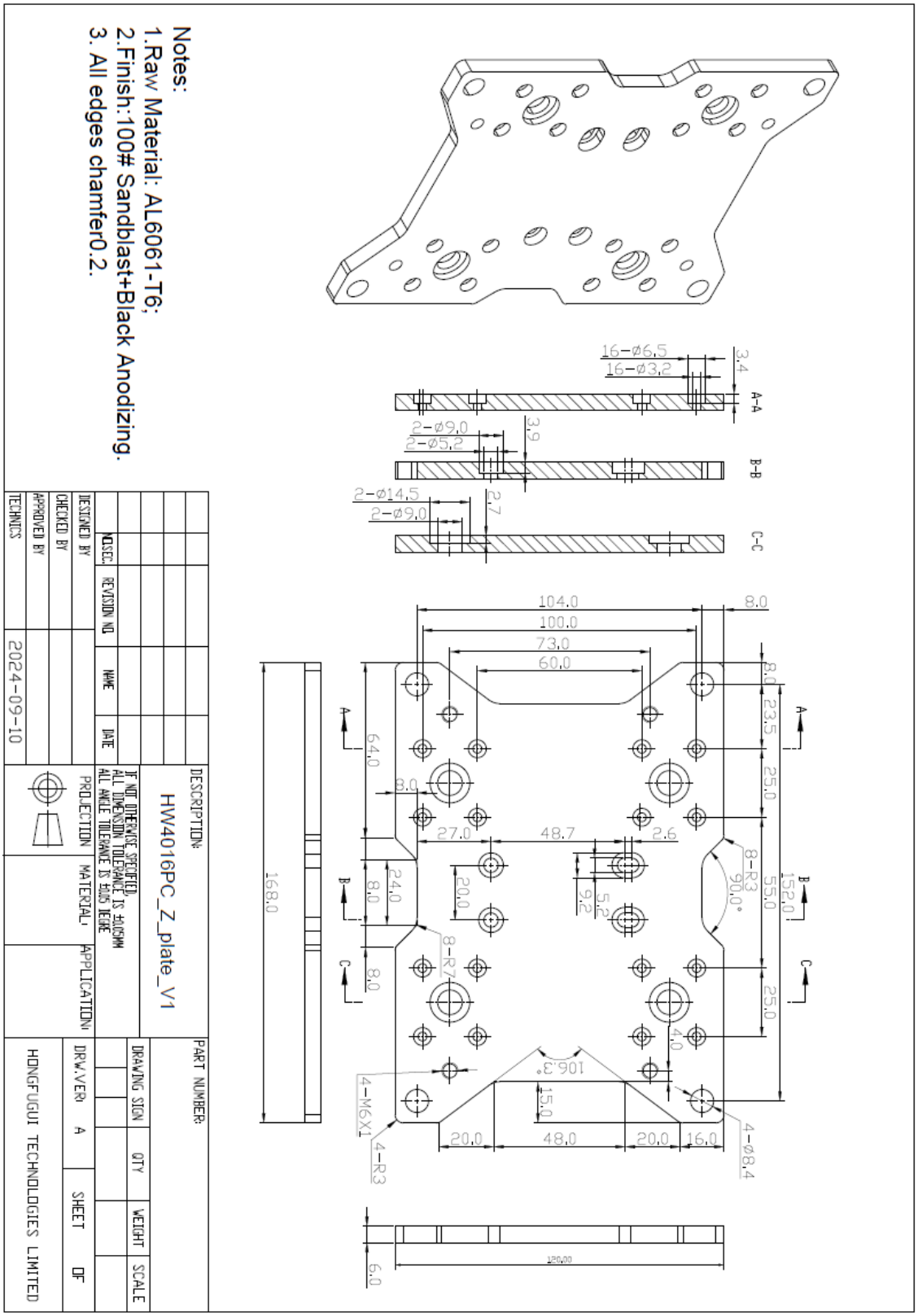

Fig. 88 Z plate technical draw by the manufacturer.

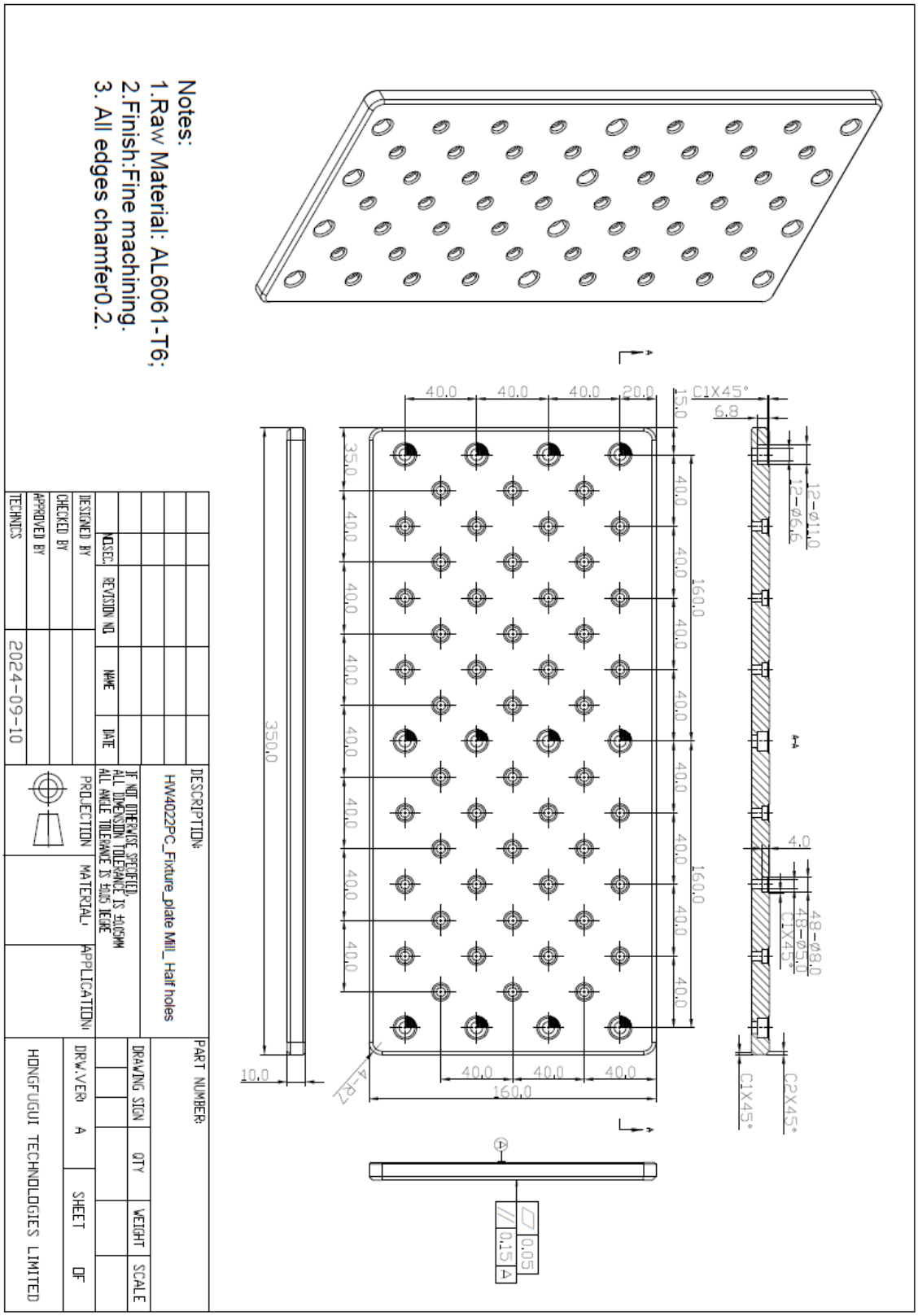

Fig. 89 Fixture plate technical draw by the manufacturer.

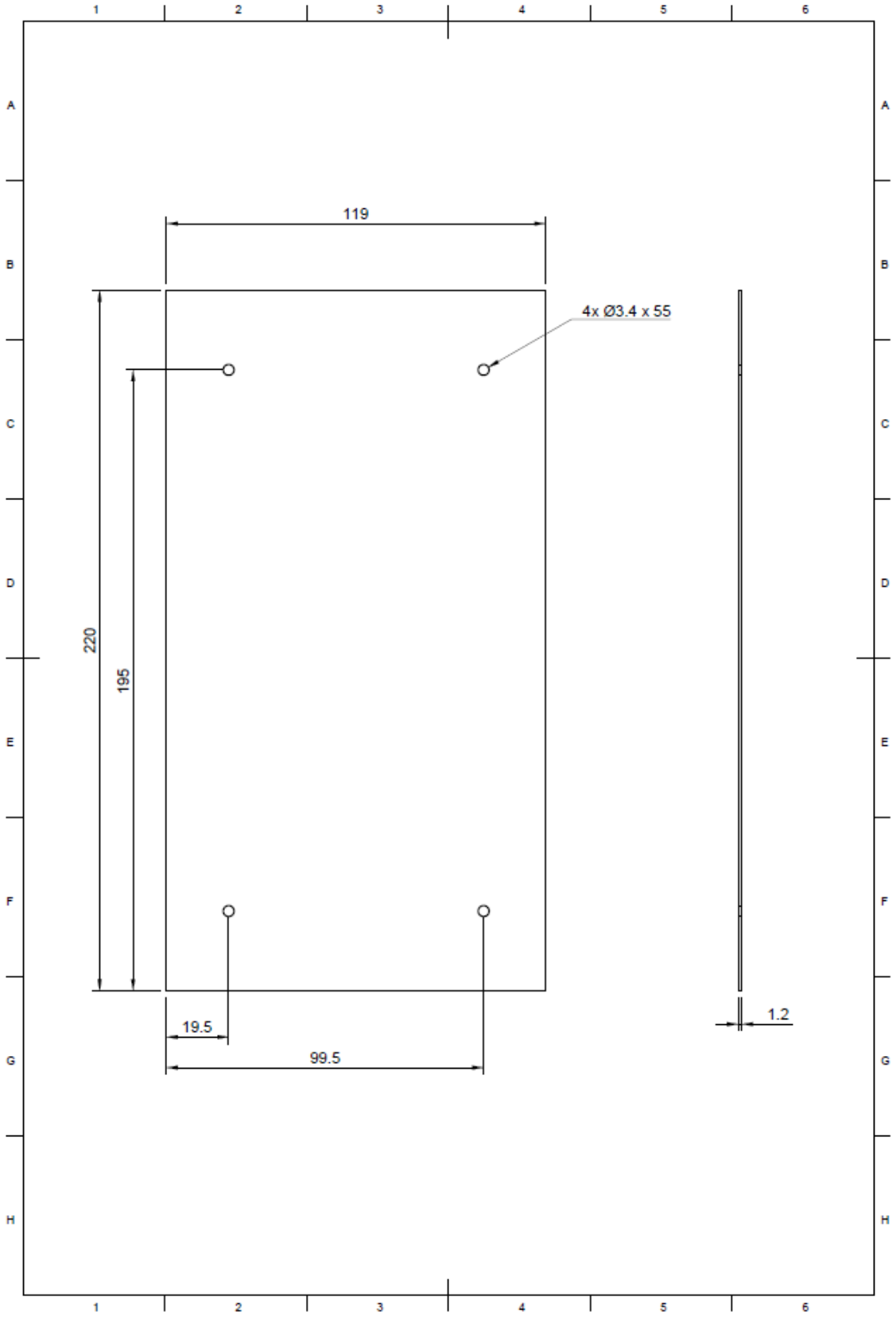

Fig. 90 Z tower shield panel technical draw.

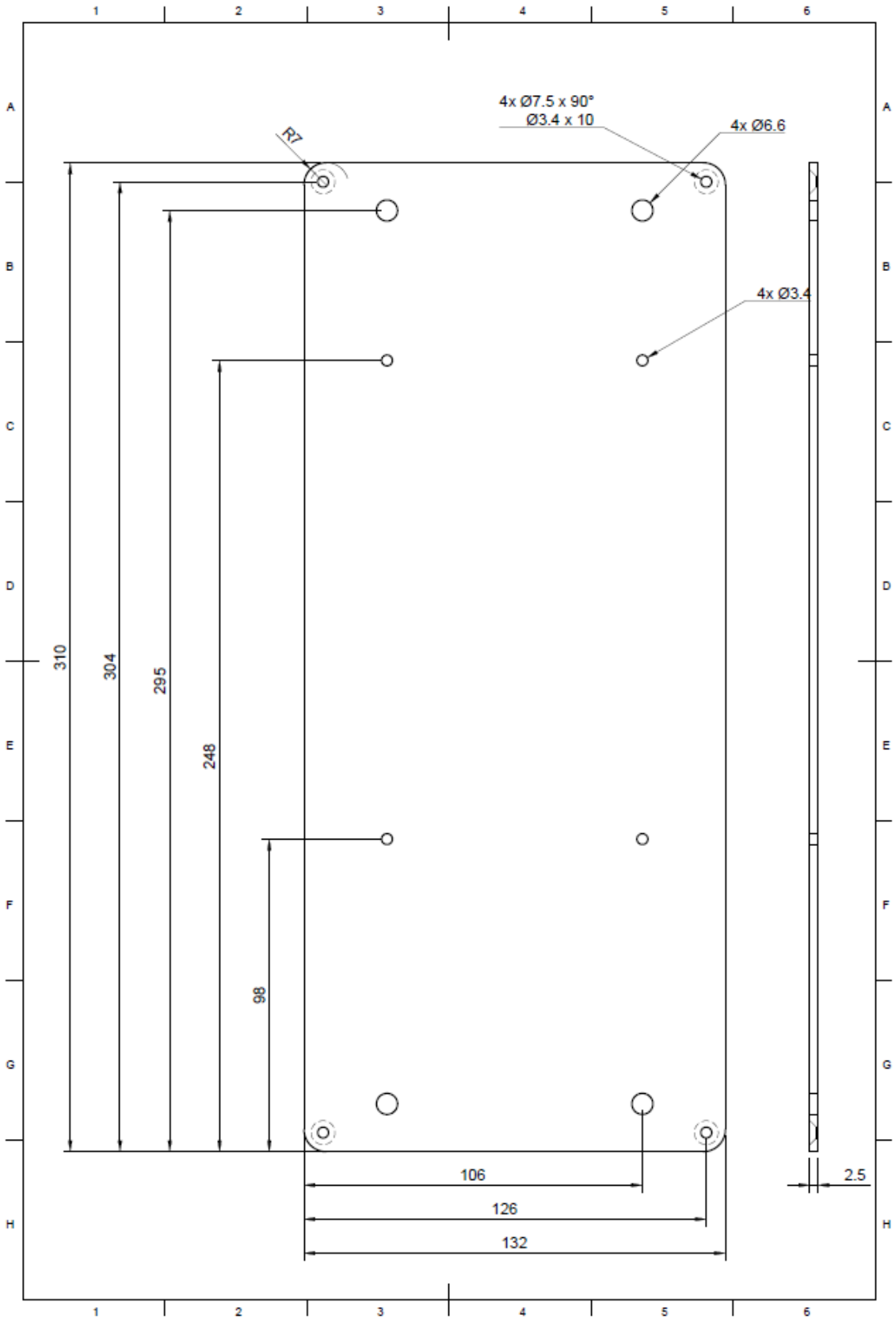

Fig. 91 Rear electronics enclosure panel technical draw.

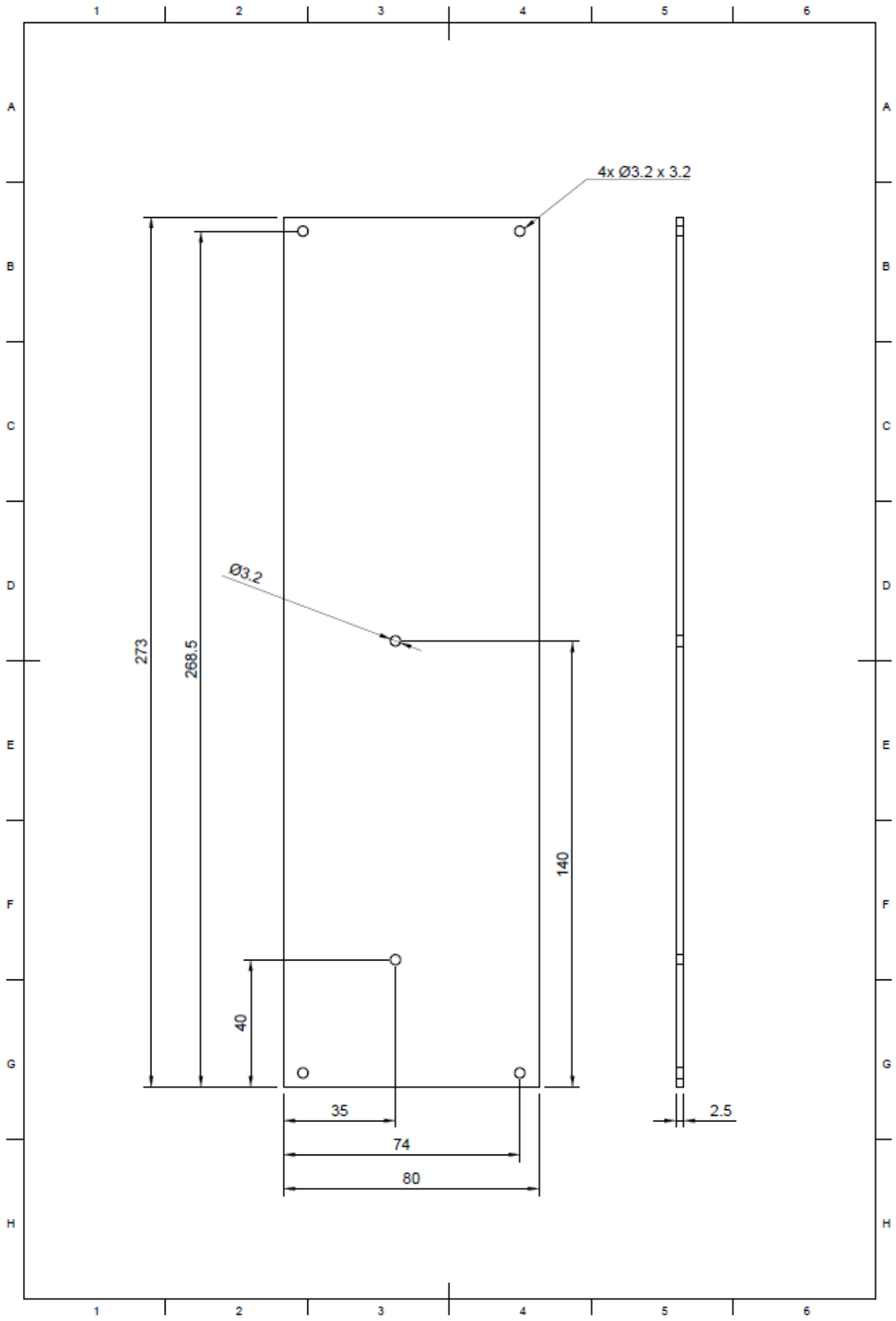

Fig. 92 Right electronics enclosure panel technical draw.

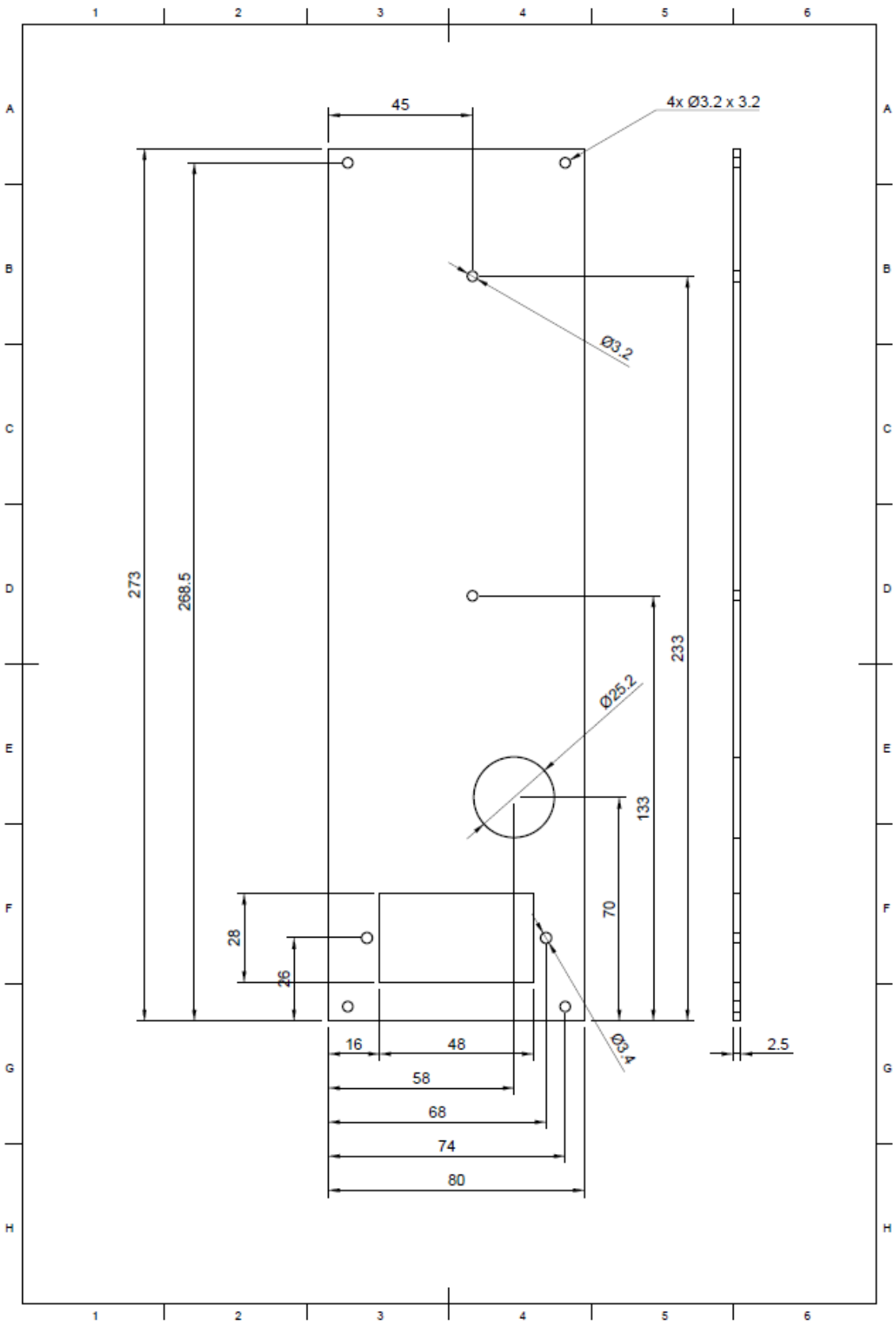

Fig. 93 Left electronics enclosure panel technical draw.

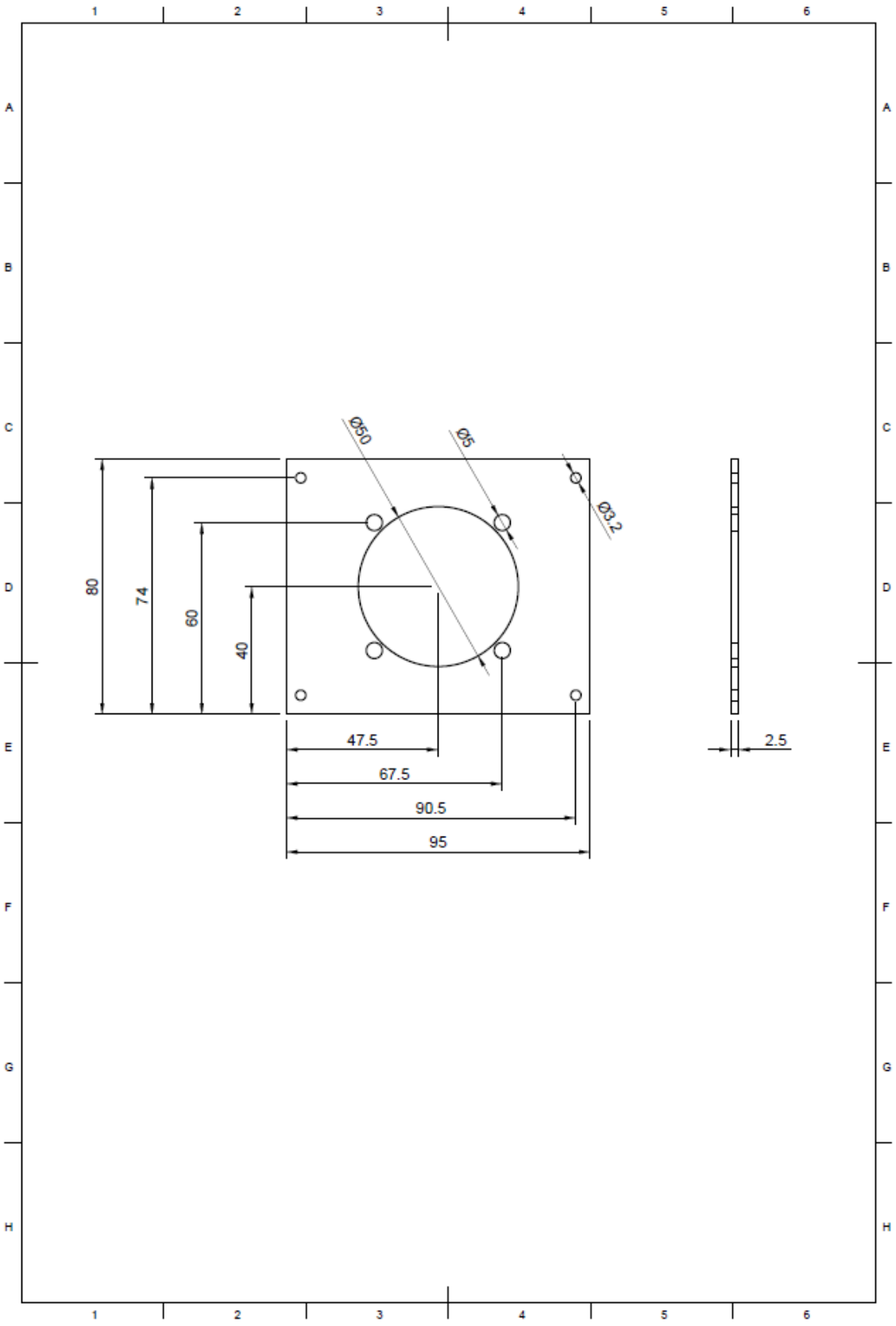

Fig. 94 Bottom electronics enclosure panel technical draw.

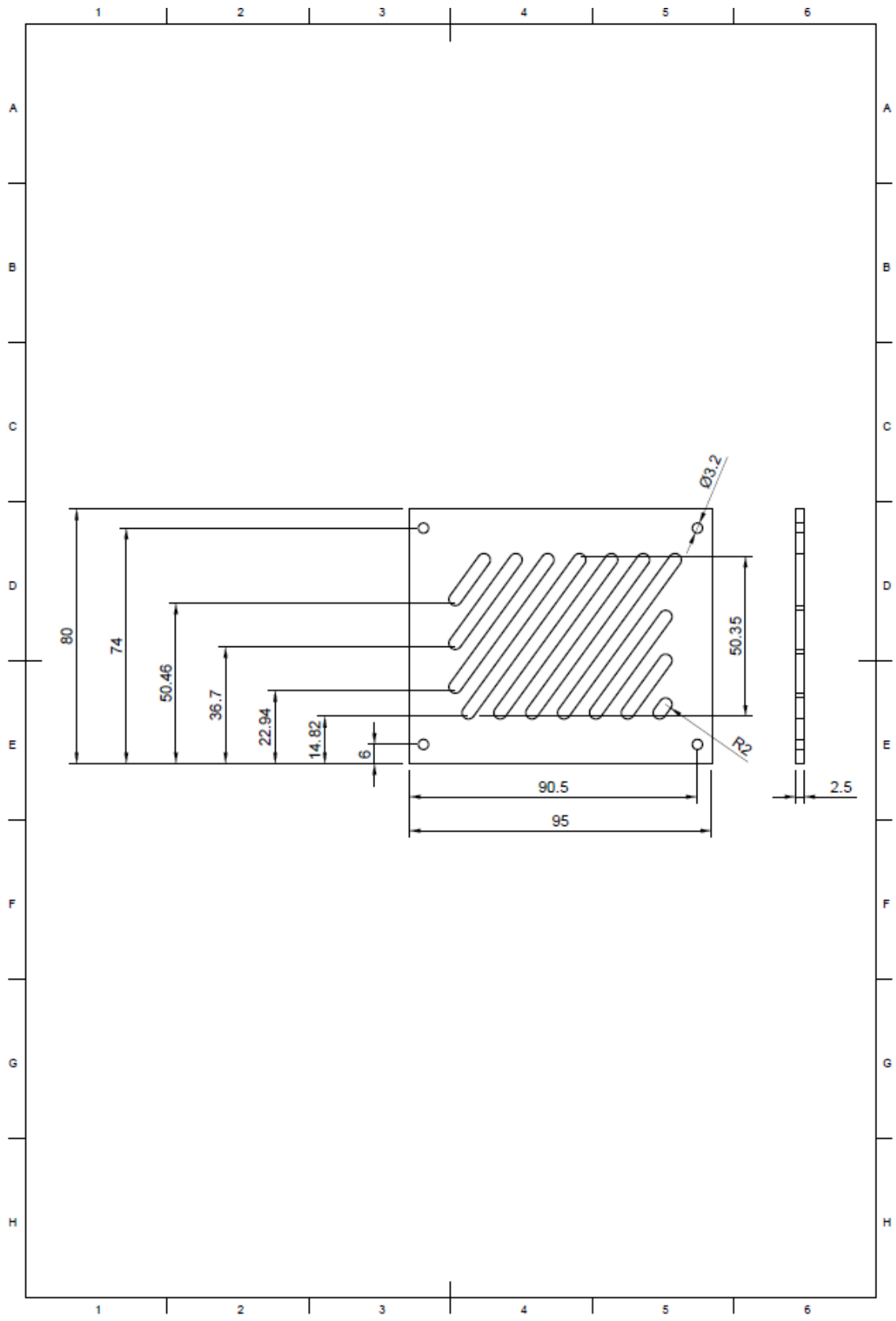

Fig. 95 Top electronics enclosure panel technical draw.

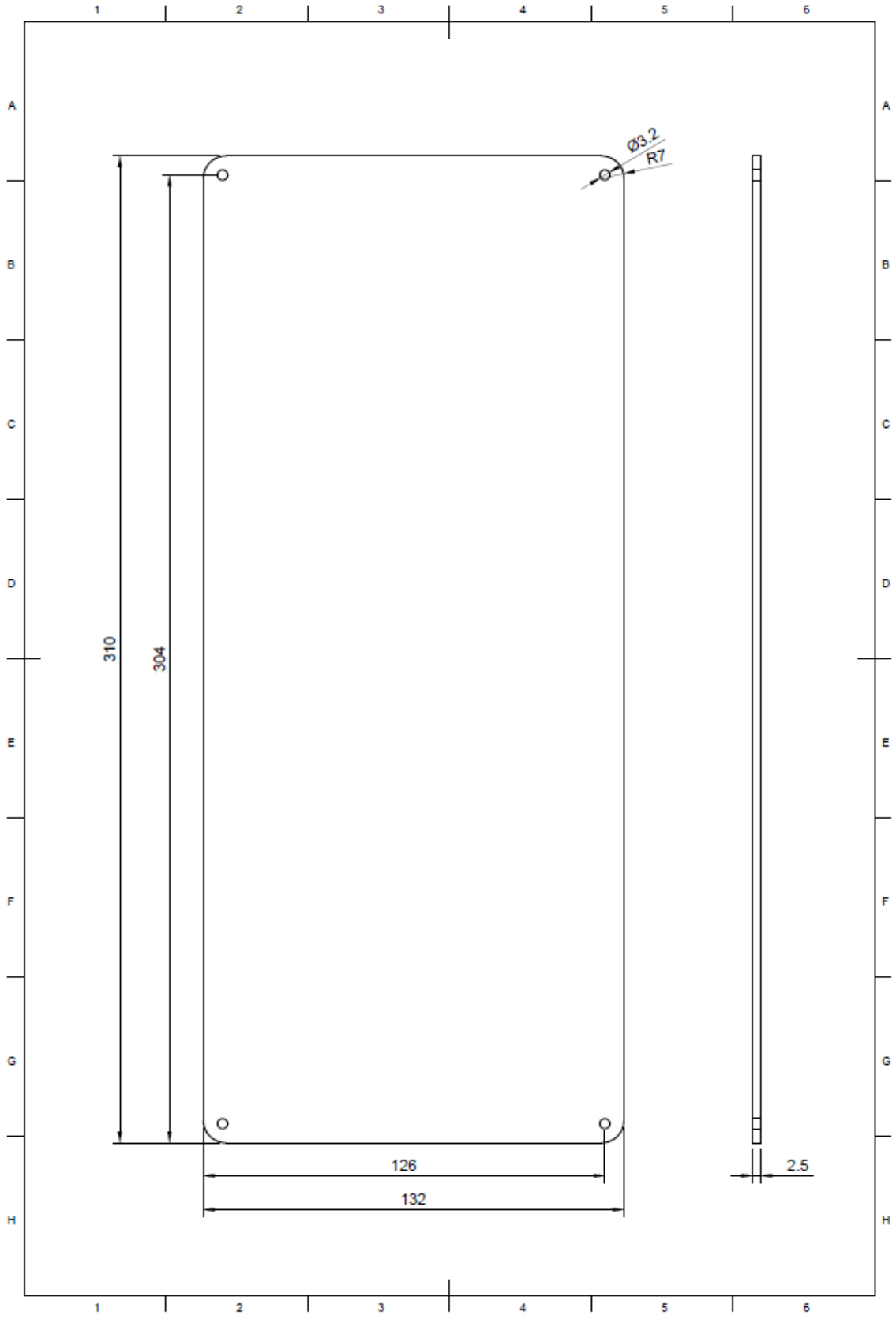

Fig. 96 Cover electronics enclosure panel technical draw.

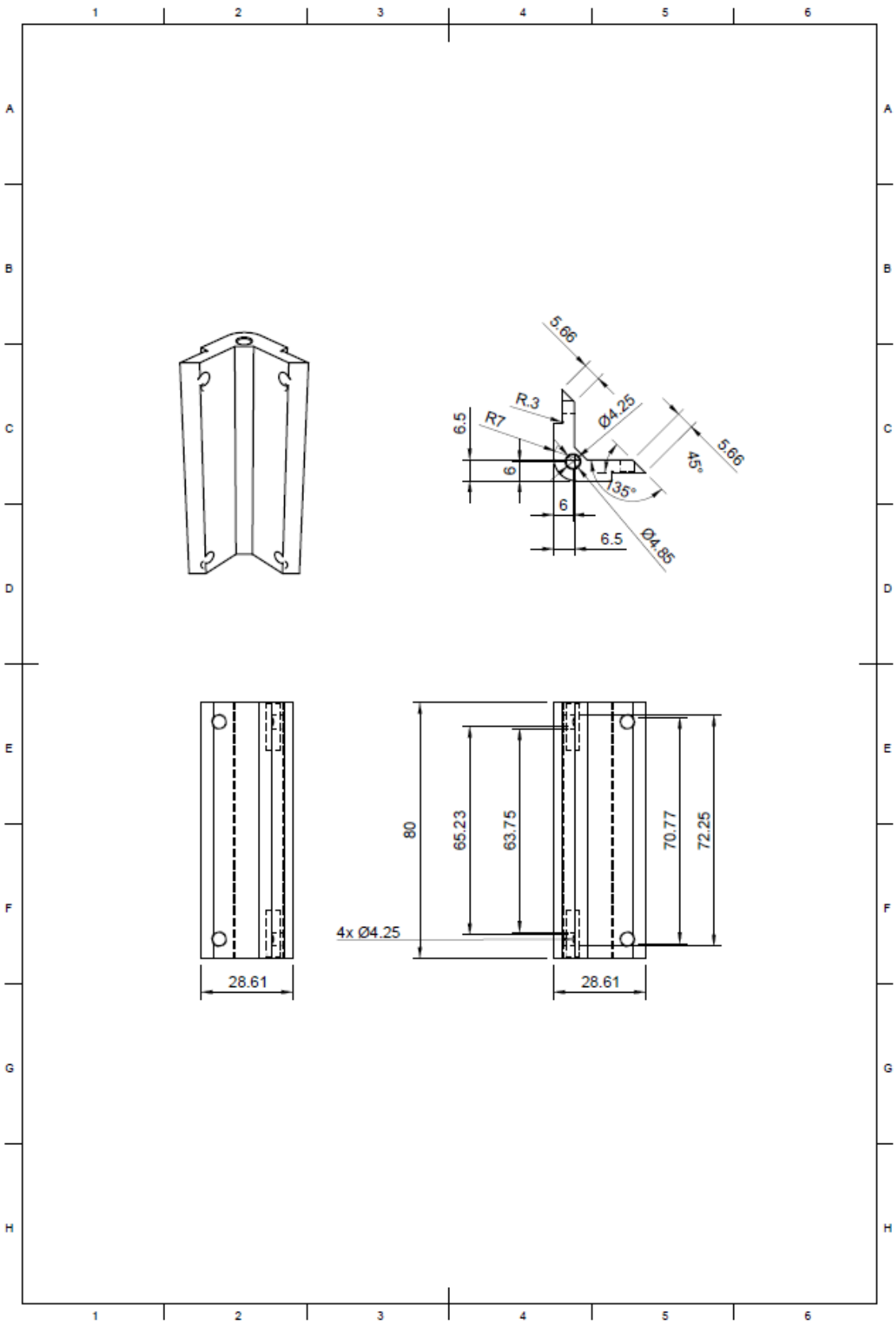

Fig. 97 Electronics enclosure 3D printed corner parts technical draw.

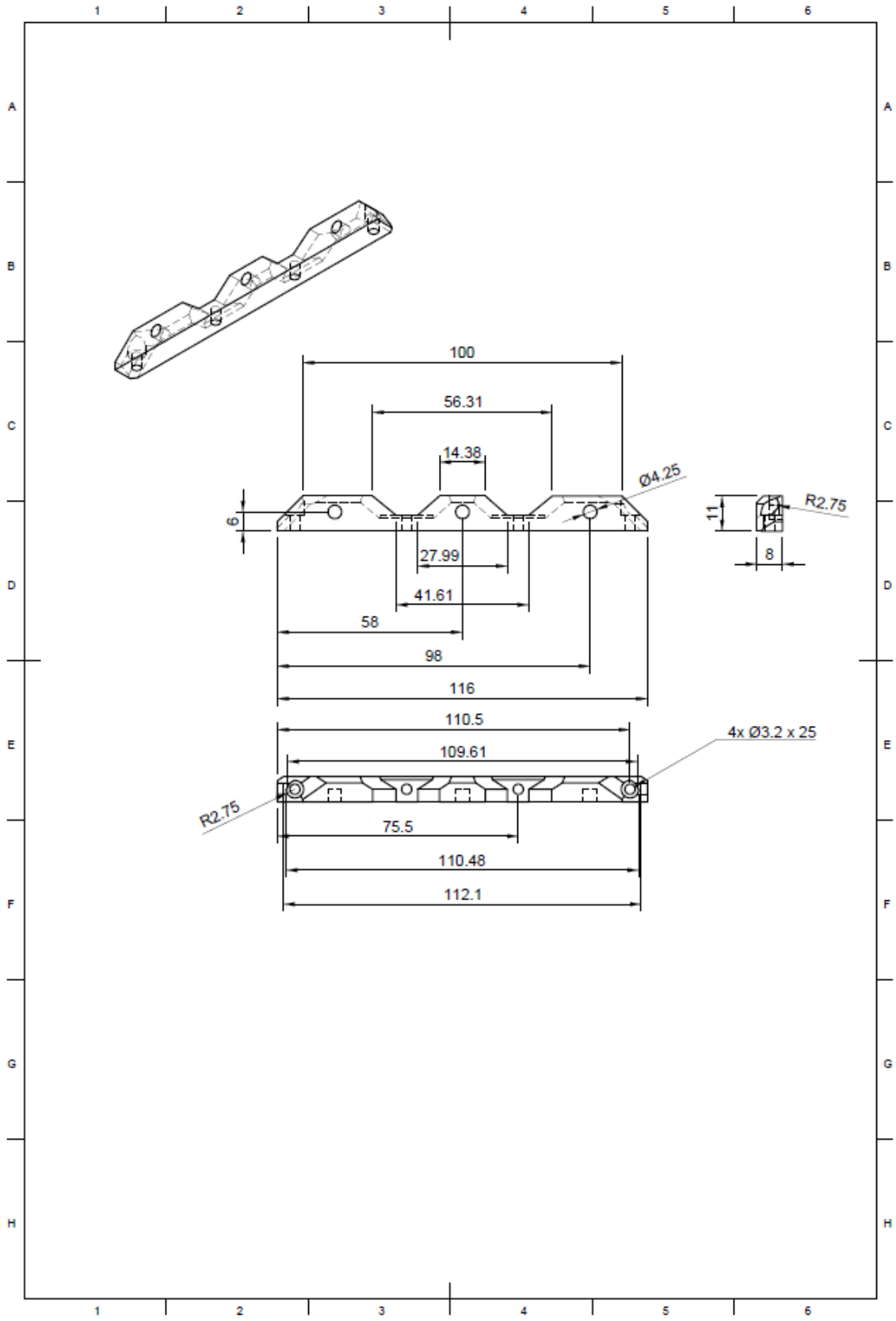

Fig. 98 Bellow gantry mount 3D printed technical draw.

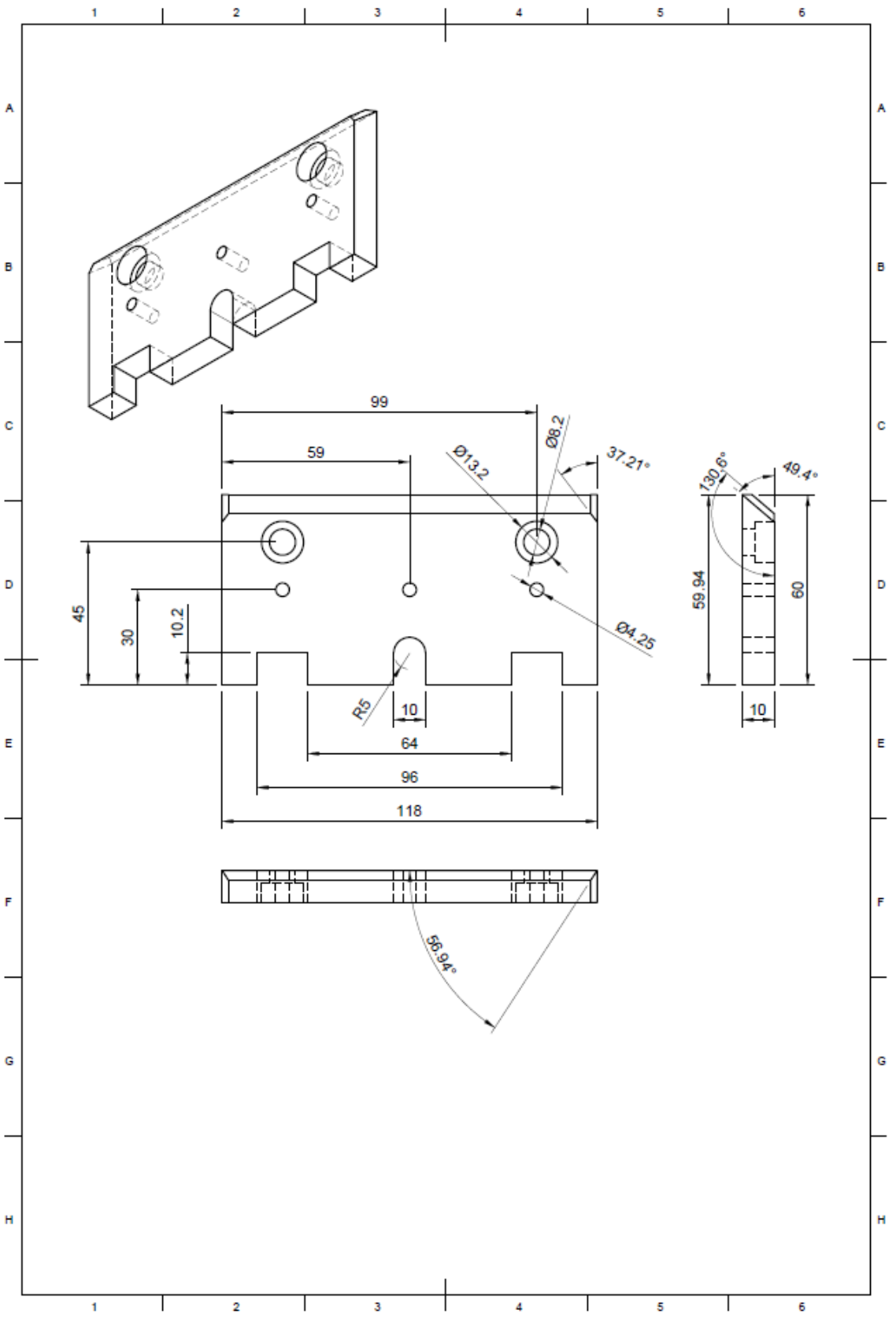

Fig. 99 Y rear bellow mount 3D printed technical draw.

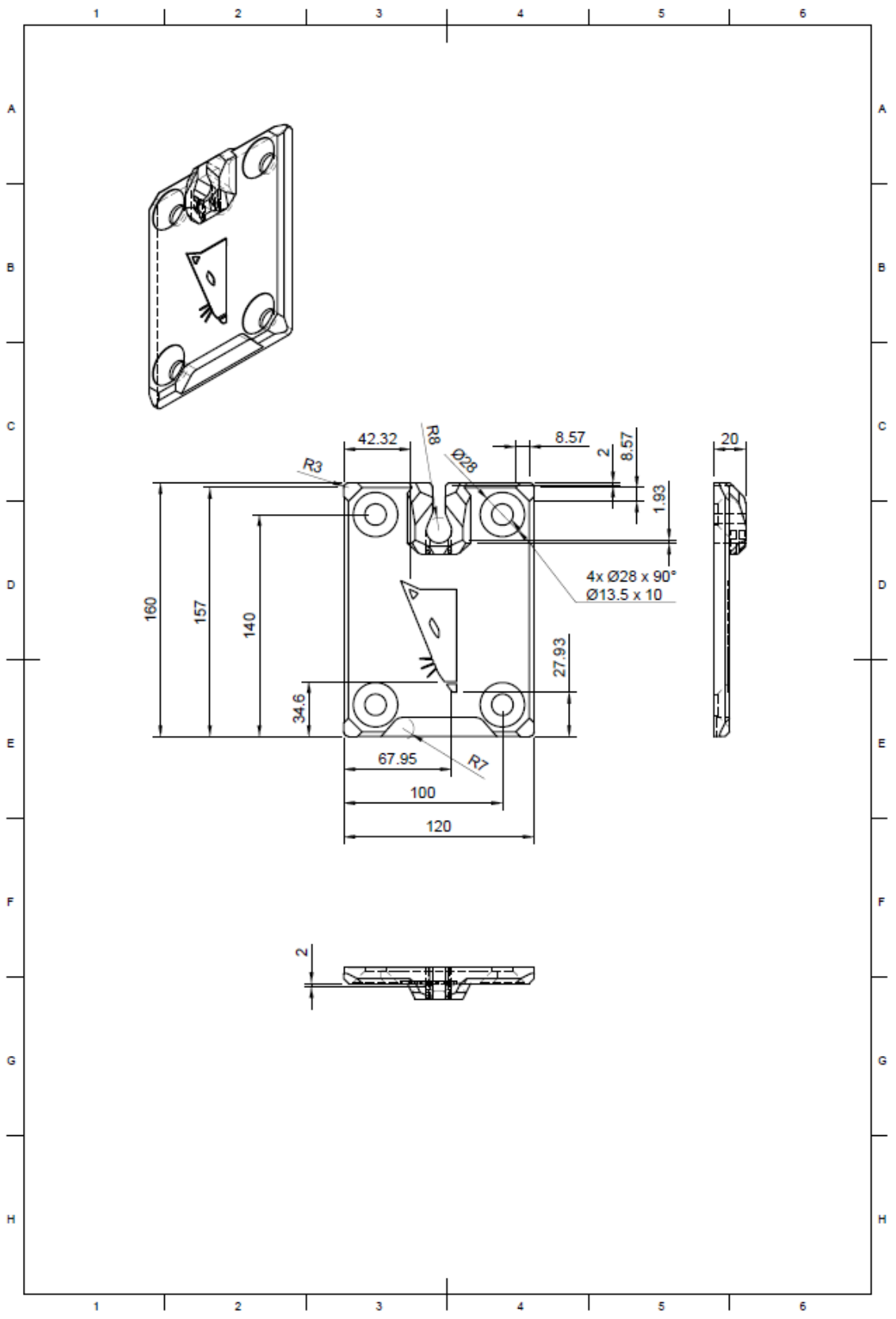

Fig. 100 Z top extrusion cover 3D printed technical draw.